Fakultät für Medizin

Institut für Diabetes und Regenerationsforschung

Identification and characterization of novel genes involved in pancreas development

Aimée Bastidas Ponce

Vollständiger Abdruck der von der Fakultät für Medizin der Technischen Universität München zur Erlangung des akademischen Grades eines

Doktors der Naturwissenschaften (Dr. rer. nat.)

genehmigten Dissertation.

Vorsitzende/-r: Prof. Dr. Dieter Saur
Prüfer der Dissertation:

1. Prof. Dr. Heiko Lickert
2. Prof. Dr. Dr. h.c. mult. Martin Hrabě de Angelis
3. Prof. Dr. Susanna Hofmann

Die Dissertation wurde am 20.08.2019 bei der Technischen Universität München eingereicht und durch die Fakultät für Medizin am 07.04.2020 angenommen.

Faculty of Medicine

Institute of Diabetes and Regeneration

Identification and characterization of novel genes involved in pancreas development

Aimée Bastidas Ponce

Supervisors:

Prof. Dr. Heiko Lickert

Abstract

The better understanding of the biological processes underlying differentiation and maturation of insulin-producing beta-cells (β-cells) is essential for establishment of novel therapeutic approaches, such as *in vivo* regeneration or cell replacement for diabetes therapy. In this PhD thesis, we investigated the mechanisms regulating endocrine cell induction, specification and lineage allocation as well as β-cell maturation and identity.

In the first part, we studied the transcriptional profiles of endocrine progenitors-precursors (EPs) at single-cell resolution by using a novel neurogenin 3 (Neurog3; Ngn3)-Venus fusion reporter mouse line. Specifically, we defined the lineage origin of $Ngn3^{low}$-expressing endocrine progenitors and analyzed their gene expression profiles at different stages of pancreas development. Next, we provided EP-enriched and –signature genes by comparing the mRNA profile of EPs and non-EPs pancreatic lineages. Notably, $Ngn3^{high}$-expressing EPs derived from diverse developmental stages express different levels of EP-signature genes that defined their fate towards α- or β-cells. Altogether, our data provide a comprehensive dataset of transcriptional changes during pancreatic lineage segregation and define a detailed roadmap of endocrinogenesis during pancreas development.

In the second part, we evaluated the functional interconnection of the transcription factors (TFs) pancreatic and duodenal homeobox 1 (Pdx1) and the Forkhead box A2 (Foxa2) during β-cell maturation. Both Pdx1 and Foxa2 play an essential role during β-cell formation and function. However, their interaction during postnatal β-cell maturation remains uncertain. To address this question, we generated a double fluorescent reporter knock-in ($FVFPBF^{DHom}$) mouse line that exhibited normal embryonic development but developed hyperglycemia at weaning age. Notably, the diabetic condition was observed only in male animals disclosing a sexual dimorphic phenotype. Deeper analysis revealed failure in β-cell maturation and sustainability of β-cell identity at postnatal stages. Altogether, establishment and analysis of $FVFPBF^{DHom}$ mouse model demonstrate a cooperative function between Pdx1 and Foxa2 to regulate β-cell maturation and preserve their identity. Overall, we provided a blueprint that can be used for efficient generation of functional β-cells from stem cells *in vitro* and uncovered novel mechanisms controlling β-cell maturation and identity. These findings will aid not only to generate functional β-cell for cell-replacement but also to define novel molecular targets to prevent loss of β-cell identity in diabetic condition.

Index

1 Introduction

The effects of modern life style, such as unhealthy diet and poor physical activity, are the reasons why diabetes represents one of the fastest growing epidemics affecting nearly 425 million people worldwide (International Federation Diabetes 2017). Diabetes results from insufficient production of insulin, due to the dysfunction of β-cells and is characterized by hyperglycemia.

Several types of diabetes have been described in regard to their cause and onset. Type 1 diabetes (T1D) is characterized by the loss of β-cells due to autoimmunity and T cell-mediated destruction, which leads to insulin deficiency. It has a strong genetic component and constitutes around 5-10% of diabetes cases affecting mainly young people. In comparison, Type 2 (T2D) represents the major proportion of diagnosed diabetic patients, with around 70%. Dysfunctional β-cells, glucolipotoxicity and insulin resistance in peripheral organs are the main features of T2D. Together T1D and T2D depict majority of diagnosed diabetic patients (around 80%, Figure 1). Moreover, maturity-onset diabetes of the young (MODY) represents a rare group of genetic diabetic diseases where dysfunction of β-cells is due to mutations in genes involved in their formation or function (Anik et al., 2015; Reis et al., 2000; Weng et al., 2001). Furthermore, during pregnancy, a particular type of diabetes can develop due to an inappropriate response to metabolic demands generating gestational diabetes (Klara Feldman et al., 2016). Within this condition the mother and the offspring are at increased risk to develop T2D after pregnancy and during their adult life, respectively (Dabelea, 2007; Damm, 2009; Petitt et al., 1985). Genetic and gestational diabetes represents the remaining 20% of diagnosed cases (Figure 1). Although current treatments are mainly based on external supply of insulin and improve the life quality of diabetes patients, they are far from providing a cure for the disease. Thus, strategies to promote β-cell replacement in the case of T1D and endogenous β-cell regeneration for T2D patients represent important options to improve future treatments. Therefore, it is of upmost importance to understand the mechanisms underlying pancreas organogenesis, β-cell differentiation and maturation together with their expansion during development.

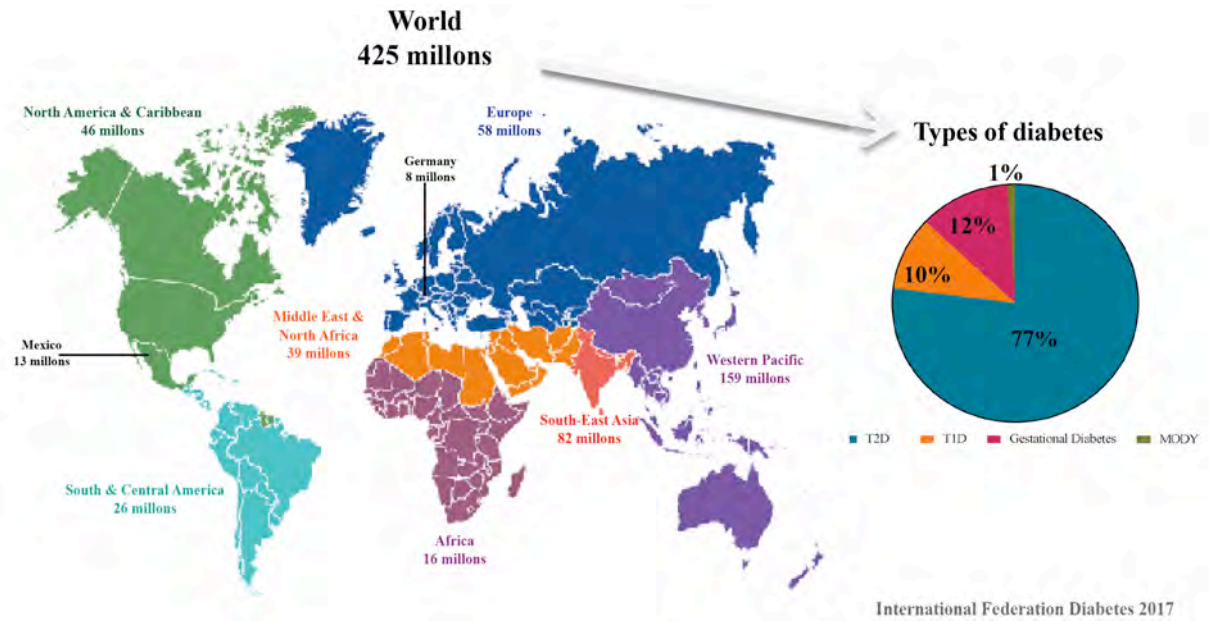

Figure 1. Global prevalence of diabetes. Worldwide incidence and distribution of diabetic persons together with percentages of diabetes types without distinction of age or gender among people. Figure modified from https://idf.org/aboutdiabetes/what-is-diabetes/facts-figures.html.

1.1 Pancreas development

The pancreas is an organ that consists of two compartments: the exocrine part produces digestive enzymes and is comprised by acinar and ductal cells; meanwhile the endocrine compartment consists of the islets of Langerhans that secrete pancreatic hormones to mediate glucose homeostasis (Islam, 2010). The islets are formed by 5 endocrine cell types: β-, alpha- (α-), delta- (δ-), PP- and epsilon- (ε-) cells that synthesize insulin, glucagon, somatostatin, pancreatic polypeptide and ghrelin, respectively (reviewed by Pan and Wright, 2011; Shih et al., 2013; Bastidas-Ponce et al., 2017).

1.1.1 Early pancreas development

In mouse, pancreas development starts around embryonic day 8.5 (E8.5) with the expression of the TFs *Pdx1* and pancreas-specific transcription factor 1a (*Ptf1a*). The specification of the dorsal and ventral buds, with the expression of *Pdx1* and *Ptf1a*, takes places in the foregut endoderm. It has been shown that the absence of either of these genes results in pancreatic agenesis in mouse (Ahlgren et al., 1996; Jonsson et al., 1994; Marty-santos and Cleaver, 2015; Offield et al., 1996) and in human (Stoffers et al., 1997; Weedon et al., 2013). At this stage, *Pdx1* and *Ptf1a* expression is regulated by upstream endoderm TFs, such as forkhead

TF Foxa2 and hepatocyte nuclear factor 6 (Hnf6) (Bastidas-Ponce et al., 2017; Pan and Wright, 2011).

Embryonic pancreas development is divided into two main stages called primary and secondary transition. The first transition takes place between E8.5 and E12.5 and is characterized by a massive proliferation of multipotent pancreatic progenitors (MPCs; $Pdx1^{+}$/$Ptf1a^{+}$ cells) (Burlison et al., 2008) and by morphogenic changes in the epithelium to generate a continuous tubular network (Villasenor et al., 2010). The MPCs give rise to all pancreatic cell types (Pan and Wright, 2011). The regulation between proliferation and maintenance of MPCs, in early pancreatic stages, has been shown as critical for the establishment of the organ size by the determination of the number of mature pancreatic cells (Villasenor et al., 2010). Due to this, a tight system that regulates proliferation and differentiation of MPCs is required; it has been shown that Notch signaling plays a critical role in this regulation (Hart et al., 2003; Norgaard et al., 2003; Apelqvist, 1999; Li et al., 2015; Murtaugh et al., 2003). Studies conducted within deficient mice for components of Notch have shown early endocrine differentiation that causes the depletion of the MPCs pool (Apelqvist et al., 1999; Fujikura et al., 2006; Jensen et al., 2000a). Additionally, reduced pancreas size and a defect in epithelial branching have been observed when the Notch pathway is repressed in MPCs by chemical approaches (Apelqvist et al., 1999).

1.1.2 Pancreas morphogenesis

The pancreas is a highly branched and tubular epithelial plexus. During the establishment of the pancreatic tube, the epithelium goes through a stratification process; follow by the polarization of the epithelial cells that then form microlumens which lastly fuse to generate a luminal network (Figure 2). MPCs form a multi-layered epithelium with cap cells in the outer layer and body cells forming the inner part (Villasenor et al., 2010; Zhou et al., 2007). Later, the cap and body cells differentiate into acinar and endocrine/ductal cells, respectively (Villasenor et al., 2010). This epithelial stratification seems to be critical for the expansion and establishment of the MPC pool (Stanger et al., 2007; Villasenor et al., 2010).

At E10.5, pancreatic epithelial cells polarize and rearrange the stratified epithelium to form microlumens that later coalesce and generate tubules (Kesavan et al., 2009; Villasenor et al., 2010). In addition, it has been shown that the Rho GTPase Cdc42 (Cell division cycle 42) establishes polarity and is required for lumen and endocrine formation during pancreatic

development. Cdc42-null pancreas displayed a defect in tubulogenesis and impairment in endocrine lineage differentiation (Kesavan et al., 2009). Moreover, deletion of Pdx1 not only blocks differentiation towards pancreatic lineages but also impairs the expansion and fusion of lumens together with pancreatic tubulogenesis (Marty-santos and Cleaver, 2016).

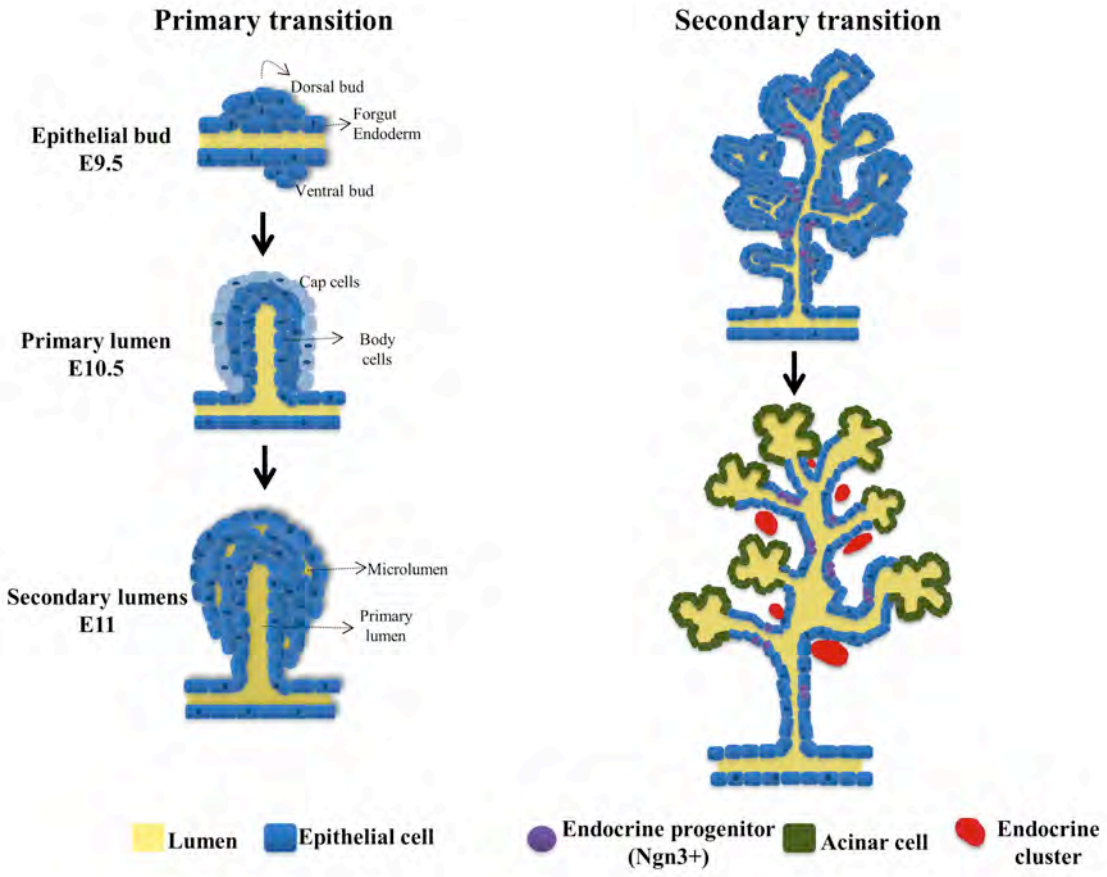

Figure 2. Pancreas development. Primary and secondary transition lead to the development of the three pancreatic cell types (acinar, duct and endocrine cells) in a plexus epithelial structure.

The segregation and differentiation of the three pancreatic lineages (acinar, duct and endocrine) take place during the secondary transition between E12.5 and E15.5. In this process the MPCs segregate into pancreatic tip or trunk domains, which allocates towards acini or bipotent endocrine/duct progenitor cells, respectively (Figure 3). During the segregation of these domains, Nkx6.1 expression is required not only to induce trunk formation but also to repress tip fate, meanwhile Ptf1a favors the generation of the tip domain (Schaffer et al., 2010). In addition, recently it was shown that pancreatic progenitor cells allocate into fate-determining niches by differential surface tension due to cell-cell contact. Cells expressing low and high p120-Catenin levels segregate into tip and trunk domains, respectively (Nyeng et al., 2019). Altogether, these data support the regulated and complex

connection between organ patterning and pancreatic cell fate during embryonic pancreas development.

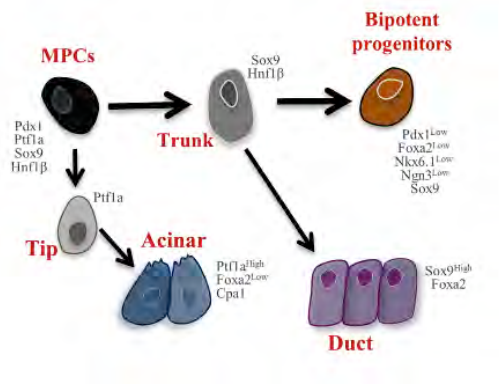

Figure 3. Pancreatic lineage differentiation. Formation of pancreatic lineages from MPCs through patterning (tip & trunk) to form ductal, acinar and bipotent cells.

1.2 Exocrine compartment

Acinar and ductal cells form the exocrine compartment, which constitutes ~95% of the adult pancreas and is responsible for the secretion of digestive enzymes to the duodenum. Acinar cell differentiation begins around E12.5, with the formation of proacini in the distal tip of the pancreatic epithelium (Marty-Santos and Cleaver, 2015). The main regulator of differentiation and maintenance of acini is the TF Ptf1a; as mice deficient of this gene have been shown to completely lack acinar cells (Krapp et al., 1998). In adult mice, acinar cells are characterized by the expression of Ptf1a, Carboxypeptidase 1 (Cpa1), amylase, elastase and trypsinogen (Pictet and Rutter, 1972; Pictet et al., 1972). Acinar and ductal cells are connected through the centroacinar (CA) cells, which express TFs as *Pdx1*, *Sox9*, *Ptf1a* and *Nkx6.1* (Kopp et al., 2011; Schaffer et al., 2010; Solar et al., 2009). It has been suggested that these cells are a reservoir for progenitor-like cells, however this has been shown only in zebrafish (Delaspre et al., 2015) and in *in vitro* studies (Rovira et al., 2010). Ductal cells arise from bipotent epithelial cells in the trunk domain and their differentiation requires the activation of Notch signaling (Hald et al., 2003; Murtaugh et al., 2003). Mature ductal cells express *Sox9*, *Hes1*, *Hnf1β* and *Glis3* (Pierreux et al., 2006). Acinar and ductal cells together form a tubular structure consisting of a main duct, which is connected to the bile duct and the duodenum as well as secondary branches connecting the acini (Reichert and Rustgi, 2011).

1.3 Endocrine compartment

The endocrine compartment represents ~5% of the adult pancreas weight and is formed by the islets of Langerhans. In rodents, β-cells represent approximately ~80% of the islet cell mass and they localize in the core part, while α- (~15%), δ-, ε- and PP-cells (combining for ~5%) reside in the periphery (Islam, 2010). Several differences have been observed when comparing human and murine pancreas with regard to the ratio of the hormone-producing endocrine cells as well as the islet architecture (Brissova, 2005; Kim et al., 2009). Different to mouse, human islets are composed of ~50% β-cells, ~40% α-cells and ~10% other endocrine cell types (Brissova, 2005; Cabrera et al., 2006). Also, in the human islets the endocrine cells are arranged in an intermingled way compared to the structure described in mice.

The allocation of endocrine cells is characterized by an increased expression of different TFs specific for each cell type, requiring a complex gene regulatory network (Arda et al., 2013; Jensen, 2004). The progression from a multipotent cell to a defined mature endocrine cell is regulated by a hierarchical TFs expression, which coordinates the identity of the differentiated cells (Pan and Wright, 2011). This allocation has been reported stage-dependent for each endocrine cell type; α-cells are produced mainly during the first transition, while β-, δ-, and PP-cells appear in the second one.

1.3.1 Endocrine differentiation and delamination

Within the pancreas, the ductal epithelium is composed of bipotent cells and provides a reservoir for endocrine progenitors (EPs; $Ngn3^{+}/Pdx1^{+}$) (Solar et al., 2009), which give rise to all endocrine cell types (Gradwohl et al., 2000; Gu et al., 2002; Johansson et al., 2007). Neurogenin 3 (Ngn3) has been shown to be the master regulator of endocrinogenesis (Gu et al., 2002), transitory Ngn3 expression, between E9.0 and E17.5, induces endocrine-specific TF cascades that initiate and segregate the endocrine cell subtypes (Petri et al., 2006; Villasenor et al., 2008). In addition, it has been shown that no endocrine cells are formed in Ngn3 null mice (Gradwohl et al., 2000), whereas ectopic expression of this TF enforces generation of hormone-expressing cells (Schwitzgebel et al., 2000) (Figure 4).

The specification between α- and β-cell fate is determined by Arx and Pax4 loop-regulated expression, where high levels of Arx give rise to α-cells and Pax4 expression to β-cells (Collombat et al., 2003). Also, β-cell determination requires the expression of Nkx6.1 and

Pdx1. Nkx6.1 expression is then restricted to Ins^{+} cells whereas Pdx1 is also found in a small portion of δ-cells. Another important TF for β-cell differentiation is Nkx2.2, which promotes β-cell program by blocking α-cell differentiation through a repressor complex (Papizan et al., 2011). In addition to Arx, α-cell differentiation relies on other TFs such as Pax6, Rfx6, Brn4, Foxa2 and MafB (Bramswig and Kaestner, 2011). Moreover, there is a tight relation between induction of β-/δ-cell program; in this regard it has been shown that expression or loss of *Pax4* in these cells defines their β- or δ-cell fate, respectively (Collombat et al., 2003). Furthermore, PP-cells are first observed during early pancreas development and the expression of transcriptional levels of PP were reported in all endocrine cells (Herrera et al., 1991). In addition, a tight relation between the α- and PP-cells differentiation programs has been observed during development, which is supported by the increase of PP-cells when Arx is overexpressed (Collombat et al., 2007) (Figure 4). Lastly, ε-cells constitute the least abundant endocrine cell type mainly found during development; due to this they remain poorly understood.

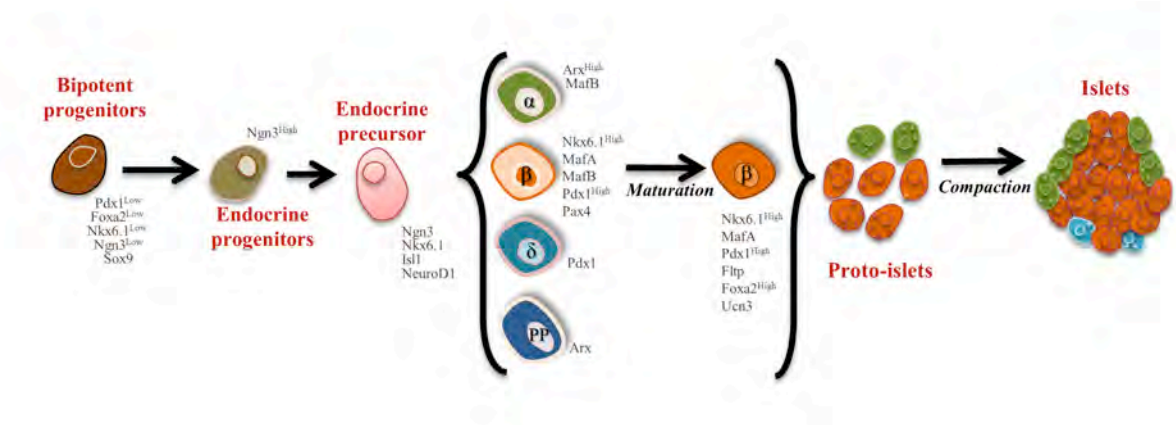

Figure 4. Endocrine lineage differentiation. Formation of endocrine populations from bipotent progenitors until the establishment of the islets of Langerhans.

During the secondary transition, when endocrine cells commit, they exit the cell cycle and leave the pancreatic epithelium in a process defined as delamination (Wang et al., 2010) to then differentiate into specific endocrine cell types that cluster and form islets (Melton, 2011). The level of Ngn3 expression has been reported as the main trigger for the endocrine cell delamination by determining the cell fate as an endocrine precursor cell ($Ngn3^{High}$) (Wang et al., 2010) or a biased progenitor cell ($Ngn3^{Low}$) (Bechard et al., 2016a). Furthermore, Notch signaling has been shown as crucial regulator of Ngn3 expression and function (Apelqvist, 1999; Jensen et al., 2000b; Lee et al., 2001). High levels of Notch block the expression and

activation of Ngn3 (Qu et al., 2013), meanwhile low levels induce Sox9 that activates Ngn3 and endocrine differentiation (Shih et al., 2012). In addition, a tight regulation has been proposed among epithelial morphogenesis and endocrine differentiation, by the requirement of polarity modifications in endocrine cells to differentiate and delaminate. For instance, modulation of apicobasal polarity by EGFR signaling in EPs ($Ngn3^{+}$) leads to constriction in the apical cell domain which triggers an increase in Ngn3 expression to become endocrine committed cells and delaminate (Gouzi et al., 2011; Löf-Öhlin et al., 2017) (Figure 5).

After delamination, endocrine cells migrate within the mesenchyme, to form proto-islets that later will become proper mature islets. Interactions of adhesion molecules, such as cadherins and integrins (Jain and Lammert, 2009) mediate the endocrine cell clustering. Particularly, E-Cadherin is important for aggregation of β-cells during development (Dahl et al., 1996), though it is downregulated during the delamination process. However, the process by which the endocrine cells cluster remains poorly understood.

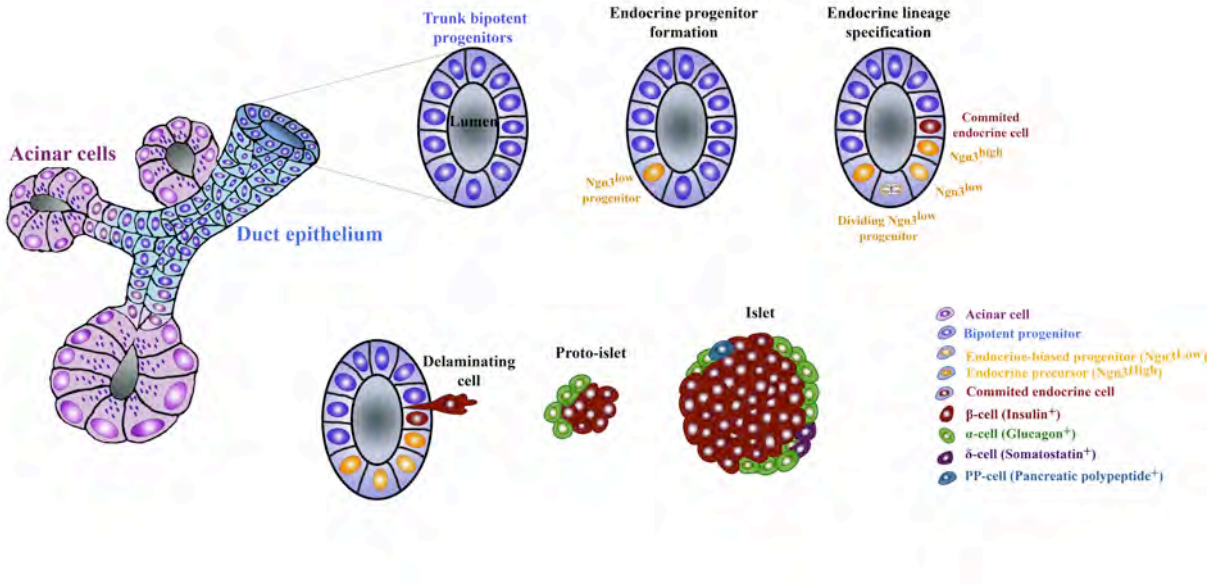

Figure 5. Schematic depiction of endocrine lineage formation and clustering during secondary transition of pancreas development (E12.5-E16.5). Endocrine-biased progenitors ($Ngn3^{low}$) emerge from the bipotent progenitors ($Ngn3^{high}$) that differentiate to all endocrine cell types. Upon differentiated endocrine cells leave the epithelium, migrate and cluster to form proto-islets that undergo maturation to produce islets of Langerhans. Modified with copyright permission from (Bastidas-Ponce et al., 2017).

1.3.2 β-cell maturation and dysfunction

In adult islets the function β-cells is to sense glucose levels and to lower blood glucose upon food intake by activating glucose uptake in the peripheral organs such as liver, muscle and adipose tissue (Islam, 2010). α-cells secrete glucagon, which acts as a counter-regulator to restore normoglycemia. Glucagon acts on the liver increasing glucose levels by glycogenolysis and gluconeogenesis upon hypoglycemia (Briant et al., 2016; Islam, 2010). Moreover, the secretion of insulin and glucagon is regulated by the somatostatin secreted from δ-cells (Hauge-Evans et al., 2009; Islam, 2010; Kanno et al., 2002). In addition, pancreatic polypeptide regulates not only endocrine secretion but also exocrine cells secretion and gut motor activity (Kojima et al., 2007; Lin and Chance, 1974). Ghrelin-secreting cells have been observed during embryonic development, however ε-cells are are very scarce in adult pancreas and their precise function remains unclear (Dezaki, 2013).

After differentiation, endocrine cells acquire their functional glucose-responsive hormone-producing phenotype. Particularly, β-cells go through postnatal maturation processes where they obtain a mature and regulated response upon glucose stimulation (Bonner-Weir et al., 2016). During this process, immature β-cells activate and upregulate their signature transcriptional profile, with the expression of genes, such as *MafA, Nkx6.1*, *Pdx1* and *NeuroD1* (Bliss and Sharp, 1992; Blum et al., 2012; Stolovich-Rain et al., 2015). Immature β-cells are characterized by displaying an unregulated insulin secretion upon high glucose levels (Asplund et al., 1969; Grasso et al., 1968; Hole et al., 1988; Obenshain et al., 1970), together with a "leaky" secretion at basal glucose levels (Bliss and Sharp, 1992; Blum et al., 2012) compared to mature β-cells.

The TFs MafA and MafB are essential for β-cell maturation. During differentiation, α- and β-cells express MafB, which progressively becomes limited only to α-cells promoting their maturation and identity (Artner et al., 2007; Conrad et al., 2015). In β-cells, a switch from MafB to MafA is critical to acquire mature identity (Nishimura et al., 2006, 2009). MafA, Pdx1 and NeuroD regulate *insulin* gene transcription by synergistically activating its promoter (Aguayo-Mazzucato et al., 2011; Gao et al., 2014; Gu et al., 2010; Melloul et al., 2002; Taylor et al., 2013; Zhang et al., 2005). Furthermore, Pdx1 and Nkx2.2 play an important role

in β-cell maturation by inducing functional β-cell markers such as insulin, the enzyme glucokinase (Gck) required to process glucose during glycolysis and the glucose transporter Glut2, demonstrating a critical role of these proteins not only during pancreas development, but also in β-cell function. In addition, it has been reported that Pdx1 is required to maintain β-cell function (Gao et al., 2014; Li et al., 2005), proper insulin secretion (Ahlgren et al., 1998) and identity by repressing α-cell program (Gao et al., 2014). Also, it has been shown that Pdx1 heterozygous animals develop diabetes in adulthood, secrete less insulin and have an increase in apoptosis (Brissova et al., 2002; Holland et al., 2005; Johnson et al., 2003). In human, mutations in the Pdx1 locus generates MODY4 (Fajans et al., 2001).

Another reported important TF to maintain the identity of functional β-cells is Foxa2 (Gao et al., 2010). This TF belongs to the Forkhead box family and acts as a pioneer TF having the capacity to open compact chromatin, which allows other genes to be bound, thus promoting dynamic regulation of gene expression (Zaret and Carroll, 2011). During pancreas development, Foxa2 has different functions during organogenesis and differentiation (Kaestner, 2010). Particularly in β-cells, deletion of Foxa2 causes a hyperinsulinemic hypoglycemic phenotype (Sund et al., 2001). Moreover, two subunits of the β-cell ATP-sensitive K^+ channel were identified as novel Foxa2 targets in islets (Sund et al., 2001). In addition, genetic fine mapping and genomic annotation confirmed that T2D risk alleles are enriched for Foxa2-bound enhancers in human (Gaulton et al., 2015; Mahajan et al., 2014).

Foxa2 and Pdx1 share several important functions, such as regulation of insulin production and modulation of the function of other TFs (Gao et al., 2007; Hani, 1999; Wang et al., 2002a). In diabetic models, the levels of both TFs appeared to be reduced in dysfunctional β-cells, suggesting that these TFs act alone or in combination to induce or to maintain β-cell identity (Russ et al., 2011; Wang et al., 2014a). Furthermore, heterozygous mice for both *Pdx1* and *Foxa2* display altered islet architecture and loss of β-cell identity resulting in severe distortion in insulin secretion and blood glucose regulation (Shih et al., 2013). Moreover, Foxa2 directly binds to *Pdx1* enhancer elements during development and deletion of Foxa1 and Foxa2, double knockout, leads to pancreas agenesis (Gao et al., 2014). Additionally, Foxa2-driven *Pdx1* expression has also been reported in differentiating β-cells (Lee et al., 2002a).

Between P9 and P14, β-cells gain the capacity to sense different levels of glucose, which is reflected by a proper secretion upon higher glucose concentrations (Blum et al., 2012). This process is characterized by the expression of Urocortin 3 (Ucn3) (Blum et al., 2012) as a marker of maturity in β-cells. Another maturation step takes place when the mice change from high-fat (mother) milk diet to a high-carbohydrate chow during weaning (around P21). In this step, β-cells obtain a compensatory proliferation feature and improve their secretory response due to a regulation of their oxidative phosphorylation (Stolovich-Rain et al., 2015). However, the detailed mechanisms and molecular players required for a full maturation of β-cells are still unknown.

Moreover, islet architecture impacts endocrine cells maturation. Cell polarity, cell-to-cell adhesion, cell-to-matrix adhesion and gap junctions together with interconnections with the surrounding tissues (vessels, nerves and the microenvironment) provide the compact structure with physiological function capable to sense glucose levels (Bader et al., 2016; Roscioni et al., 2016). In this regard, Wnt/planar cell polarity (PCP) components have been shown to trigger the expression of β-cell maturation markers in 2D and 3D *in vitro* cultures of mouse and humans (Bader et al., 2016), which could be a reflection of their function in islet compaction (Roscioni et al., 2016). How the arrangement of endocrine cells within the islet affects their functions remains still uncertain. Due to this, understanding the principles of endocrine cell formation during development is not only important to generate these cells *in vitro* but also to trigger regeneration of adult islets in diabetic condition.

In certain conditions of elevated metabolic and functional activity such as diabetes, β-cells lose their proper function and identity, resulting in β-cell dysfunction (Weir and Bonner-Weir, 2004). Different causes have been related to this phenomenon, such as oxidative stress, high levels of glucose and lipids, and inflammatory cytokines (Guo et al., 2013; Jonas et al., 1999; Prentki and Nolan, 2006; Prentki et al., 1992). Dysfunctional β-cells exhibit an altered gene expression signature characterized by a low expression of their specific TFs (Guo et al., 2013). Likewise, a reduced expression of maturation and functional markers such as Ucn3, Glut2 and MafA is observed. In some cases, dysfunctional β-cells become less mature, expressing embryonic markers like Ngn3 and displaying a poly-hormonal phenotype (Wang et al., 2014a), within these changes they go through a process defined as dedifferentiation. In addition, it has been shown that dedifferentiated β-cells have altered capacity to respond to different glucose levels, demonstrating an impact on their functional properties (Kahn et al.,

2006; Marx, 2002), particularly a decrease in the first and second insulin secretion phase during the GSIS analysis (Pørksen et al., 2002) (Figure 6).

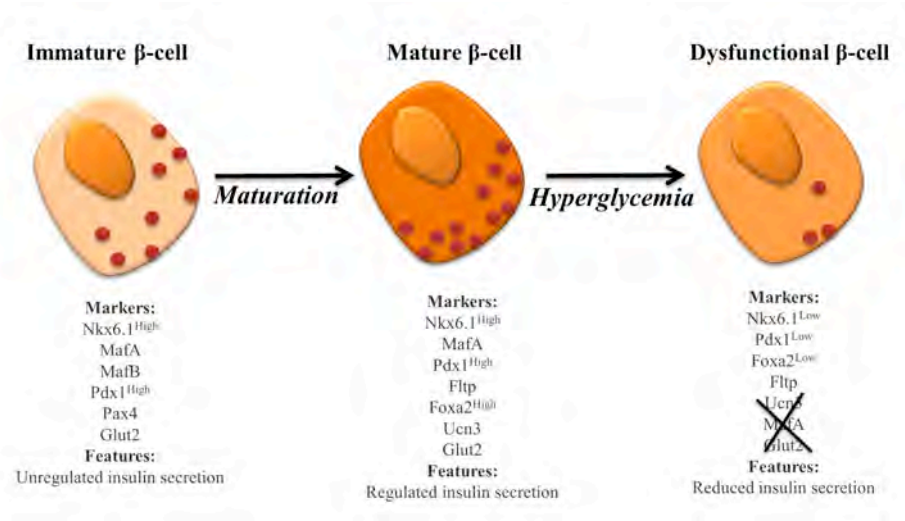

Figure 6. Different types of β-cells. β-cell maturation process is required for the proper establishment of identity and functional features.

Recently, the dedifferentiation process has been observed to be a major mode of β-cell failure in diabetes (Talchai et al., 2012). Dedifferentiated β-cells have been identified in T1D and T2D and are characterized by a progenitor-like or immature state accompanied by an impaired insulin secretion (Brereton et al., 2014; Dahan et al., 2017; Jonas et al., 1999; Laybutt et al., 2003; Ross Laybutt et al., 2002; Talchai et al., 2012; Wang et al., 2014a). Importantly, dedifferentiated β-cells have also been observed in T2D human, suggesting a conserved mechanism from mouse to human (Cinti et al., 2016). In this regard, a deeper understanding of β-cell (de)differentiation, heterogeneity and plasticity in health and disease gives the opportunity to design drugs that specifically target certain islet cell subpopulations in order to trigger regeneration (Roscioni et al., 2016a).

1.3.3 Regeneration of β-cells

Numerous approaches have been investigated to regenerate endogenous β-cells (Figure 7), particularly triggering endogenous expansion of β-cells and differentiating other cell types towards the β-cell fate. In regard to the β-cell proliferation capacity, it has been shown that new β-cells in adult islets are formed by self-replication (Dor et al., 2004). However, this is very limited due to the low β-cell proliferation rate (Finegood et al., 1995; Teta et al., 2005)

and its age dependency (Gregg et al., 2012; Meier et al., 2008). Furthermore, β-cell proliferation has been observed in certain conditions with high metabolic demand, such as pregnancy (Sorenson and Brelje, 1997; Parsons et al 1992 and Teta 2007) or obesity (Linnemann et al., 2014). Moreover, in rodents injury and pathological conditions like pancreatectomy, partial duct ligation (PDL), and the use of low-dose of Streptozotocin (STZ) can trigger regenerative β-cell responses (Bonner-Weir et al., 1993; Rankin and Kushner, 2009; Senée et al., 2006). Particularly, animal disease modelling like pancreatic duct ligation reinforces the β-cell replication resulting in a robust β-cell proliferation (Teta et al., 2005, 2007).

During embryonic pancreas development, EPs expressing ($Ngn3^+$ cells) differentiate and form a new β-cell (Katsuta et al., 2012). In adult mice, these EPs come from the pancreatic ductal epithelium (Bonner-weir et al., 2004), and they have been observed after partial pancreatectomy and PDL (Bonner-Weir et al., 1993). Also, treatments such as Gastrin (Téllez and Montanya, 2014) and the GLP-1 agonist Exendin 4 (Xu et al., 1999) induce Ngn3 expression and increase β-cell neogenesis in rodents. However, the rate of $Ngn3^+$ cell formation is low and the specific mechanism that triggers β-cell neogenesis remains uncertain and controversial, thus a deeper understanding of this process represents an approach to regenerate of functional β-cell mass.

Stressful conditions such as dysfunction or loss of β-cell mass trigger the conversion of several cell types into β-cell fate in a process called transdifferentiation (Shen et al., 2003). In mice with nearly complete ablated β-cell mass, a stage-dependent degree of cell plasticity within the islet has been observed. In juvenile mice efficient reprogramming of δ-cells has been observed (Chera et al., 2014;) meanwhile in adulthood α-cells transdifferentiate towards β-cells (Chera et al., 2014; Thorel et al., 2010). Other pancreatic cells, such as acinar cells, have shown reprogramming capacity when undergo through injury as in PDL (Pan et al., 2013) or by the re-expression of developmental TFs (Ngn3, Pdx1, and MafA) (Zhou et al., 2008) acquiring β-cell features.

Altogether, these findings prove the plasticity of all pancreatic cells and show their ability to expand and differentiate to generate new β-cells. However, the requirement of harsh challenging conditions such as total ablation and the low transdifferentiation efficiency disclose the need of further investigation to uncover the precise mechanisms that define the differentiation towards β-cell fate.

In vitro generation of insulin producing cells, for replacement of the dysfunctional β-cells, has been considered an attractive alternative; however and despite the efforts and success differentiating Ins^+ β-like cells (Blum et al., 2012; Pagliuca et al., 2014; Rezania et al., 2014), further investigation is required to differentiate fully mature β-cells in a controlled manner. In addition, this might shed light on the pathogenesis of diabetes and reveal molecular targets for treatments.

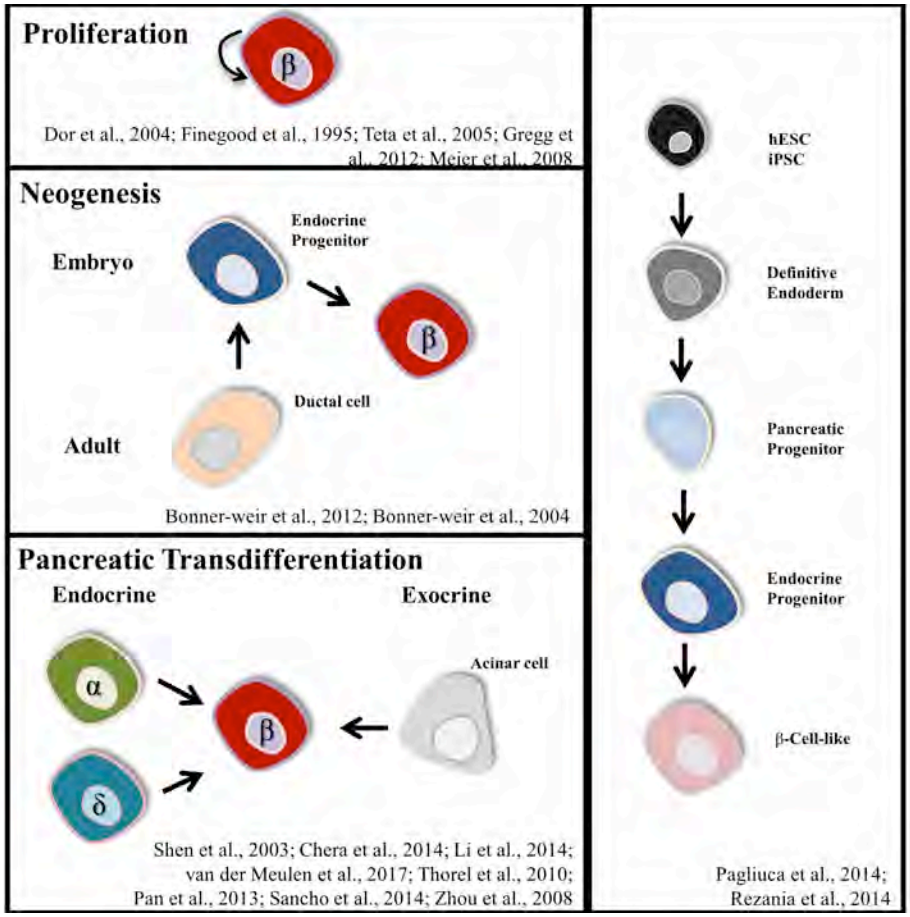

Figure 7. Strategies for *in vivo* regeneration and *in vitro* differentiation of β-cells. Different approaches to regenerate β-cell.

2 Aims of the thesis

Understanding the biological processes underlying differentiation, maturation and function of β-cells can potentially create novel approaches for diabetes therapy. Therefore, in this thesis, I addressed the following aims:

Aim 1: Analysis of the endocrine lineage development on a single cell level. A detailed and time-resolved description of all determinants involved in pancreatic endocrinogenesis will enhance the understanding of islet cell neogenesis. Hence, we investigated in a stage-dependent manner the gene regulatory programs during endocrine cell induction from multipotent and bipotent progenitors, as well as endocrine specification and lineage allocation, using single cell RNA sequencing and computational analysis. This can serve as roadmap for the generation of endocrine cells from stem cells and may allow to trigger endocrine neogenesis for *in vivo* regeneration of β-cells.

Aim 2: Analysis of the cooperative function of Foxa2 and Pdx1 during β-cell maturation.

A comprehensive understanding of the β-cell maturation process will allow to determinate the factors required for the acquisition of a functional β-cell phenotype. Thus, we investigated the synergistic regulatory function of Pdx1 and Foxa2 during post-natal development of β-cells using a novel reporter mouse line FVFPBF^{DHom}. This provided useful information to improve the generation, *in vitro,* of functional mature β-like cells for replacement therapies.

3 Methods

Animal studies. The animal experiments were carried out in compliance with the German Animal Protection Act, the guidelines of the Society of Laboratory Animals (GV-SOLAS) and Federation of Laboratory Animal Science Associations (FELASA).

Blood glucose level analysis. Mice were maintained in standard conditions, fed and watered ab libitum or fasted 6 hrs before the measurements. Blood glucose values were determined from venous blood using an automatic glucose monitor (Glucometer Elite, Bayer).

Tissue isolation and processing. Organs were dissected, washed in 1X PBS and transferred to RIPA buffer containing proteinase inhibitors, crushed manually or using a tissue homogenizer or a water sonicator always on ice to avoid protein degradation. Afterwards the lysate was centrifuged (12000 rpm, 4 °C, 10 min), and the supernatant transferred into a new tube and stored at ≥20 °C.

Pancreatic insulin content. Pancreatic insulin content was determined using acid ethanol extraction method. Therefore, the pancreas was dissected, washed in 1X PBS and transferred into an acid-ethanol solution (5mL 1.5% HCl in 70% EtOH), the tissue was homogenized using a tissue homogenizer and incubated at -20 °C during 24 hrs. After that a second round of acid-ethanol solution was added follow by another 24 hrs incubation at -20 °C. The homogenize tissue was centrifuged (2000 rpm, 15 min, 4 °C) and the supernatant transferred into a new tube and neutralized with 1M Tris pH 7.5. Insulin was measured using a mouse insulin ELISA and normalized over the protein concentration that was determined by BCA protein assay.

Islet isolation. The pancreatic islets of Langerhans were isolated from mice via collagenase digestion of the pancreas, islet purification and hand picking. In detail, the collagenase P (Roche) solution (1 mg/mL in G-solution) was injected in the common bile duct after sealing the connection of the central pancreatic duct with the duodenum using a clamp. After inflating the pancreas with the collagenase, the pancreas was dissected and transferred into 3 mL of collagenase P solution. The pancreas was digested at 37 °C for 15 min (mixing after 7.5 min), placed on ice, the digestive reaction was stopped by adding 15 mL of cold G-solution. The tube was centrifuged (1620 rpm, 3 min, 4 °C), the pellet washed 2x with 20 mL of G-solution and suspended in 5.5 mL of the gradient medium. The suspension (2^{nd} phase) was added slowly on the 2.5 mL remaining gradient medium (1^{st} phase) and finally 6 mL of G-solution

were added slowly on top to form the 3rd phase. After 10 min of incubation at RT the gradient was centrifuged (1700 rpm, 10 min, RT, acceleration 3, brake 0) resulting in an islet enriched interphase between the middle and the upper phase. This interphase was pipetted into a pre-wet cell strainer (70 μm) and washed 2x with 10 mL G-solution. To harvest the islets the cell strainer was turned and washed to deposit the islets into a petri dish. To purify the islets, the islets were handpicked under the microscope and cultured in culture medium.

Single cell suspension. In order to achieve a single cell suspension of islets, the islets were handpicked in an 1.5 mL Eppendorf tube, pelleted (800 rpm, 1 min) washed with PBS (-Mg/Ca) and digested with 0.25% Trypsin with EDTA (Gibco) at 37 °C for 8 min. During this time the cells have to be pipetted 5x up and down with a 1 mL pipette every 2-3 min. The digestion was stopped by culture medium and centrifuged (1200 rpm, 5 min). The cell pellet was suspended in FACS buffer and filtered through a filter (35 nm).

FACS sorting. The FACS sorting of endocrine cells was done using the FACS-Aria III (BD). In general, the single cells were gated according to their FSC-A (front scatter area) and SSC-A (side scatter area). Singlets were gated dependent on the FSC-W (front scatter width) and FSC-H (front scatter height) and dead cells were excluded using the marker 7AAD (eBioscience). The FVF endocrine populations were discriminated upon their Venus fluorescence emission at 488 nm and the β- and α-lineages according to their BFP emission at 405 nm (positive and negative respectively). To enrich for β-cells the distinct SSC-A high populations were gated. In order to isolate RNA from FACS sorted cells, the cells were sorted directly into Qiazol (Qiagen).

Glucose stimulated insulin secretion (GSIS). Before performing the GSIS, the freshly isolated islets were cultured O/N in culture medium to recover. Islets were transferred in a 96 well plate, into a cultured a modified Krebs Ringer phosphate HEPES (KRPH) buffer supplemented with 2.8 mM glucose for 1 h. Then the islets were sequentially incubated with different glucose concentrations in modified KRPH buffer for 2 hrs each step (2.8, 16.7 and 2.8 glucose), then the islets were incubated in KCl to release all the insulin content. Afterwards the islets were dissolved in RIPA supplemented with proteinase inhibitors. All samples were stored until use at -20 °C.

RNA isolation. Dependent on the amount of RNA, the miRNA micro kit (Qiagen) or miRNA mini kit (Qiagen) was used. The RNA isolation was carried out according to the kit manual. In addition, the optional step for the DNA degradation was performed by DNase I treatment. The RNA was eluted in 14 μL of nuclease-free water for immediate use or stored at -80 °C.

RNA amplification. If the amount of RNA was low, the RNA was amplified using the Ovation® PicoSL WTA SystemV2 (Nugen). Therefore, between 500 pg and 50 ng RNA were used and the amplification was performed according to the kit manual. Furthermore, all cDNAs have to be degraded by DNAZap to prohibit primer contaminations. Afterwards the PCR purification kit was used to purify the resulting cDNA.

Reverse transcription. The reverse transcription transcribes RNA into cDNA. For cDNA preparation the SuperScript Vilo cDNA and cDNA synthesis kit (Life Technologies and Promega respectively) was used. The cDNA synthesis was carried out according to the kit manual. Afterwards the cDNA was stored at ≥20 °C.

Quantitative PCR (qPCR). The qPCR was performed using TaqMan™ probes (Life Technologies) and 25 ng cDNA per reaction. Each reaction consisted of 4.5 µL cDNA in nuclease-free water, 5 µL TaqMan™ Advanced master mix (Life Technologies) and 0.5 µL TaqMan probe™ (Life Technologies). After sealing the 96-well plate (Life Technologies) and its centrifugation (1500 rpm, 5 min), the qPCR was performed using Viia7 (Thermo Fisher Scientific). The data was analysed using excel. The C_t-values, a point of linear slope of fluorescence, were normalized among samples, transformed to linear expression values, normalized on reference genes and on the control samples.

$$\text{Relative expression (gene)} = (2^{\text{Ct (mean genes)} - \text{Ct (gene)}}) / (2^{\text{Ct (mean references)} - \text{Ct (reference)}})$$

$$\text{Normalized expression (gene)} = \text{Relative expression (gene)} / \text{Relative expression}_{\text{control}} \text{ (gene)}$$

Cryosections. The dissected pancreas was fixed in 4% paraformaldehyde (PFA) for 2-24 hrs at 4 °C. After fixation, the tissue was cryoprotected in a sequential gradient of 10%, 30% sucrose in PBS (1-2 hrs each RT). After, the pancreas was incubated in 30% sucrose and tissue embedding medium (Leica) (1:1) O/N at 4 ºC. The pancreas was orientated in an embedding mold, frozen using dry ice and stored at -80 °C. To prepare cryosections the embedded and frozen pancreas was cut in 20 µm sections using a cryostat (Leica), mounted on a glass slide (Thermo Fisher Scientific) and dried for 10 min at RT before use or storage at -20 °C.

Sections Immunostainings. The cryosections were rehydrated by 3x washing with 1X PBS, permeabilized with 0.2% Triton X-100 in H_2O for 15 min and blocked in blocking solution (PBS, 0.1% Tween-20, 1% donkey serum, 5% FCS) for 1-2 hrs. Afterwards, the sections were incubated with the primary antibody in blocking solution O/N at 4 °C. Prior to the incubation

in secondary antibody in blocking solution the sections were rinsed 3x and washed 3x with 1X PBS. Finally after being incubated during 3-5 hrs with the 2nd antibody, the sections were stained for DAPI (1:500 in 1X PBS) for 30 min, rinsed and washed 3x with 1X PBS and mounted using or self-made Elvanol. Pictures were taken on a Leica DMI 6000 microscopy using LAS AF software.

Immunostainings of islets In contrast to cryosections, islets were transferred into a 96 well plate, fixed in 2% PFA for 15 min at 37 °C, permeabilized with 0.5% Triton X-100 in H_2O for 30 min and blocked in blocking solution (PBS, 0.2% Tween-20, 1% donkey serum, 5% FCS) for 2 hrs. Afterwards, the islets were incubated with the primary antibody in blocking solution O/N at 4 °C. Prior to the incubation in secondary antibody in blocking solution the sections were rinsed 3x and washed 3x for 10 min with 1X PBS-T. Incubation of the islet with the 2nd antibody during 3-4 hrs at RT in blocking buffer, the islets were stained for DAPI (1:500 in 1X PBS) for 30 min, rinsed and washed 3x with 1X PBS-T and mounted using self-made Elvanol on a cover slip equipped with a spacer (Life Technologies). Pictures were taken on a Leica DMI 6000 microscopy using LAS AF software.

Microscopy & Analysis The acquired images were analyzed using Leica LAS AF software and/or Imaris (Bitplane) software. Imaris was used to quantify nuclear stainings.

The **statistical analysis** was carried out using Excel or Graphpad Prism. If not otherwise indicated a two-sided and unpaired *t*-test was used. *indicated *P*-values >0.05, ** > 0.01, *** > 0.001 and **** > 0.0001.

4 Publications for dissertation

Bastidas-Ponce A*, Tritschler S*, Dony L, Scheibner K, Tarquis-Medina M, Salinno C, Schirge S, Burtscher I, Böttcher A, Theis FJ[+], Lickert H[+], Bakhti M[+]. **Comprehensive single cell mRNA profiling reveals a detailed roadmap for pancreatic endocrinogenesis.** Development. 2019 Jun 17;146(12) (*Co-first author; [+]Co-corresponding).

Summary: This paper provides a high-resolution single cell gene expression profile of the distinct pancreatic and endocrine populations during endocrinogenesis. Additionally, we identified novel signature genes for endocrine progenitor and precursors associated with cell fate. This disclosed novel markers and molecular programs that can be used to improve the *in vitro* generation of β-like cells.

Declaration of contribution: *In vivo* studies were performed primarily by me with the support of Jessica Jaki and Marta Tarquis-Medina. Moreover, organ dissection was performed with the support of Marta Tarquis-Medina. All tissue handling, immunohistochemistry and qPCR analysis were done by myself. Further, sorting of samples was performed by Katharina Scheibner. scRNAseq analysis was performed by Sophie Tritschler, Dony Leander, Ciro Salinno and Dr. Mostafa Bakhti. Figure design was done by Dr. Mostafa, Sophie Tritschler and me. Finally, the manuscript was written and editing by Dr. Mostafa Bakhti, Dr. Heiko Lickert, Sophie Tritschler and me. All the co-authors contributed on discussion and reviewing of the final manuscript.

Bastidas-Ponce A*, Roscioni SS, Burtscher I, Bader E, Sterr M, Bakhti M, Lickert H. **Foxa2 and Pdx1 cooperatively regulate postnatal maturation of pancreatic β-cells.** Mol Metab. 2017 Mar 25;6(6):524-534 (*First author).

Summary: This paper shows the functional link between Foxa2 and Pdx1 during postnatal β-cells maturation. We observed that impairment of this cooperative function results in a hyperglycemic phenotype with reduce Pdx1 expression and lose of β-cell identity and function. This revealed that failure in β-cell maturation leads to diabetes upon dysregulation of Pdx1, this patomechanism could be used to identifying further targets to regenerate β-cells.

Declaration of contribution: *In vivo* studies were performed primarily by me with the support of Sara Roscioni and Erik. Moreover, organ dissection was performed with the support of Sara Roscioni. Tissue handling, immunohistochemistry were done by myself. Meanwhile qPCR analysis by Erik Bader and Chip-seq analysis was performed by Michael Sterr. The mouse line was generated by Dr. Ingo Burtscher. Dr. Bakhti and I performed the Western Blot analysis. Figure design was done by Dr. Mostafa and me. Finally, the manuscript was written by Dr. Mostafa Bakhti, Dr. Heiko Lickert and me with editing, discussion and reviewing among all the co-authors.

5 Discussion

5.1 Analysis of the endocrine lineage development on a single cell level

Here we provided a roadmap of the gene expression profile during pancreatic endocrinogenesis on a single cell level. By using a novel Ngn3 reporter mouse line, we were capable to enrich the endocrine population and analysed distinct pancreatic (MPCs, acinar, ductal) and endocrine populations (progenitors, precursors, Fev^+ and hormone-expressing lineages) during the secondary transition. We described in a spatio-temporal high-resolution not only the molecular mechanisms that regulate endocrine formation and lineage allocation during pancreas development but also identify novel markers and pathways that define different endocrine subpopulations. These data might improve regenerative therapies by triggering endogenous regeneration of β-cells in diabetic conditions.

5.1.1 A novel endocrine reporter mouse line, Ngn3-Venus fusion

Endocrine progenitors (EPs) are characterized by the expression of the master regulatory TF Ngn3 and loss-of-function leads to failure of endocrine lineage induction (Gradwohl et al., 2000). Several reporter mouse lines have been generated to study endocrine lineage induction and segregation, however due to the Ngn3 transient expression this represents a challenge. Previously, Ngn3 reporter mouse lines were generated by knock-out/knock-in strategy (Kim et al., 2015) or by expressing a fluorescent protein under the regulation of the *Ngn3* promoter (Mellitzer et al., 2004). However, these mouse lines showed limitations due to the stability of the fluorescents proteins or the heterozygous condition which impair EPs formation (Wang et al., 2010). To overcome this, we generated a novel Ngn3-Venus fusion (NVF) reporter mouse line that accurately mirrors the transient endogenous protein expression and follows its dynamic regulation. The NVF mice allowed us to selectively isolate an enriched number of EPs during the secondary transition (E12.5-E15.5) to perform a single cell transcriptomic analysis during the endocrine formation.

5.1.2 Defining endocrine progenitors with a single cell approach

By sorting NVF^+ cells and epithelial cells (NVF^-;$EpCam^+$) and performing scRNAseq, we distinguished 8 main clusters (MPCs, tip, trunk, acinar, ductal, EPs, Fev^{high} and endocrine cells) defined by known and non-described markers during endocrinogenesis (E12.5-15.5). Additionally, we confirmed the ductal epithelium as the major contributor for the formation the $Ngn3^{low}$ EPs, as it was shown before by a lineage tracing study that used $Hnf1\beta^+$ cells (Solar et al., 2009). A sustained generation of EPs ($Ngn3^{low}$ cells) at E15.5 was detected, supporting the idea that the EP pool formation is a continues process (Bechard et al., 2016b).

An unprecedented high number of EPs was isolated by sorting NVF^+ cells, this enrichment allowed us to obtain a unique set of transient endocrine signature genes. When comparing $Ngn3^+$ EPs with non-EPs ($Ngn3^-$) 58 new signature genes for the EPs were disclosed. Among them some with already described function in EPs, such as *Amotl2* (Scavuzzo et al., 2018), *Cdkn1a* (Miyatsuka et al., 2011) and others. In addition, we revealed some genes with unknown function in endocrinogenesis, as the cell-cycle inhibitors *Gadd45a* and *Btg2* (Krentz et al., 2018) and the Notch inhibitors *Numb1* and *Hes6* and more. Assessment of their function by knocking-out these genes will provide insights into the paths for the establishment of EPs. Furthermore, this could be used to improve the *in vitro* generation of β-like cells or to trigger endogenous β-cell neogenesis in diabetic conditions.

5.1.3 Specification of endocrine cell types

Committed endocrine precursors ($Ngn3^{high}$ cells) will give rise to hormone-expressing cells; recently Fev^+ cells were reported as a novel cluster of endocrine cells during endocrinogenesis. They were found between $Ngn3^{high}$ EPs and hormone-expressing endocrine cells in mouse and human (Byrnes et al., 2018; Krentz et al., 2018; Ramond et al., 2018). In our survey, we confirmed by RNA velocity that endocrine cells acquire a Fev^{high} stage characterized by low levels of Ngn3 expression together with the expression of several early endocrine gene markers indicating their progression towards differentiated endocrine cells.

By calculating cell-to-cell distance in a Partition-based graph abstraction (PAGA) analysis we associated the fate of Ngn3^{high} EPs towards α- or β-cells and disclosed different population of EPs (Ngn3^{high}). This indicate that endocrine cell types are specified in the Ngn3^{high}-state precursor, as was described before by Desgraz et al., where they showed unipotency of EPs expressing high levels of *Ngn3* (Desgraz and Herrera, 2009). In mouse, endocrine cells are allocated in a step-wise manner and EPs are consecutively specified into α-cells, β-cells, PP-cells and δ-cells during the secondary transition (Johansson et al., 2007). In accordance, we identified in a stage-dependent manner differential expression of EP-signature genes that were related to the allocation between hormone-expressing cells. This included some non-described genes during endocrine cells segregation (*Neurod2*, *Steap1*, *Upk3bl*, *Gng13* and *Gm8773*). Furthermore, we described in early stages (E12.5 & E13.5) that Ngn3^{high} EPs expressed *Steap1*, *Gng13* and *Gm8773* and were strongly connected towards α-cell fate, meanwhile in later stages (E14.5 & E15.5) Ngn3^{high} EPs are expressing *Neurod2* and *Upk3bl* and generate β-cells.

5.2 Analysis of the interconnection between Foxa2 and Pdx1 activity during β-cell development and function

Here we show that Pdx1 and Foxa2 are not only crucial TFs for the adult function of β-cells but also have a cooperative function during β-cell maturation. By generating and using a double knock-in reporter ($FVFPBF^{DHom}$) mouse, we evaluated the functional relationship between these TFs and observed that $FVFPBF^{DHom}$ males developed hyperglycemia due to reduced Pdx1 levels in juvenile and adult islets. In addition, we detected impairment in islet architecture, reduction in the β-cell population and loss of endocrine cellular identity at weaning age. Altogether, these data disclosed a genetic interaction between *Pdx1* and *Foxa2* required to sustain functional mature β-cell identity.

5.2.1 Pdx1-BFP fusion as a novel pancreatic reporter mouse line

Pdx1 determinates pancreas development (Ahlgren et al., 1998) and function of adult β-cells (Gao et al., 2014). In order to dissect its function several reporter mouse lines and cell lines (i.e embryonic stem cells (ESCs), induced pluripotent stem cells (IPSCs)) have been generated and widely used. Here, we generated a novel Pdx1-BFP (PBF) reporter mouse line, which accurately reflects the spatio-temporal protein expression and regulation of the endogenous Pdx1 protein. Previously, other Pdx1 reporter mouse lines that were generated replaced the open reading frame of Pdx1 on one allele resulting in heterozygous mouse that suffers the impairments in pancreas development, generating MODY4 (Offield et al., 1996). Therefore, all knock-in/knock-out reporter mice that had been generated were used as heterozygous (Holland et al., 2005; Potter et al., 2012) and exhibit an altered endocrine formation and differentiation (Wang et al., 2010). To overcome these limitations, different strategies have been employed to analyze the activity of Pdx1, as the use of a secretory luciferase reporter under the control of the Pdx1 promoter (Nishimura et al., 2013) using an indirect measurement of Pdx1 activity with the secreted Gaussia princeps luciferase (GLuc). Also, constitutive and time-specific conditional Pdx1 reporter mouse lines have been designed by taking advantage of the Cre-LoxP system and the mTmG reporter mouse model (Muzumdar et al., 2007). This Pdx1-Cre x mTmG reporter mouse line (Snyder et al., 2013) represent a powerful tool for lineage tracing of $Pdx1^{+}$ cells although they lack the capacity to

follow the endogenous dynamic Pdx1 expression in a spatio-temporal manner (Miyazaki et al., 2016; Wu et al., 1997). Thus, we generated a new transgenic mouse line by fusing the blue fluorescent protein (BFP) to the Pdx1 gene. In contrast to previous Pdx1 reporter mouse lines, our Pdx1-BFP (PBF) shows an accurate and comparable expression matching the endogenous Pdx1 and PBF during the whole embryonic pancreas development and a specific PBF expression in adult β-cells. Additionally, homozygous PBF mice showed no detectable endocrine phenotype, if not a modest influence on expression levels and proper glucose homeostasis in the adult state. These properties will allow us to isolate at different developmental stages (MPCs, EPs, β-cells) $Pdx1^{+}$ cells to then perform a deeper analysis of their expression profile. Therefore, understanding the regulatory transitions on $Pdx1^{+}$ cells in a stage-dependent manner with a single cell or bulk approach will disclose lineage relationships and molecular changes during endocrinogenesis.

5.2.2 FVFPBFDHom a dimorphic diabetes mouse model

Despite the requirement of Pdx1 expression and the interaction of Foxa1/2 with the Pdx1 enhancer during development (Gao et al., 2008), no obvious defect in embryonic pancreas development was observed. Pdx1 and Foxa2 are required to maintain the adult β-cell function, both independently from each other (Gao et al., 2014a; Li et al., 2005; Gao et al., 2010) as well as in combination exerting a synergistic effect (Shih et al., 2013). To investigate Pdx1 and Foxa2 expression domains and their functional interconnection in adult islets, we generated the FVFPBF double homozygous ($FVFPBF^{DHom}$) reporter mice by crossing FVF (Burtscher et al., 2013) and PBF mouse lines. In FVFPBF mice both FVF and PBF proteins mirror the expression of endogenous Foxa2 and Pdx1, respectively.

However, a dimorphic phenotype was observed in $FVFPBF^{DHom}$ mice, males develop hyperglycemia by weaning age, whereas females develop gestational diabetes. Recently, difference in susceptibility to develop diabetes has previously been shown to be dependent on sex in mice and human (Vital et al., 2006). We found lower blood glucose levels in females compared to male littermates disclosing a protective phenotype. Sex hormones, particularly estrogen, have been place as the reason of the development of sexual dimorphism in diverse diseases including diabetes (Alonso-Magdalena et al., 2008; Root-Bernstein et al., 2014; Yuchi et al., 2015). Recently, it was shown that the sexual dimorphism in the develop of liver cancer depends on Foxa1/2 interactions with the androgen and estrogen receptors (Li et al., 2012). Important to note, we also found the estrogen-signaling pathway to be highly regulated

by Foxa2 and Pdx1 binding. However, how Foxa2 and Pdx1 regulate each other and their combinatorial effect on sex hormones regulation in islets and/or its potential role on the onset and in the development of diabetes require further investigation.

5.2.3 Reduction of Pdx1 expression during β-cell maturation leads to hyperglycemia

FVFPBF^{DHom} mice displayed reduced levels of Pdx1 expression. Recently, Spaeth et al., described a hyperglycemic phenotype during weaning age due to the reduced levels of Pdx1 by the disruption of the autoregulatory loop of Pdx1 in its cis-regulatory elements Area IV (Spaeth et al., 2017). It has been shown that by binding to *cis*-regulatory elements (Area I and IV), Pdx1 regulates its own expression through an autoregulatory positive feedback loop (Gerrish et al., 2001; Gerrish et al., 2004; Marshak et al., 2000). Thus, we speculate that the fusion of Venus to Foxa2 and BFP to Pdx1 in FVFPBF^{DHom} mice perhaps reduces DNA binding or cooperative binding between the TFs and prevents that cofactors co-bind to Pdx1 resulting in a reduction of the levels of Pdx1 expression, which leads to develop a hyperglycemic condition.

Heterozygous mice for both Pdx1 and Foxa2 have altered β-cell identity with severe consequences on insulin secretion and blood glucose levels (Shih et al., 2013). Moreover, both Foxa2 and Pdx1 levels appeared to be reduced in dedifferentiated β-cells, as in the case of diabetes models (Russ et al., 2011; Wang et al., 2014b). Furthermore, it was recently shown that in T2D GSK3 downregulates Pdx1 expression by regulating its phosphorylation which results in reduced levels of Glut2 and insulin expression and secretion (Sacco et al., 2019). High blood glucose levels, reduced expression of Pdx1 and Glut2 together with the impaired insulin secretion observed in FVFPBF^{DHom} males support the requirement of a tight regulation of Pdx1 expression for the maintenance of functional β-cell mass.

5.2.4 Defective maturation and β-cell identity in FVFPBFDHom mice

Endocrine cells acquire their mature functional phenotype in the postnatal stage. Mature cells are characterized by the expression of a set of genes that confine identity features, secretory capacity and a regulated-response upon glucose stimulation (Bonner-Weir et al., 2016). Mature β-cells are characterized by the expression of genes such as Nkx2.2 (Doyle and Sussel, 2007), MafA (Kaneto and Matsuoka, 2015; Nishimura et al., 2015), Flattop (Bader et al., 2016) and Ucn3 (Blum et al., 2012). Reduce levels of Ucn3 were observed in FVFPBF^{DHom} mice, indicating a defect in the maturation process, where the few cells that acquired Ucn3 expression failed in maintaining and preserving their mature (β-cell) identity. This might imply a regulatory function of Foxa2 or Pdx1a independently or cooperatively on the Ucn3 gene; however, a deeper analysis of this possible regulatory link is required.

In addition, we investigated whether the metabolic changed due to the dietary switch at weaning age (Stolovich-Rain et al., 2015) could trigger the hyperglycemic condition in FVFPBF^{DHom} male mice. When we compared P18 pre-weaned (high carbohydrate chow) mice with high-fat milk diet both sacrifice at P25, no difference between the dietary conditions was observed, exhibiting similarly high blood glucose levels. This indicated a genetic predisposition in FVFPBF^{DHom} mice to develop diabetes rather than an effect of the environmental factors.

We also found polyhormonal endocrine cells among the FVFPBF^{DHom} islets. This could be explained by reduced levels of Pdx1 which has been shown to be required in adult islets to block the α-cell program (Ahlgren et al., 1998; Gao et al., 2014). Furthermore, specific deletion of Pdx1 in β-cells by Ins-Cre activity leads to hyperglycemia due to the reprograming of these cells towards α-cells (Gao et al., 2014). Supporting this notion it has been shown that upon exogenous Pdx1 expression in the embryonic endocrine progenitors perinatal α-cells convert into β-cells passing through a polyhormonal (glucagon-insulin) state (Yang et al., 2011). In addition, Pdx1 suppresses *MafB* and *glucagon* gene expression in β-cells. Then, in β-cells with lower levels of Pdx1 expression, this inhibitory function is lost and α-cell program gets upregulated (Gao et al., 2014). The observation of increased levels of *MafB* in

the FVFPBF^{DHom} mice, suggests that β-cells transdifferentiate towards α-cells partially through derepression of this gene due to low expression levels of Pdx1. In addition, the polyhormonal phenotype could be related to the glucotoxic condition generating a plastic environment where endocrine cells lose their identities and particularly β-cells dedifferentiate into a more embryonic like state (Bonner-Weir et al., 2016). Supporting these results, similar polyhormonal β-cells have been described upon deletion of Nkx2.2, a regulator of β-cell plasticity (Gutiérrez et al., 2017), thus revealing a plasticity feature of endocrine cells which could be employed to trigger differentiation towards β-cell lineage in regenerative therapies. Thus, the impairment in β-cell maturation together with the hyperglycemia phenotype in FVFPBF^{DHom} mice likely leads to reduced numbers of β-cell, to the loss of β-cell identity and to transdifferentiation towards other endocrine cell types, mainly α-cells. Yet, it is not clear whether these polyhormonal cells result from a transdifferentiation process as it has been described in juvenile mice when β-cells are completely ablated (Chakravarthy et al., 2017) or if the hyperglycemic condition modified the plasticity status of the β-cells (Bonner-Weir et al., 2016; Gutiérrez et al., 2017).

FVFPBF^{DHom} mice showed disrupted islet architecture, with loss of cell-to-cell adhesion compared to the control mice. An altered islet architecture is already found in heterozygous mice for both Pdx1 and Foxa2 (Shih et al., 2013) and it has been shown that islet architecture impacts endocrine cell maturation (Bader et al., 2016; Roscioni et al., 2016b). Additionally, it has been shown that cell adhesion molecules as E-Cadherin and β-catenin are required to maintain the islet structure and proper secretory function in β-cells (Hodgkin et al., 2007; Rogers et al., 2018; Sorrenson et al., 2016). During pancreas development, in has been shown that Pdx1 is not only required to regulate E-Cadherin expression but also its maintenance (Marty-Santos and Cleaver, 2016). In addition, ChIP-Seq data have revealed that both E-Cadherin and β-catenin promoters are bound by Pdx1 in β-cells (Khoo et al., 2012; Teo et al., 2015). Recently, it was revealed that reduced levels of β-catenin result in disruption of intracellular actin remodeling and thus a dysregulation in insulin secretion (Sorrenson et al., 2016). The reduced expression levels of Pdx1 in FVFPBF^{DHom} mice and its regulatory link with E-Cadherin and β-catenin might therefore explain the observed disruption of islet architecture and defect in insulin secretion.

5.2.5 Cooperative regulation of Pdx1 and Foxa2 in mature β-cells

Foxa2 and Pdx1 share important functions, such as regulation of insulin production and secretion as well as modulation of TFs (Gao et al., 2008; Hani, 1999; Wang et al., 2002). In addition, Foxa2 has been shown to drive Pdx1 expression also in differentiated β-cells (Lee et al., 2002b). By ChIP-seq analysis we identified 5976 loci to be co-occupied by both Foxa2 and Pdx1 in the islets. Including genes involved in β-cell maturation and function such as *MafA*, *Ins1*, and *Slc2a2 (Glut2)*, this explained their downregulation in the FVFPBF^{DHom} islets. Consequently, this suggested that due to the steric hindrance of the fluorescent tag the correct co-binding of Foxa2 and Pdx1 is restricted. Remarkably, a similar cooperatively function of FOXA2 and PDX1 has been identified in human. For example, in hESC-derived pancreatic progenitors they bind to enhancer regions of the *PTF1A* gene and it has been shown that this binding can be abolished by occurring mutations, thus resulting in pancreatic agenesis (Weedon et al., 2013).

6 References

Aguayo-Mazzucato, C., Koh, A., El Khattabi, I., Li, W.C., Toschi, E., Jermendy, A., Juhl, K., Mao, K., Weir, G.C., Sharma, A., et al. (2011). Mafa expression enhances glucose-responsive insulin secretion in neonatal rat beta cells. Diabetologia.

Ahlgren, U., Jonsson, J., Edlund, H., Alpert, S., Hanahan, D., Teitelman, G., Ang, S.-L., Wierda, A., Wong, D., Stevens, K.A., et al. (1996). The morphogenesis of the pancreatic mesenchyme is uncoupled from that of the pancreatic epithelium in IPF1/PDX1-deficient mice. Development.

Ahlgren, U., Jonsson, J., Jonsson, L., Simu, K., and Edlund, H. (1998). β-cell-specific inactivation of the mouse Ipf1/Pdx1 gene results in loss of the β-cell phenotype and maturity onset diabetes. Genes Dev.

Alonso-Magdalena, P., Ropero, A.B., Carrera, M.P., Cederroth, C.R., Baquié, M., Gauthier, B.R., Nef, S., Stefani, E., and Nadal, A. (2008). Pancreatic insulin content regulation by the Estrogen receptor ERα. PLoS One *3*.

Anik, A., Çatli, G., Abaci, A., and Böber, E. (2015). Maturity-onset diabetes of the young (MODY): An update. J. Pediatr. Endocrinol. Metab.

Apelqvist, A. (1999). Notch signalling controls pancreatic cell differentiation. Nature *400*, 877–881.

Apelqvist, Å., Li, H., Sommer, L., Beatus, P., Anderson, D.J., Honjo, T., Hrabě De Angelis, M., Lendahl, U., and Edlund, H. (1999). Notch signalling controls pancreatic cell differentiation. Nature.

Arda, H.E., Benitez, C.M., and Kim, S.K. (2013). Gene regulatory networks governing pancreas development. Dev. Cell.

Artner, I., Blanchi, B., Raum, J.C., Guo, M., Kaneko, T., Cordes, S., Sieweke, M., and Stein, R. (2007). MafB is required for islet beta cell maturation. Proc. Natl. Acad. Sci.

Asplund, K., Westman, S., and Hellerström, C. (1969). Glucose stimulation of insulin secretion from the isolated pancreas of foetal and newborn rats. Diabetologia *5*, 260–262.

Bader, E., Migliorini, A., Gegg, M., Moruzzi, N., Gerdes, J., Roscioni, S.S., Bakhti, M., Brandl, E., Irmler, M., Beckers, J., et al. (2016). Identification of proliferative and mature β-cells in the islets of Langerhans. Nature *535*, 430–434.

Bastidas-Ponce, A., Scheibner, K., Lickert, H., and Bakhti, M. (2017). Cellular and molecular mechanisms coordinating pancreas development. Development.

Bechard, M.E., Bankaitis, E.D., Hipkens, S.B., Ustione, A., Piston, D.W., Yang, Y.P., Magnuson, M.A., and Wright, C.V.E. (2016a). Precommitment low-level neurog3 expression defines a long-lived mitotic endocrine-biased progenitor pool that drives production of endocrine-committed cells. Genes Dev. *30*, 1852–1865.

Bechard, M.E., Bankaitis, E.D., Hipkens, S.B., Ustione, A., Piston, D.W., Yang, Y.P., Magnuson, M.A., and Wright, C.V.E. (2016b). Precommitment low-level neurog3 expression defines a long-lived mitotic endocrine-biased progenitor pool that drives production of endocrine-committed cells. Genes

Dev. *30*, 1852–1865.

Bliss, C.R., and Sharp, G.W. (1992). Glucose-induced insulin release in islets of young rats: time-dependent potentiation and effects of 2-bromostearate. Am. J. Physiol. *263*, E890-6.

Blum, B., Hrvatin, S., Schuetz, C., Bonal, C., Rezania, A., and Melton, D. a (2012). Functional beta-cell maturation is marked by an increased glucose threshold and by expression of urocortin 3. Nat. Biotechnol. *30*, 261–264.

Bonner-weir, S., Toschi, E., Inada, A., Reitz, P., Sy, F., Aye, T., Sharma, A., Toschi, E., Inada, A., Reitz, P., et al. (2004). The pancreatic ductal epithelium serves as a potential pool of progenitor cells. Pediatr. Diabetes.

Bonner-Weir, S., Baxter, L.A., Schuppin, G.T., and Smith, F.E. (1993). A second pathway for regeneration of adult exocrine and endocrine pancreas: A possible recapitulation of embryonic development. Diabetes.

Bonner-Weir, S., Aguayo-Mazzucato, C., and Weir, G.C. (2016). Dynamic development of the pancreas from birth to adulthood. Ups. J. Med. Sci. *121*, 155–158.

Bramswig, N.C., and Kaestner, K.H. (2011). Transcriptional regulation of α-cell differentiation. Diabetes, Obes. Metab.

Brereton, M.F., Iberl, M., Shimomura, K., Zhang, Q., Adriaenssens, A.E., Proks, P., Spiliotis, I.I., Dace, W., Mattis, K.K., Ramracheya, R., et al. (2014). Reversible changes in pancreatic islet structure and function produced by elevated blood glucose. Nat. Commun.

Briant, L., Salehi, A., Vergari, E., Zhang, Q., and Rorsman, P. (2016). Glucagon secretion from pancreatic α-cells. Ups. J. Med. Sci.

Brissova, M. (2005). Assessment of Human Pancreatic Islet Architecture and Composition by Laser Scanning Confocal Microscopy. J. Histochem. Cytochem. *53*, 1087–1097.

Brissova, M., Shiota, M., Nicholson, W.E., Gannon, M., Knobel, S.M., Piston, D.W., Wright, C.V.E., and Powers, A.C. (2002). Reduction in pancreatic transcription factor PDX-1 impairs glucose-stimulated insulin secretion. J. Biol. Chem.

Burlison, J.S., Long, Q., Fujitani, Y., Wright, C.V.E., and Magnuson, M.A. (2008). Pdx-1 and Ptf1a concurrently determine fate specification of pancreatic multipotent progenitor cells. Dev. Biol.

Burtscher, I., Barkey, W., and Lickert, H. (2013). Foxa2-venus fusion reporter mouse line allows live-cell analysis of endoderm-derived organ formation. Genesis *51*, 596–604.

Byrnes, L.E., Wong, D.M., Subramaniam, M., Meyer, N.P., Gilchrist, C.L., Knox, S.M., Tward, A.D., Ye, C.J., and Sneddon, J.B. (2018). Lineage dynamics of murine pancreatic development at single-cell resolution. Nat. Commun. *9*, 1–17.

Cabrera, O., Berman, D.M., Kenyon, N.S., Ricordi, C., Berggren, P.-O., and Caicedo, A. (2006). The unique cytoarchitecture of human pancreatic islets has implications for islet cell function. Proc. Natl. Acad. Sci. U. S. A. *103*, 2334–2339.

Chakravarthy, H., Gu, X., Enge, M., Dai, X., Wang, Y., Damond, N., Downie, C., Liu, K., Wang, J., Xing, Y., et al. (2017). Converting Adult Pancreatic Islet α Cells into β Cells by Targeting Both

Dnmt1 and Arx. Cell Metab.

Chera, S., Baronnier, D., Ghila, L., Cigliola, V., Jensen, J.N., Gu, G., Furuyama, K., Thorel, F., Gribble, F.M., Reimann, F., et al. (2014). Diabetes recovery by age-dependent conversion of pancreatic δ-cells into insulin producers. Nature *514*, 503–507.

Cinti, F., Bouchi, R., Kim-Muller, J.Y., Ohmura, Y., Sandoval, P.R., Masini, M., Marselli, L., Suleiman, M., Ratner, L.E., Marchetti, P., et al. (2016). Evidence of β-cell dedifferentiation in human type 2 diabetes. J. Clin. Endocrinol. Metab.

Collombat, P., Mansouri, A., Hecksher-sørensen, J., Serup, P., Krull, J., Gradwohl, G., and Gruss, P. (2003). Opposing actions of Arx and Pax4 in endocrine pancreas development Opposing actions of Arx and Pax4 in endocrine pancreas development. *4*, 2591–2603.

Collombat, P., Hecksher-Sørensen, J., Krull, J., Berger, J., Riedel, D., Herrera, P.L., Serup, P., and Mansouri, A. (2007). Embryonic endocrine pancreas and mature β cells acquire α and PP cell phenotypes upon Arx misexpression. J. Clin. Invest.

Conrad, E., Dai, C., Spaeth, J., Guo, M., Cyphert, H.A., Scoville, D., Carroll, J., Yu, W.-M., Goodrich, L. V., Harlan, D.M., et al. (2015). The MAFB transcription factor impacts islet α-cell function in rodents and represents a unique signature of primate islet β-cells. Am. J. Physiol. - Endocrinol. Metab.

Dabelea, D. (2007). The predisposition to obesity and diabetes in offspring of diabetic mothers. Diabetes Care.

Dahan, T., Ziv, O., Horwitz, E., Zemmour, H., Lavi, J., Swisa, A., Leibowitz, G., Ashcroft, F.M., Veld, P.I. t., Glaser, B., et al. (2017). Pancreatic β-Cells express the fetal islet hormone gastrin in rodent and human diabetes. Diabetes.

Dahl, U., Sjødin, a, and Semb, H. (1996). Cadherins regulate aggregation of pancreatic beta-cells in vivo. Development *122*, 2895–2902.

Damm, P. (2009). Future risk of diabetes in mother and child after gestational diabetes mellitus. Int. J. Gynecol. Obstet.

Delaspre, F., Beer, R.L., Rovira, M., Huang, W., Wang, G., Gee, S., Del Carmen Vitery, M., Wheelan, S.J., and Parsons, M.J. (2015). Centroacinar cells are progenitors that contribute to endocrine pancreas regeneration. Diabetes.

Desgraz, R., and Herrera, P.L. (2009). Pancreatic neurogenin 3-expressing cells are unipotent islet precursors. Development *136*, 3567–3574.

Dezaki, K. (2013). Ghrelin function in insulin release and glucose metabolism. Endocr. Dev. *25*, 135–143.

Dor, Y., Brown, J., Martinez, O.I., and Melton, D.A. (2004). Adult pancreatic β-cells are formed by self-duplication rather than stem-cell differentiation. Nature.

Doyle, M.J., and Sussel, L. (2007). Nkx2.2 regulates β-cell function in the mature islet. Diabetes.

Fajans, S.S., Bell, G.I., and Polonsky, K.S. (2001). Molecular Mechanisms and Clinical Pathophysiology of Maturity-Onset Diabetes of the Young. N. Engl. J. Med.

Finegood, D.T., Scaglia, L., and Bonner-Weir, S. (1995). Dynamics of ??-cell mass in the growing rat pancreas: Estimation with a simple mathematical model. Diabetes.

Fujikura, J., Hosoda, K., Iwakura, H., Tomita, T., Noguchi, M., Masuzaki, H., Tanigaki, K., Yabe, D., Honjo, T., and Nakao, K. (2006). Notch/Rbp-j signaling prevents premature endocrine and ductal cell differentiation in the pancreas. Cell Metab.

Gao, N., White, P., Doliba, N., Golson, M.L., Matschinsky, F.M., and Kaestner, K.H. (2007). Foxa2 Controls Vesicle Docking and Insulin Secretion in Mature ?? Cells. Cell Metab. *6*, 267–279.

Gao, N., LeLay, J., Vatamaniuk, M.Z., Rieck, S., Friedman, J.R., and Kaestner, K.H. (2008). Dynamic regulation of Pdx1 enhancers by Foxa1 and Foxa2 is essential for pancreas development. Genes Dev.

Gao, N., Le Lay, J., Qin, W., Doliba, N., Schug, J., Fox, A.J., Smirnova, O., Matschinsky, F.M., and Kaestner, K.H. (2010). Foxa1 and Foxa2 maintain the metabolic and secretory features of the mature beta-cell. Mol. Endocrinol. (Baltimore, Md) *24*, 1594–1604.

Gao, T., McKenna, B., Li, C., Reichert, M., Nguyen, J., Singh, T., Yang, C., Pannikar, A., Doliba, N., Zhang, T., et al. (2014). Pdx1 maintains β cell identity and function by repressing an α cell program. Cell Metab.

Gaulton, K.J., Ferreira, T., Lee, Y., Raimondo, A., Mägi, R., Reschen, M.E., Mahajan, A., Locke, A., William Rayner, N., Robertson, N., et al. (2015). Genetic fine mapping and genomic annotation defines causal mechanisms at type 2 diabetes susceptibility loci. Nat. Genet. *47*, 1415–1425.

Gerrish, K., Cissell, M. a, and Stein, R. (2001). The role of hepatic nuclear factor 1 alpha and PDX-1 in transcriptional regulation of the pdx-1 gene. J. Biol. Chem. *276*, 47775–47784.

Gerrish, K., Van Velkinburgh, J.C., and Stein, R. (2004). Conserved transcriptional regulatory domains of the pdx-1 gene. Mol. Endocrinol. *18*, 533–548.

Gouzi, M., Kim, Y.H., Katsumoto, K., Johansson, K., and Grapin-Botton, A. (2011). Neurogenin3 initiates stepwise delamination of differentiating endocrine cells during pancreas development. Dev. Dyn.

Gradwohl, G., Dierich, a, LeMeur, M., and Guillemot, F. (2000). Neurogenin3 Is Required for the Development of the Four Endocrine Cell Lineages of the Pancreas. Proc. Natl. Acad. Sci. U. S. A. *97*, 1607–1611.

Grasso, S., Saporito, N., Messina, A., and Reitano, G. (1968). Plasma insulin, glucose and free fatty acid (FFA) response to various stimuli in the premature infant. Diabetes *17*, 306.

Gregg, B.E., Moore, P.C., Demozay, D., Hall, B.A., Li, M., Husain, A., Wright, A.J., Atkinson, M.A., and Rhodes, C.J. (2012). Formation of a human β-cell population within pancreatic islets is set early in life. J. Clin. Endocrinol. Metab.

Gu, C., Stein, G.H., Pan, N., Goebbels, S., Hörnberg, H., Nave, K.A., Herrera, P., White, P., Kaestner, K.H., Sussel, L., et al. (2010). Pancreatic β Cells Require NeuroD to Achieve and Maintain Functional Maturity. Cell Metab.

Gu, G., Dubauskaite, J., and Melton, D.A. (2002). Direct evidence for the pancreatic lineage: NGN3+ cells are islet progenitors and are distinct from duct progenitors. Development.

Guo, S., Dai, C., Guo, M., Taylor, B., Harmon, J.S., Sander, M., Robertson, R.P., Powers, A.C., and Stein, R. (2013). Inactivation of specific β cell transcription factors in type 2 diabetes. J. Clin. Invest. *123*, 3305–3316.

Gutiérrez, G.D., Bender, A.S., Cirulli, V., Mastracci, T.L., Kelly, S.M., Tsirigos, A., Kaestner, K.H., and Sussel, L. (2017). Pancreatic β cell identity requires continual repression of non-β cell programs. J. Clin. Invest.

Hald, J., Hjorth, J.P., German, M.S., Madsen, O.D., Serup, P., and Jensen, J. (2003). Activated Notch1 prevents differentiation of pancreatic acinar cells and attenuate endocrine development. Dev. Biol.

Hani, E.H. (1999). Defective mutations in the insulin promoter factor-1 (IPF-1) gene in late-onset type 2 diabetes mellitus. J. Clin. Invest. 104, R41-R48 *104*, R41–R48.

Hart, A., Papadopoulou, S., and Edlund, H. (2003). Fgf10 maintains notch activation, stimulates proliferation, and blocks differentiation of pancreatic epithelial cells. Dev. Dyn.

Hauge-Evans, A.C., King, A.J., Carmignac, D., Richardson, C.C., Robinson, I.C.A.F., Low, M.J., Christie, M.R., Persaud, S.J., and Jones, P.M. (2009). Somatostatin secreted by islet δ-cells fulfills multipleRoles as a paracrine regulator of islet function. Diabetes.

Herrera, P.L., Huarte, J., Sanvito, F., Meda, P., Orci, L., and Vassalli, J.D. (1991). Embryogenesis of the murine endocrine pancreas; early expression of pancreatic polypeptide gene. Development.

Hodgkin, M.N., Rogers, G.J., and Squires, P.E. (2007). Colocalization between β-catenin and insulin suggests a novel role for the adherens junction in β-cell function [6]. Pancreas.

Hole, R.L., Pian-Smith, M.C., and Sharp, G.W. (1988). Development of the biphasic response to glucose in fetal and neonatal rat pancreas. Am. J. Physiol. *254*, E167-74.

Holland, A.M., Go, L.J., Naselli, G., MacDonald, R.J., and Harrison, L.C. (2005). Conditional Expression Demonstrates the Role of the Maintenance and Regeneration of {b}-Cells in the Adult. Diabetes *54*, 2586–2595.

Islam, M.S. (2010). The islets of Langerhans.

Jain, R., and Lammert, E. (2009). Cell-cell interactions in the endocrine pancreas. Diabetes. Obes. Metab. *11 Suppl 4*, 159–167.

Jensen, J. (2004). Gene Regulatory Factors in Pancreatic Development. Dev. Dyn.

Jensen, J., Heller, R.S., Funder-Nielsen, T., Pedersen, E.E., Lindsell, C., Weinmaster, G., Madsen, O.D., and Serup, P. (2000a). Independent development of pancreatic and β-cells from Neurogenin3-expressing precursors: A role for the notch pathway in repression of premature differentiation. Diabetes.

Jensen, J., Pedersen, E.E., Galante, P., Hald, J., Heller, R.S., Ishibashi, M., Kageyama, R., Guillemot, F., Serup, P., and Madsen, O.D. (2000b). Control of endodermal endocrine development by Hes-1. Nat. Genet. *24*, 36–44.

Johansson, K.A., Dursun, U., Jordan, N., Gu, G., Beermann, F., Gradwohl, G., and Grapin-Botton, A. (2007). Temporal Control of Neurogenin3 Activity in Pancreas Progenitors Reveals Competence Windows for the Generation of Different Endocrine Cell Types. Dev. Cell *12*, 457–465.

Johnson, J.D., Ahmed, N.T., Luciani, D.S., Han, Z., Tran, H., Fujita, J., Misler, S., Edlund, H., and Polonsky, K.S. (2003). Increased islet apoptosis in Pdx1+/- mice. J. Clin. Invest. *111*, 1147–1160.

Jonas, J.C., Sharma, A., Hasenkamp, W., Ilkova, H., Patanè, G., Laybutt, R., Bonner-Weir, S., and Weir, G.C. (1999). Chronic hyperglycemia triggers loss of pancreatic beta cell differentiation in an animal model of diabetes. J. Biol. Chem. *274*, 14112–14121.

Jonsson, J., Carlsson, L., Edlund, T., and Edlund, H. (1994). Insulin-promoter-factor 1 is required for pancreas development in mice. Nature.

Kaestner, K.H. (2010). The FoxA factors in organogenesis and differentiation. Curr. Opin. Genet. Dev.

Kahn, S.E., Hull, R.L., and Utzschneider, K.M. (2006). Mechanisms linking obesity to insulin resistance and type 2 diabetes. Nature *444*, 840–846.

Kaneto, H., and Matsuoka, T.A. (2015). Role of pancreatic transcription factors in maintenance of mature ??-cell function. Int. J. Mol. Sci. *16*, 6281–6297.

Kanno, T., Göpel, S.O., Rorsman, P., and Wakui, M. (2002). Cellular function in multicellular system for hormone-secretion: Electrophysiological aspect of studies on α-, β- and δ-cells of the pancreatic islet. Neurosci. Res. *42*, 79–90.

Katsuta, H., Aguayo-Mazzucato, C., Katsuta, R., Akashi, T., Hollister-Lock, J., Sharma, A.J., Bonner-Weir, S., and Weir, G.C. (2012). Subpopulations of GFP-marked mouse pancreatic ??-cells differ in size, granularity, and insulin secretion. Endocrinology *153*, 5180–5187.

Kesavan, G., Sand, F.W., Greiner, T.U., Johansson, J.K., Kobberup, S., Wu, X., Brakebusch, C., and Semb, H. (2009). Cdc42-mediated tubulogenesis controls cell specification. Cell *139*, 791–801.

Khoo, C., Yang, J., Weinrott, S.A., Kaestner, K.H., Naji, A., Schug, J., and Stoffers, D.A. (2012). Research Resource: The Pdx1 Cistrome of Pancreatic Islets. Mol. Endocrinol. (Baltimore, Md) *26*, 521–533.

Kim, A., Miller, K., Jo, J., Kilimnik, G., Wojcik, P., and Hara, M. (2009). Islet architecture: A comparative study. Islets *1*, 129–136.

Kim, Y.H., Larsen, H.L., Rué, P., Lemaire, L.A., Ferrer, J., and Grapin-Botton, A. (2015). Cell Cycle–Dependent Differentiation Dynamics Balances Growth and Endocrine Differentiation in the Pancreas. PLoS Biol. *13*, 1–25.

Klara Feldman, R., Tieu, R.S., and Yasumura, L. (2016). Gestational diabetes screening the international association of the diabetes and pregnancy study groups compared with carpenter-coustan screening. Obstet. Gynecol.

Kojima, S., Ueno, N., Asakawa, A., Sagiyama, K., Naruo, T., Mizuno, S., and Inui, A. (2007). A role for pancreatic polypeptide in feeding and body weight regulation. Peptides *28*, 459–463.

Kopp, J.L., Dubois, C.L., Schaffer, A.E., Hao, E., Shih, H.P., Seymour, P.A., Ma, J., and Sander, M. (2011). Sox9+ ductal cells are multipotent progenitors throughout development but do not produce new endocrine cells in the normal or injured adult pancreas. Development.

Krapp, A., Knöfler, M., Ledermann, B., Bürki, K., Berney, C., Zoerkler, N., Hagenbüchle, O., and

Wellauer, P.K. (1998). The bHLH protein PTF1-p48 is essential for the formation of the exocrine and the correct spatial organization of the endocrine pancreas. Genes Dev.

Krentz, N.A.J., Xu, E.E., Lynn, F.C., Sasaki, S., Lee, M.Y.Y., Maslova, A., and Sproul, S.L.J. (2018). Single-Cell Transcriptome Profiling of Mouse and hESC-Derived Pancreatic Progenitors. Stem Cell Reports *11*, 1551–1564.

Laybutt, D.R., Glandt, M., Xu, G., Ahn, Y.B., Trivedi, N., Bonner-Weir, S., and Weir, G.C. (2003). Critical reduction β-cell mass results in two distinct outcomes over time. Adaptation with impaired glucose tolerance or decompensated diabetes. J. Biol. Chem.

Lee, C.S., Sund, N.J., Vatamaniuk, M.Z., Matschinsky, F.M., Stoffers, D.A., and Kaestner, K.H. (2002a). Foxa2 controls Pdx1 gene expression in pancreatic β-cells in vivo. Diabetes.

Lee, C.S., Sund, N.J., Vatamaniuk, M.Z., Matschinsky, F.M., Stoffers, D.A., and Kaestner, K.H. (2002b). Foxa 2. *51*.

Lee, J.C., Smith, S.B., Watada, H., Lin, J., Scheel, D., Wang, J., Mirmira, R.G., and German, M.S. (2001). Regulation of the pancreatic pro-endocrine gene neurogenin3. Diabetes *50*, 928–936.

Li, K., Zhu, S., Russ, H.A., Xu, S., Xu, T., Zhang, Y., Ma, T., Hebrok, M., and Ding, S. (2014). Small molecules facilitate the reprogramming of mouse fibroblasts into pancreatic lineages. Cell Stem Cell *14*, 228–236.

Li, Y., Cao, X., Li, L.X., Brubaker, P.L., Edlund, H., and Drucker, D.J. (2005). β-Cell Pdx1 expression is essential for the glucoregulatory, proliferative, and cytoprotective actions of glucagon-like peptide-1. Diabetes.

Li, Z., Tuteja, G., Schug, J., and Kaestner, K.H. (2012). Foxa1 and Foxa2 are essential for sexual dimorphism in liver cancer. Cell *148*, 72–83.

Lin, T.M., and Chance, R.E. (1974). Candidate hormones of the gut. VI. Bovine pancreatic polypeptide (BPP) and avian pancreatic polypeptide (APP). Gastroenterology *67*, 737–738.

Linnemann, A.K., Baan, M., and Davis, D.B. (2014). Pancreatic -Cell Proliferation in Obesity. Adv. Nutr. An Int. Rev. J.

Löf-Öhlin, Z.M., Nyeng, P., Bechard, M.E., Hess, K., Bankaitis, E., Greiner, T.U., Ameri, J., Wright, C. V., and Semb, H. (2017). EGFR signalling controls cellular fate and pancreatic organogenesis by regulating apicobasal polarity. Nat. Cell Biol.

Mahajan, A., Go, M.J., Zhang, W., Below, J.E., Gaulton, K.J., Ferreira, T., Horikoshi, M., Johnson, A.D., Ng, M.C.Y., Prokopenko, I., et al. (2014). Genome-wide trans-ancestry meta-analysis provides insight into the genetic architecture of type 2 diabetes susceptibility. Nat. Genet.

Marshak, S., Benshushan, E., Shoshkes, M., Havin, L., Cerasi, E., and Melloul, D. (2002). Functional Conservation of Regulatory Elements in the pdx-1 Gene: PDX-1 and Hepatocyte Nuclear Factor 3beta Transcription Factors Mediate beta -Cell-Specific Expression. Mol. Cell. Biol.

Marty-santos, L., and Cleaver, O. (2015). Pdx1 regulates pancreas tubulogenesis and E-cadherin expression. Development 101–112.

Marty-Santos, L., and Cleaver, O. (2015). Progenitor Epithelium: Sorting Out Pancreatic Lineages. J.

Histochem. Cytochem. *63*, 559–574.

Marty-Santos, L., and Cleaver, O. (2016). Pdx1 regulates pancreas tubulogenesis and E-cadherin expression. Development.

Marx, J. (2002). Unraveling the causes of diabetes. Science *296*, 686–689.

Meier, J.J., Butler, A.E., Saisho, Y., Monchamp, T., Galasso, R., Bhushan, A., Rizza, R.A., and Butler, P.C. (2008). β-cell replication is the primary mechanism subserving the postnatal expansion of β-cell mass in humans. Diabetes.

Mellitzer, G., Martín, M., Sidhoum-Jenny, M., Orvain, C., Barths, J., Seymour, P.A., Sander, M., and Gradwohl, G. (2004). Pancreatic Islet Progenitor Cells in Neurogenin 3-Yellow Fluorescent Protein Knock-Add-On Mice. Mol. Endocrinol. *18*, 2765–2776.

Melloul, D., Marshak, S., and Cerasi, E. (2002). Regulation of insulin gene transcription. Diabetologia.

Melton, D.A. (2011). Using stem cells to study and possibly treat type 1 diabetes. Philos. Trans. R. Soc. B Biol. Sci.

van der Meulen, T., Mawla, A.M., DiGruccio, M.R., Adams, M.W., Nies, V., Dólleman, S., Liu, S., Ackermann, A.M., Cáceres, E., Hunter, A.E., et al. (2017). Virgin Beta Cells Persist throughout Life at a Neogenic Niche within Pancreatic Islets. Cell Metab.

Miyatsuka, T., Kosaka, Y., Kim, H., and German, M.S. (2011). Neurogenin3 inhibits proliferation in endocrine progenitors by inducing Cdkn1a. Proc. Natl. Acad. Sci.

Miyazaki, S., Tashiro, F., and Miyazaki, J.I. (2016). Transgenic expression of a single transcription factor Pdx1 induces transdifferentiation of pancreatic acinar cells to endocrine cells in adult mice. PLoS One.

Murtaugh, L.C., Stanger, B.Z., Kwan, K.M., and Melton, D.A. (2003). Notch signaling controls multiple steps of pancreatic differentiation. Proc. Natl. Acad. Sci.

Muzumdar, M.D., Tasic, B., Miyamichi, K., Li, N., and Luo, L. (2007). A global double-fluorescent cre reporter mouse. Genesis.

Nishimura, W., Kondo, T., Salameh, T., El Khattabi, I., Dodge, R., Bonner-Weir, S., and Sharma, A. (2006). A switch from MafB to MafA expression accompanies differentiation to pancreatic β-cells. Dev. Biol.

Nishimura, W., Bonner-Weir, S., and Sharma, A. (2009). Expression of MafA in pancreatic progenitors is detrimental for pancreatic development. Dev. Biol.

Nishimura, W., Eto, K., Miki, A., Goto, M., Kawaguchi, M., Nammo, T., Udagawa, H., Hiramoto, M., Shimizu, Y., Okamura, T., et al. (2013). Quantitative assessment of Pdx1 promoter activity in vivo using a secreted luciferase reporter system. Endocrinology.

Nishimura, W., Takahashi, S., and Yasuda, K. (2015). MafA is critical for maintenance of the mature beta cell phenotype in mice. Diabetologia.

Norgaard, G.A., Jensen, J.N., and Jensen, J. (2003). FGF10 signaling maintains the pancreatic

progenitor cell state revealing a novel role of Notch in organ development. Dev. Biol.

Obenshain, S.S., Adam, P.A., King, K.C., Teramo, K., Raivio, K.O., Räihä, N., and Schwartz, R. (1970). Human fetal insulin response to sustained maternal hyperglycemia. N. Engl. J. Med. *283*, 566–570.

Offield, M.F., Jetton, T.L., Labosky, P.A., Ray, M., Stein, R.W., Magnuson, M.A., Hogan, B.L.M., and Wright, C.V.E. (1996). PDX-1 is required for pancreatic outgrowth and differentiation of the rostral duodenum Martin. Development.

Pagliuca, F.W., Millman, J.R., G??rtler, M., Segel, M., Van Dervort, A., Ryu, J.H., Peterson, Q.P., Greiner, D., and Melton, D.A. (2014). Generation of functional human pancreatic ?? cells in vitro. Cell *159*, 428–439.

Pan, F.C., and Wright, C. (2011). Pancreas organogenesis: From bud to plexus to gland. Dev. Dyn.

Pan, F.C., Bankaitis, E.D., Boyer, D., Xu, X., Van de Casteele, M., Magnuson, M.A., Heimberg, H., and Wright, C.V.E. (2013). Spatiotemporal patterns of multipotentiality in Ptf1a-expressing cells during pancreas organogenesis and injury-induced facultative restoration. Development.

Papizan, J.B., Singer, R.A., Tschen, S.I., Dhawan, S., Friel, J.M., Hipkens, S.B., Magnuson, M.A., Bhushan, A., and Sussel, L. (2011). Nkx2.2 repressor complex regulates islet ??-cell specification and prevents ??-to-??-cell reprogramming. Genes Dev.

Petitt, D.J., Bennett, P.H., Knowler, W.C., Baird, H.R., and Aleck, K.A. (1985). Gestational diabetes mellitus and impaired glucose tolerance during pregnancy. Long-term effects on obesity and glucose tolerance in the offspring. Diabetes.

Petri, A., Ahnfelt-Rønne, J., Frederiksen, K.S., Edwards, D.G., Madsen, D., Serup, P., Fleckner, J., and Heller, R.S. (2006). The effect of neurogenin3 deficiency on pancreatic gene expression in embryonic mice. J. Mol. Endocrinol.

Pictet, R., and Rutter, W.J. (1972). Development of the embryonic endocrine pancreas. Handb. Physiol. 25–66.

Pictet, R.L., Clark, W.R., Williams, R.H., and Rutter, W.J. (1972). An ultrastructural analysis of the developing embryonic pancreas. Dev. Biol.

Pierreux, C.E., Poll, A. V., Kemp, C.R., Clotman, F., Maestro, M.A., Cordi, S., Ferrer, J., Leyns, L., Rousseau, G.G., and Lemaigre, F.P. (2006). The Transcription Factor Hepatocyte Nuclear Factor-6 Controls the Development of Pancreatic Ducts in the Mouse. Gastroenterology.

Pørksen, N., Hollingdal, M., Juhl, C., Butler, P., Veldhuis, J.D., and Schmitz, O. (2002). Pulsatile insulin secretion: detection, regulation, and role in diabetes. Diabetes *51 Suppl 1*, S245-54.

Potter, L.A., Choi, E., Hipkens, S.B., Wright, C.V.E., and Magnuson, M.A. (2012). A recombinase-mediated cassette exchange-derived cyan fluorescent protein reporter allele for Pdx1. Genesis.

Prentki, M., and Nolan, C.J. (2006). Islet beta cell failure in type 2 diabetes. J. Clin. Invest. *116*, 1802–1812.

Prentki, M., Vischer, S., Glennon, M.C., Regazzi, R., Deeney, J.T., and Corkey, B.E. (1992). Malonyl-CoA and long chain acyl-CoA esters as metabolic coupling factors in nutrient-induced insulin

secretion. J. Biol. Chem. *267*, 5802–5810.

Qu, X., Afelik, S., Jensen, J.N., Bukys, M.A., Kobberup, S., Schmerr, M., Xiao, F., Nyeng, P., Veronica Albertoni, M., Grapin-Botton, A., et al. (2013). Notch-mediated post-translational control of Ngn3 protein stability regulates pancreatic patterning and cell fate commitment. Dev. Biol. *376*, 1–12.

Ramond, C., Beydag-Tasöz, B.S., Azad, A., van de Bunt, M., Petersen, M.B.K., Beer, N.L., Glaser, N., Berthault, C., Gloyn, A.L., Hansson, M., et al. (2018). Understanding human fetal pancreas development using subpopulation sorting, RNA sequencing and single-cell profiling. Development *145*, dev165480.

Rankin, M.M., and Kushner, J.A. (2009). Adaptive β-cell proliferation is severely restricted with advanced age. Diabetes.

Reichert, M., and Rustgi, A.K. (2011). Pancreatic ductal cells in development, regeneration, and neoplasia. J. Clin. Invest.

Reis, A.F., Ye, W.Z., Dubois-Laforgue, D., Bellanne-Chantelot, C., Timsit, J., and Velho, G. (2000). Mutations in the insulin promoter factor-1 gene in late-onset type 2 diabetes mellitus. Eur. J. Endocrinol. *143*, 511–513.

Rezania, A., Bruin, J.E., Arora, P., Rubin, A., Batushansky, I., Asadi, A., O'Dwyer, S., Quiskamp, N., Mojibian, M., Albrecht, T., et al. (2014). Reversal of diabetes with insulin-producing cells derived in vitro from human pluripotent stem cells. Nat Biotechnol *32*, 1121–1133.

Rogers, C.D., Sorrells, L.K., and Bronner, M.E. (2018). A catenin-dependent balance between N-cadherin and E-cadherin controls neuroectodermal cell fate choices. Mech. Dev.

Root-Bernstein, R., Podufaly, A., and Dillon, P.F. (2014). Estradiol binds to insulin and insulin receptor decreasing insulin binding in vitro. Front. Endocrinol. (Lausanne). *5*, 1–13.

Roscioni, S.S., Migliorini, A., Gegg, M., and Lickert, H. (2016a). Impact of islet architecture on β-cell heterogeneity, plasticity and function. Nat. Rev. Endocrinol.

Roscioni, S.S., Migliorini, A., Gegg, M., and Lickert, H. (2016b). Impact of islet architecture on β-cell heterogeneity, plasticity and function. Nat. Rev. Endocrinol.

Ross Laybutt, D., Sharma, A., Sgroi, D.C., Gaudet, J., Bonner-Weir, S., and Weir, G.C. (2002). Genetic regulation of metabolic pathways in β-cells disrupted by hyperglycemia. J. Biol. Chem.

Rovira, M., Scott, S.-G., Liss, A.S., Jensen, J., Thayer, S.P., and Leach, S.D. (2010). Isolation and characterization of centroacinar/terminal ductal progenitor cells in adult mouse pancreas. Proc. Natl. Acad. Sci.

Russ, H.A., Sintov, E., Anker-Kitai, L., Friedman, O., Lenz, A., Toren, G., Farhy, C., Pasmanik-Chor, M., Oron-Karni, V., Ravassard, P., et al. (2011). Insulin-Producing cells generated from dedifferentiated human pancreatic beta cells expanded in vitro. PLoS One *6*.

Sacco, F., Seelig, A., Humphrey, S.J., Krahmer, N., Volta, F., Reggio, A., Marchetti, P., Gerdes, J., and Mann, M. (2019). Phosphoproteomics Reveals the GSK3-PDX1 Axis as a Key Pathogenic Signaling Node in Diabetic Islets. Cell Metab.

Sancho, R., Gruber, R., Gu, G., and Behrens, A. (2014). Loss of Fbw7 reprograms adult pancreatic

ductal cells into ??, ??, and ?? cells. Cell Stem Cell *15*, 139–153.

Scavuzzo, M.A., Hill, M.C., Chmielowiec, J., Yang, D., Teaw, J., Sheng, K., Kong, Y., Bettini, M., Zong, C., Martin, J.F., et al. (2018). Endocrine lineage biases arise in temporally distinct endocrine progenitors during pancreatic morphogenesis. Nat. Commun.

Schaffer, A.E., Freude, K.K., Nelson, S.B., and Sander, M. (2010). Nkx6 transcription factors and Ptf1a function as antagonistic lineage determinants in multipotent pancreatic progenitors. Dev. Cell.

Schwitzgebel, V.M., Scheel, D.W., Conners, J.R., Kalamaras, J., Lee, J.E., Anderson, D.J., Sussel, L., Johnson, J.D., and German, M.S. (2000). Expression of neurogenin3 reveals an islet cell precursor population in the pancreas. Development.

Senée, V., Chelala, C., Duchatelet, S., Feng, D., Blanc, H., Cossec, J.-C., Charon, C., Nicolino, M., Boileau, P., Cavener, D.R., et al. (2006). Mutations in GLIS3 are responsible for a rare syndrome with neonatal diabetes mellitus and congenital hypothyroidism. Nat. Genet. *38*, 682–687.

Shen, C.N., Horb, M.E., Slack, J.M.W., and Tosh, D. (2003). Transdifferentiation of pancreas to liver. Mech. Dev.

Shih, H.P., Kopp, J.L., Sandhu, M., Dubois, C.L., Seymour, P. a, Grapin-Botton, A., and Sander, M. (2012). A Notch-dependent molecular circuitry initiates pancreatic endocrine and ductal cell differentiation. Development *139*, 2488–2499.

Shih, H.P., Wang, A., and Sander, M. (2013). Pancreas organogenesis: from lineage determination to morphogenesis. Annu. Rev. Cell Dev. Biol. *29*, 81–105.

Snyder, C.S., Harrington, A.R., Kaushal, S., Mose, E., Lowy, A.M., Hoffman, R.M., and Bouvet, M. (2013). A dual-color genetically engineered mouse model for multispectral imaging of the pancreatic microenvironment. Pancreas.

Solar, M., Cardalda, C., Houbracken, I., Martín, M., Maestro, M.A., De Medts, N., Xu, X., Grau, V., Heimberg, H., Bouwens, L., et al. (2009). Pancreatic Exocrine Duct Cells Give Rise to Insulin-Producing β Cells during Embryogenesis but Not after Birth. Dev. Cell.

Sorenson, R.L., and Brelje, T.C. (1997). Adaptation of islets of Langerhans to pregnancy: β-cell growth, enhanced insulin secretion and the role of lactogenic hormones. In Hormone and Metabolic Research, p.

Sorrenson, B., Cognard, E., Lee, K.L., Dissanayake, W.C., Fu, Y., Han, W., Hughes, W.E., and Shepherd, P.R. (2016). A critical role for β-catenin in modulating levels of insulin secretion from β-cells by regulating actin cytoskeleton and insulin vesicle localization. J. Biol. Chem. *291*, 25888–25900.

Spaeth, J.M., Gupte, M., Perelis, M., Yang, Y.P., Cyphert, H., Guo, S., Liu, J.H., Guo, M., Bass, J., Magnuson, M.A., et al. (2017). Defining a Novel Role for the Pdx1 Transcription Factor in Islet β-Cell Maturation and Proliferation During Weaning. Diabetes.

Stanger, B.Z., Tanaka, A.J., and Melton, D. a (2007). Organ size is limited by the number of embryonic progenitor cells in the pancreas but not the liver. Nature *445*, 886–891.

Stoffers, D. a, Ferrer, J., Clarke, W.L., and Habener, J.F. (1997). Early-onset type-II diabetes mellitus (MODY4) linked to IPF1. Nat. Genet. *17*, 138–139.

Stolovich-Rain, M., Enk, J., Vikesa, J., Nielsen, F., Saada, A., Glaser, B., and Dor, Y. (2015). Weaning Triggers a Maturation Step of Pancreatic ?? Cells. Dev. Cell *32*, 535–545.

Sund, N.J., Vatamaniuk, M.Z., Casey, M., Ang, S.W., Magnuson, M.A., Stoffers, D.A., Matschinsky, F.M., and Kaestner, K.H. (2001). Tissue-specific deletion of Foxa2 in pancreatic β cells results in hyperinsulinemic hypoglycemia. Genes Dev. *15*, 1706–1715.

Talchai, C., Xuan, S., Lin, H. V., Sussel, L., and Accili, D. (2012). Pancreatic β cell dedifferentiation as a mechanism of diabetic β cell failure. Cell *150*, 1223–1234.

Taylor, B.L., Liu, F.F., and Sander, M. (2013). Nkx6.1 Is Essential for Maintaining the Functional State of Pancreatic Beta Cells. Cell Rep.

Téllez, N., and Montanya, E. (2014). Gastrin induces ductal cell dedifferentiation and β-cell neogenesis after 90% pancreatectomy. J. Endocrinol.

Teo, A.K.K., Tsuneyoshi, N., Hoon, S., Tan, E.K., Stanton, L.W., Wright, C.V.E., and Dunn, N.R. (2015). PDX1 binds and represses hepatic genes to ensure robust pancreatic commitment in differentiating human embryonic stem cells. Stem Cell Reports *4*, 578–590.

Teta, M., Long, S.Y., Wartschow, L.M., Rankin, M.M., and Kushner, J.A. (2005). Very slow turnover of beta-cells in aged adult mice. Diabetes *54*, 2557–2567.

Teta, M., Rankin, M.M., Long, S.Y., Stein, G.M., and Kushner, J.A. (2007). Growth and regeneration of adult beta cells does not involve specialized progenitors. Dev. Cell *12*, 817–826.

Thorel, F., Népote, V., Avril, I., Kohno, K., Desgraz, R., Chera, S., and Herrera, P.L. (2010). Conversion of adult pancreatic alpha-cells to beta-cells after extreme beta-cell loss. Nature *464*, 1149–1154.

Villasenor, A., Chong, D.C., and Cleaver, O. (2008). Biphasic Ngn3 expression in the developing pancreas. Dev. Dyn. *237*, 3270–3279.

Villasenor, A., Chong, D.C., Henkemeyer, M., and Cleaver, O. (2010). Epithelial dynamics of pancreatic branching morphogenesis. Development *137*, 4295–4305.

Vital, P., Larrieta, E., and Hiriart, M. (2006). Sexual dimorphism in insulin sensitivity and susceptibility to develop diabetes in rats. J. Endocrinol. *190*, 425–432.

Wang, H., Gauthier, B.R., Hagenfeldt-Johansson, K.A., Iezzi, M., and Wollheim, C.B. (2002a). Foxa2 (HNF3??) controls multiple genes implicated in metabolism-secretion coupling of glucose-induced insulin release. J. Biol. Chem.

Wang, H., Gauthier, B.R., Hagenfeldt-Johansson, K.A., Iezzi, M., and Wollheim, C.B. (2002b). Foxa2 (HNF3??) controls multiple genes implicated in metabolism-secretion coupling of glucose-induced insulin release. J. Biol. Chem. *277*, 17564–17570.

Wang, S., Yan, J., Anderson, D.A., Xu, Y., Kanal, M.C., Cao, Z., Wright, C.V.E., and Gu, G. (2010). Neurog3 gene dosage regulates allocation of endocrine and exocrine cell fates in the developing mouse pancreas. Dev. Biol.

Wang, Z., York, N.W., Nichols, C.G., and Remedi, M.S. (2014a). Pancreatic β cell dedifferentiation in diabetes and redifferentiation following insulin therapy. Cell Metab.

Wang, Z., York, N.W., Nichols, C.G., and Remedi, M.S. (2014b). Pancreatic ?? cell dedifferentiation in diabetes and redifferentiation following insulin therapy. Cell Metab. *19*, 872–882.

Weedon, M.N., Cebola, I., Patch, A., Flanagan, S.E., Franco, E. De, Caswell, R., Rodríguez-seguí, S.A., Shaw-smith, C., Cho, C.H., Allen, H.L., et al. (2013). Recessive mutations in a distal PTF1A enhancer cause isolated pancreatic agenesis. Nat. Publ. Gr. *46*, 61–64.

Weir, G.C., and Bonner-Weir, S. (2004). Five stages of evolving beta-cell dysfunction during progression to diabetes. Diabetes *53 Suppl 3*, S16-21.

Weng, J., Macfarlane, W.M., Lehto, M., Gu, H.F., Shepherd, L.M., Ivarsson, S.A., Wibell, L., Smith, T., and Groop, L.C. (2001). Functional consequences of mutations in the MODY4 gene (IPF1) and coexistence with MODY3 mutations. Diabetologia *44*, 249–258.

Wu, K.L., Gannon, M., Peshavaria, M., Offield, M.F., Henderson, E., Ray, M., Marks, A., Gamer, L.W., Wright, C. V, and Stein, R. (1997). Hepatocyte nuclear factor 3beta is involved in pancreatic beta-cell-specific transcription of the pdx-1 gene. Mol. Cell. Biol.

Xu, G., Stoffers, D.A., Habener, J.F., and Bonner-Weir, S. (1999). Exendin-4 stimulates both β-cell replication and neogenesis, resulting in increased β-cell mass and improved glucose tolerance in diabetic rats. Diabetes.

Yang, Y., Thorel, F., Boyer, D.F., Herrera, P.L., and Wright, C.V.E. (2011). Context-specific α-to- β-cell reprogramming by forced Pdx1 expression service re programming by forced Pdx1 expression. Genes Dev. 1680–1685.

Yuchi, Y., Cai, Y., Legein, B., De Groef, S., Leuckx, G., Coppens, V., Van Overmeire, E., Staels, W., De Leu, N., Martens, G., et al. (2015). Estrogen Receptor ?? Regulates ??-Cell Formation During Pancreas Development and Following Injury. Diabetes *64*, 3218–3228.

Zaret, K.S., and Carroll, J.S. (2011). Pioneer transcription factors: Establishing competence for gene expression. Genes Dev.

Zhang, C., Moriguchi, T., Kajihara, M., Esaki, R., Harada, A., Shimohata, H., Oishi, H., Hamada, M., Morito, N., Hasegawa, K., et al. (2005). MafA Is a Key Regulator of Glucose-Stimulated Insulin Secretion. Mol. Cell. Biol.

Zhou, Q., Law, A.C., Rajagopal, J., Anderson, W.J., Gray, P. a., and Melton, D. a. (2007). A Multipotent Progenitor Domain Guides Pancreatic Organogenesis. Dev. Cell *13*, 103–114.

Zhou, Q., Brown, J., Kanarek, A., Rajagopal, J., and Melton, D.A. (2008). In vivo reprogramming of adult pancreatic exocrine cells to β-cells. Nature.

7 Publications

Sachs S*, **Bastidas-Ponce A***, Tritschler S*, Bakhti M, Böttcher A, Sánchez-Garrido MA, Tarquis-Medina M, Kleinert M, Fischer K, Jall S, Harger A, Bader E, Roscioni S, Ussar S, Feuchtinger A, Yesildag B, Neelakandhan A, Jensen CB, Cornu M, Yang B, Finan B, DiMarchi RD, Tschöp MH, Theis FJ, Hofmann SM, Müller TD, Lickert H. Targeted pharmacological therapy restores β-cell function for diabetes remission. Nature Metabolism. 2020 Feb;2(2):192-209. (*First authors).

Bakhti M, Scheibner K, Tritschler S, **Bastidas-Ponce A**, Tarquis-Medina M, Theis FJ, Lickert H. Establishment of a high-resolution 3D modeling system for studying pancreatic epithelial cell biology in vitro. Mol Metab. 2019 Dec; 30:16-29.

Salinno C, Cota P, **Bastidas-Ponce A**, Tarquis-Medina M, Lickert H, Bakhti M. β-cell maturation and identity in health and disease. Int J Mol Sci. 2019 Oct 30;20(21):5417.

Scheibner K, Bakhti M, **Bastidas-Ponce A** and Heiko Lickert. Wnt signaling: implications in endoderm development and pancreas organogenesis. Curr Opin Cell Biol. 2019 Aug 1;61:48-55

Bastidas-Ponce A*, Tritschler S*, Dony L, Scheibner K, Tarquis-Medina M, Salinno C, Schirge S, Burtscher I, Böttcher A, Theis FJ, Lickert H, Bakhti M. Comprehensive single cell mRNA profiling reveals a detailed roadmap for pancreatic endocrinogenesis. Development. 2019 Jun 17;146(12). (*First co-authors).

Bakhti M, **Bastidas-Ponce A**, Lickert H. Sorting out fate determination. Dev Cell. 2019 Apr 8;49(1):1-3.

Fischer DS, Fiedler AK, Kernfeld EM, Genga RMJ, **Bastidas-Ponce A**, Bakhti M, Lickert H, Hasenauer J, Maehr R, Theis FJ. Inferring population dynamics from single-cell RNA-sequencing time series data. Nat Biotechnol. 2019 Apr;37(4):461-468.

Quarta C, Clemmensen C, Zhu Z, Yang B, Joseph SS, Lutter D, Yi CX, Graf E, García-Cáceres C, Legutko B, Fischer K, Brommage R, Zizzari P, Franklin BS, Krueger M, Koch M, Vettorazzi S, Li P, Hofmann SM, Bakhti M, **Bastidas-Ponce A**, Lickert H, Strom TM, Gailus-Durner V, Bechmann I, Perez-Tilve D, Tuckermann J, Hrabě de Angelis M, Sandoval D, Cota D, Latz E, Seeley RJ, Müller TD, DiMarchi RD, Finan B, Tschöp MH. Molecular integration of incretin and glucocordicoid action reverses immunometabolic dysfunction and obesity. Cell Metab. 2017 Oct 3;26(4):620-632.e6.

Bastidas-Ponce A*, Scheibner K*, Lickert H, Bakhti M. Cellular and molecular mechanisms coordinating pancreas development. Development. 2017 Aug 15;144(16):2873-2888. Review. (*First co-authors).

Guerrero-Flores G, **Bastidas-Ponce A**, Collazo-Navarrete O, Guerra-Crespo M, Covarrubias L. Functional determination of the differentiation potential of ventral mesencephalic neural precursor cells during dopaminergic neurogenesis. Dev Biol. 2017 Sep 1;429(1):56-70.

Bastidas-Ponce A, Roscioni SS, Burtscher I, Bader E, Sterr M, Bakhti M, Lickert H. Foxa2 and Pdx1 cooperatively regulate postnatal maturation of pancreatic β-cells. Mol Metab. 2017 Mar 25;6(6):524-534. doi: 10.1016/j.molmet.2017.03.007. eCollection 2017 Jun.

8 Abbreviations

°C	Centigrade
Arx	Aristaless related homeobox
BCA	bicinchoninic acid **assay**
BFP	Blue Fluorescent protein
Brn4	Brain-Specific Homeobox/POU Domain Protein 4
Cdc42	Cell division cycle 42
DNA	Deoxyribonucleic acid
E	Embryonic day
EDTA	Ethylenediaminetetraacetic acid
EGFR	Epidermal growth factor receptor
ELISA	Enzyme-Linked ImmunoSorbent Assay
EPs	Endocrine progenitors
ESCs	Embryonic stem cells
EtOH	ethyl alcohol
ε-cells	Epsilon-cells
FELASA	Federation of Laboratory Animal Science Associations
Foxa2	Forkhead box A2
FSC-A	front scatter area
FSC-H	front scatter height
FSC-W	front scatter width
FVF	Foxa2 Venus Fusion
$FVFPBF^{DHom}$	FVFPBF Doble Homozygous
$FVFPBF^{DHom}$	FVF PBF Double Homozygous
Gck	Glucokinase
GFP	Green Flourescent Protein
Glis3	GLIS Family Zinc Finger 3
GLP-1	Glucagon like peptide-1
Glut2	Gluco0se transporter 2
GSIS	Glucose stimulated insulin secretion
GV-SOLAS	Guidelines of the Society of Laboratory Animals
HCl	Hydrochloric acid
Hes1	Hairy and enhancer of split-1
Hnf1β	Hepatocyte nuclear factor 1β
hrs	hours
Ins	Insulin
IPSCs	Induced pluripotent stem cells
KCl	potassium chloride
KRPH	Krebs Ringer phosphate HEPES
MafA/B	MAF BZIP Transcription Factor A/B
min	minutes
mL	millilitre
mM	miliMolar
MODY	Maturity-onset diabetes of the young
MPCs	Multipotent pancreatic progenitors

MPCs	Multipotent *pancreatic* progenitor
mTmG	membrane Tomatoe membrane GFP
Ngn3	Neurogening 3
NeuroD1	Neuronal Differentiation 1
ng	nanogram
Nkx2.2	Homeobox protein Nkx-2.2
Nkx6.1	Homeobox protein Nkx-6.1
O/N	Overnight
P	Postnatal day
PAGA	Partition-based graph abstraction
Pax6 and 4	Paired box protein Pax-6 and 4
PBF	Pdx1 BFP Fusion
PBS	Phosphate-buffered saline
PCP	Planar cell polarity
PCR	Polymerase chain reaction
PDL	partial duct ligation
Pdx1	Pancreatic and duodenal homeobox 1
PFA	Paraformaldehyde
pg	picogram
PP-cells	PP-cells
Ptf1a	Pancreas-specific transcription factor 1a
qPCR	Quantitative PCR
Rfx6	Regulatory factor X 6
RNA	Ribonucleic acid
rpm	revolution per minute
RT	Room temperature
scRNAseq	single cell RNA sequencing
Sox9	SRY-Box 9
SSC-A	side scatter area
STZ	Streptozotocin
T1D	Type 1 diabetes
T2D	Type 2 diabetes
TFs	Transcriptional factors
Ucn3	Urocortin 3
Wnt	wingless signaling
α-cells	Alpha-cells
β-cells	Beta-cells
β-cells	Beta-cells
δ-cells	Delta-cells
µL	microliter
µm	micrometer

9 Acknowledgements

“Because there is no other way… from all, to all, by all”

To my **family**, the strength to smile every day, because they are the infinite love that is imprinted in my stepping, the strong base that holds my structure despite differences... just an embrace of the particular me. As I've been saying while ago... the best context that I could ask for... thanks a lot!!!

Mom, my own "mamacita"... I want to explain you better that you gave me wings, you allowed me to fly, it is you the one that pulled down every scary stuff with a simple touch during nightmares... huge thanks for letting me be. **Marlon**, my dear dad... the reason to jump the big lake, to explore this part of the planet, the one that with stories and experiences fed the curiosity, the direction in certain ways... let's just meet in between lines as our traditional side. **Bro**... my kid, the balance part to let me complain, the requirement of breath away or steam out, my sidekick in the dark, might be you don't even know who you are for me, maybe you need to learn the art of read encrypted. To my **grandma**, for the faith and the blind love on this creature that enjoy every chance around you my beloved motivation. Ants, uncles, cousins, nieces, nephews and so on… let’s celebrate because it is finally done!

To **Heiko** for share the gamble that allowed me to be part of this project, my pleasure to be in IDR and be the loud troublemaker with tequila taste. Thanks for the opportunity to work with you and to be part of your whole picture. **Ingo** for cheering the exotic among the cold, the wild side of hiking ice, sledding bones, swim the wave away and more. To **Donna**, for made my life easier in each step, since day minus I got your help, despite my mess, my constant inquiring not only about travels, holidays, work, mice but beyond, let’s keep running.

To my mentors, by definition... you guys provided different tools for this great scientific journey. **Heiko**, **Ingo**, **Aurelia**, **Sara** and **Mostafa**. To each and one of you for the discussion, techniques, tips, tricks and laughs… more than thanks. For the management and technical support, all you that made it smooth for me. Not only for the part of ordering, organizing and so on but also for the care of my image, the laughs, the dancing around, the emergency case, the whole thing... thanks a lot **Kerstin**, **Jessi**, **Anne**, **Gaby**, **Robert**, **Julia B**, **Elke**, **Bianca**, **Jürgen**, **Lisa** and **Ines**.

To Syt (Sh…) group, **Mostafa** for the walking together my dear husband in science, the big pain that teaches me constantly about growing, patience, pushing and beyond, it has been being a pleasure to work with you and even bigger one to be your friend. **Marta** for the company, the learning and not only Spanish, for the support, complains and confidence to be next to me in this personal and scientific journey huge thanks. **Kathi** dear chica… what a trip, nice to share more than I thought and have you driving around; it is being a great pleasure.

Jessi, many thanks for being patient with the Mexican mess, for the growing together and the friendship. **Anne**, cool to share laughs and talks in knap still. **Bianca**, for the nice German taste in the short and shy time of you being around. **Ciro**, the adopted child, liliiiii… for the shared craziness, the confidence to discuss and the hard-core way to believe, you are a lot and more dude, the looking balance. **Perla**, our last annoying acquisition… thanks for the patience in the scary start that lead to writing lessons and long salty almonds and coffee talks. Outsider of this group but my company in project **Stephan**, thanks for the chance, to be patient with me and my times together with the apologetic pushing being that you open to share between work, snacks and coconut cakes. **IDR IDR IDR**... up and down to all of you thanks a lot.

From here and there, what a wonderful sharing among all you guys... my annexed family, my friends around. The ones that danced, laughed, drank, complained and more with me, this a part of you. What a big mess we had made here, just to think about it make a smile came along, so many cultures and differences merge together and get along as a big puzzle made on purpose. Dear **flower** (**Sara**) thanks for let me be part of your life, for the joy of your kids and family, all the talks, crazy blood patterns among loud laughs without any doubt one of the best things that happened in my life was meeting you. **Pallavi** what to say that we didn't scream or cry out in our Garching journeys, hope it has been more than clear how much I thank life for having you around. My **darling** (**Lisann**), one of the best taste of Germany, great to know you in your best context your family which I enjoy a lot, my open girly relationship in this side of the world you are a huge part of my life and getting ride of me won't be easy. **Christian**, mi **bebe** (amor)… it is being a pleasure having you next to me all this time, my drinking sidekick and full time support, I am your biggest fan and maybe you don't know but you sign a forever and ever with me. **Noah**, my first italian, the basketball remind and the Spanish that helped adaptation. **Dapeng**, my great friend that made my first stage here so much fun and different to what I knew. **Erik**, the color match of my favorite cuajo, so much fun between forks and laughs. **Francesco**, my dark humor alive, thanks for the fun, the flat and the taste that came with an ass. **Julia**, my dear mess walking what a surprise to have you around with the latino taste on board. A real pleasure to share a journey with you all.

Not always easy or forever, just the exact time to share, to all of you that shape what is now the job done. Chronological mention seems more accurate than alphabetical or contribution: **Donna, Pallavi, Noah, Mostafa, Dapeng, Sara, Ingo, Robert, Erik, Lisann, Marta, Francesco, Julia, Christian, Matthias, Annalisa, Kathi, Ciro, Stephan, Noel, Sarah, Jessi**. My long distance, always there no matter the water, time or whatever between us: **Angel**, my dear bitches: **Gigi** and **Chio, Inti, Ivanito, Chris, Eve, Alma, Chela, Cynthia, Yesenia, Luis Enrique, Harry, Francisco Delgado and Pio.** To the short but significant ones that manage to smile, drink, dance, laugh, jump and share a piece of them with me.

To all, without encrypted messages or many bla bla bla… I love you all and I appreciate each of one of you as part of my life.

© 2019. Published by The Company of Biologists Ltd | Development (2019) 146, dev173849. doi:10.1242/dev.173849

RESEARCH ARTICLE

Comprehensive single cell mRNA profiling reveals a detailed roadmap for pancreatic endocrinogenesis

Aimée Bastidas-Ponce[1,2,3,4,*], Sophie Tritschler[1,5,6,*], Leander Dony[5,6,7], Katharina Scheibner[1,2,3,4], Marta Tarquis-Medina[1,2,3,4], Ciro Salinno[1,2,3,4], Silvia Schirge[1,2,3], Ingo Burtscher[1,2,3], Anika Böttcher[1,2,3], Fabian J. Theis[5,8,‡], Heiko Lickert[1,2,3,4,‡] and Mostafa Bakhti[1,2,3,‡]

ABSTRACT

Deciphering mechanisms of endocrine cell induction, specification and lineage allocation *in vivo* will provide valuable insights into how the islets of Langerhans are generated. Currently, it is ill defined how endocrine progenitors segregate into different endocrine subtypes during development. Here, we generated a novel neurogenin 3 (Ngn3)-Venus fusion (NVF) reporter mouse line, that closely mirrors the transient endogenous Ngn3 protein expression. To define an *in vivo* roadmap of endocrinogenesis, we performed single cell RNA sequencing of 36,351 pancreatic epithelial and NVF^{+} cells during secondary transition. This allowed *Ngn3*^{low} endocrine progenitors, *Ngn3*^{high} endocrine precursors, *Fev*$^{+}$ endocrine lineage and hormone^{+} endocrine subtypes to be distinguished and time-resolved, and molecular programs during the step-wise lineage restriction steps to be delineated. Strikingly, we identified 58 novel signature genes that show the same transient expression dynamics as *Ngn3* in the 7260 profiled *Ngn3*-expressing cells. The differential expression of these genes in endocrine precursors associated with their cell-fate allocation towards distinct endocrine cell types. Thus, the generation of an accurately regulated NVF reporter allowed us to temporally resolve endocrine lineage development to provide a fine-grained single cell molecular profile of endocrinogenesis *in vivo*.

KEY WORDS: Endocrine progenitor-precursor, Neurog3, Single cell RNA sequencing, Endocrinogenesis, Endocrine cell allocation, Mouse

INTRODUCTION

In rodents, pancreatic endocrine cells are generated at two distinct stages (transitions) during embryonic development. The first transition [embryonic day (E) 9.0-12.5] produces mainly glucagon-producing α-cells, whereas all other endocrine cell types (insulin-producing β-cells, somatostatin-producing δ-cells, pancreatic polypeptide-producing PP-cells and ghrelin-producing ε-cells) are mainly generated during the secondary transition (E12.5-15.5) and thereafter. At both stages, endocrine cells are derived from the endocrine progenitor-precursor (EP) pool (Bastidas-Ponce et al., 2017a). EPs are marked by the transient expression of the transcription factor (TF) neurogenin 3 (Neurog3, hereafter called Ngn3) and are derived from Sox9^{+} bipotent ductal/endocrine progenitors, which are located within the pancreatic epithelium (Gradwohl et al., 2000; Gu et al., 2002; Kopp et al., 2011; Seymour et al., 2007; Shih et al., 2012). Upon lineage priming and specification, EPs express low levels of Ngn3 and by receiving additional signals these mitotic and non-committed Ngn3^{low} cells (which we refer to as endocrine progenitors) increase the levels of Ngn3 to become determined Ngn3^{high} EPs (to which we refer to as endocrine precursors) (Bechard et al., 2016; Pan and Wright, 2011; Wang et al., 2010). Further differentiation of Ngn3^{high} precursors generates distinct endocrine subtypes of the aforementioned hormone-expressing lineages. Changes in the gene regulatory networks, extracellular signaling cues from the respective niche and epithelial states (non-polarized versus polarized and epithelialized) cooperatively orchestrate the specification and determination of EPs (Apelqvist, 1999; Arda et al., 2013; Bankaitis et al., 2015, 2018; Cortijo et al., 2012; Löf-Öhlin et al., 2017). Yet, during progressive lineage restriction from specified EP progenitors to determined EP precursors the molecular signature changes over time and the mechanisms underpinning lineage allocation towards a specific endocrine subtype fate have remained largely elusive. Although several recent studies (Byrnes et al., 2018; Krentz et al., 2018; Ramond et al., 2018; Scavuzzo et al., 2018; Sharon et al., 2019; Stanescu et al., 2016; Yu et al., 2018, 2019) have shed light on the transcriptional profiles of EPs, the importance of these cells for endocrine cell formation still necessitates a comprehensive temporally resolved and fine-grained mapping of gene expression on the single cell level. The low percentage of EPs within the embryonic pancreas together with the limitation of transgenic reporter lines to reflect accurately the transient expression of the Ngn3 protein have been major obstacles to establishing a detailed roadmap of endocrinogenesis.

Here, we generated a novel reporter mouse line, in which the endogenous Ngn3 is fused to a very bright Venus fluorescence reporter protein (Ngn3-Venus fusion; NVF). The NVF reporter mirrors transient endogenous Ngn3 protein levels and allows specific isolation of EPs in the narrow time window when they actually express Ngn3. Single cell RNA sequencing (scRNA-seq) analysis of EP-enriched pancreatic epithelial cells highlighted the step-wise dynamic changes in gene expression programs from bipotent cells to EP progenitors and precursors, and finally to differentiated endocrine cells as well as ductal and acinar cells. We found a set of 58 previously undescribed EP-signature genes that are

[1]Institute of Diabetes and Regeneration Research, Helmholtz Zentrum München, D-85764 Neuherberg, Germany. [2]German Center for Diabetes Research (DZD), D-85764 Neuherberg, Germany. [3]Institute of Stem Cell Research, Helmholtz Zentrum München, D-85764 Neuherberg, Germany. [4]Technical University of Munich, School of Medicine, 81675 Munich, Germany. [5]Institute of Computational Biology, Helmholtz Zentrum München, D-85764 Neuherberg, Germany. [6]Technical University of Munich, School of Life Sciences Weihenstephan, 85354 Freising, Germany. [7]Max Planck Institute of Psychiatry, Kraepelinstr. 2-10, 80804 Munich, Germany. [8]Technical University of Munich, Department of Mathematics, 85748 Garching b. Munich, Germany.
*These authors contributed equally to this work

‡Authors for correspondence (fabian.theis@helmholtz-muenchen.de; heiko.lickert@helmholtz-muenchen.de; mostafa.bakhti@helmholtz-muenchen.de)

F.J.T., 0000-0002-2419-1943; H.L., 0000-0002-4597-8825; M.B., 0000-0002-2307-1122

Received 15 November 2018; Accepted 21 May 2019

Development (2019) 146, dev173849. doi:10.1242/dev.173849

specifically expressed in EPs in a similar transient manner as Ngn3. Furthermore, we found that several of these EP-signature genes are differentially expressed in endocrine precursors derived from different developmental stages that defines their lineage restriction towards specific endocrine subtypes. Altogether, our data provide a comprehensive single cell survey of stage-dependent and lineage-specific gene regulation during EP induction, specification and segregation.

RESULTS

NVF mirrors the endogenous Ngn3 protein expression pattern

We generated an NVF reporter mouse line, in which the *Ngn3* translational stop codon was removed and Venus was fused in-frame with *Ngn3* using a previously described strategy (Petrezselyova et al., 2015). Heterozygous intercrosses produced offspring with normal Mendelian distribution and homozygous *Ngn3*$^{Venus/Venus}$ animals were fertile and indistinguishable from wild-type (WT) littermates (data not shown). To assess whether the NVF reporter reflects the endogenous Ngn3 expression pattern during development, we performed immunostaining of embryonic pancreata from heterozygous *Ngn3*$^{Venus/+}$ mice at E12.5-18.5. Using antibodies against Ngn3 and Venus, we detected a similar nuclear expression pattern of NVF and endogenous Ngn3 in pancreatic sections from different developmental stages (Fig. 1A; Fig. S1A). Plot profile analysis of staining by Venus and two different Ngn3 antibodies also revealed a similar pattern of nuclear signals between NVF and Ngn3 in pancreatic sections (Fig. S1B). Furthermore, using markers of the pancreatic tubular epithelium, such as Sox9, Nkx6-1, Mucin-1 (Muc1), EpCAM and E-cadherin (cadherin 1), we found that NVF^{+} cells exist as both intra- and extra-epithelial cells (Fig. 1B). This data is in line with the idea that at the Ngn3-expressing state, EP progenitors get specified in the pancreatic epithelium and endocrine precursor delaminate into the surrounding mesenchyme to form proto-islet clusters (Gouzi et al., 2011; Sharon et al., 2019). During development, Ngn3 is expressed at low levels in progenitors, reach peak levels in precursors and the levels are reduced upon differentiation of the precursors into the endocrine hormone^{+} lineage (Bechard et al., 2016). To find out whether the NVF protein reflects the transient expression pattern of endogenous Ngn3 protein, we stained E18.5 pancreatic sections and quantified the number of differentiated hormone^{+} endocrine cells that still expressed Ngn3 protein. We observed a subtle and weak NVF signal in the nucleus or cytoplasm of a minor fraction of the hormone^{+} endocrine cells (less than 0.6%) (Fig. 1C,D), confirming that the NVF reporter protein shows a similar transient expression pattern to that of the endogenous Ngn3 protein.

It has been shown that haploinsufficiency of Ngn3 alters endocrine cell development and post-translational modifications of this protein affect its activity (Azzarelli et al., 2017; Krentz et al., 2017; Wang et al., 2010). To confirm that the fusion protein truly represents the activity of endogenous Ngn3 protein, we first checked the expression of several downstream target genes, including *Neurod1*, *Pax4* and *Arx*. Quantitative PCR (qPCR) analysis revealed no significant differences in the expression levels of these genes in isolated epithelial cells from WT and homozygous NVF pancreata at E15.5 (Fig. S1C). Next, we analyzed endocrine cell composition in WT and NVF reporter embryos. E15.5 and E18.5 pancreata from WT and homozygous NVF embryos showed comparable α-, β-, δ- and PP-cell composition (Fig. 1E,F; Fig. S1D). Furthermore, qPCR data demonstrated comparable expression levels of key endocrine cell markers in isolated islets from adult WT and homozygous NVF mice (Fig. S1E). These data were supported by the detection of normal fasting blood glucose levels in adult homozygous *Ngn3*$^{Venus/Venus}$ animals (Fig. S1F) and by comparable levels of glucose-stimulated insulin secretion of isolated WT and *Ngn3*$^{Venus/Venus}$ islets (Fig. S1G). Altogether, our analyses indicate that the NVF reporter is transiently expressed in EPs and reflects a spatiotemporal expression pattern mirroring the endogenous Ngn3 protein. Furthermore, the fusion of Venus to Ngn3 does not have a significant impact on TF function during endocrine cell development.

Single cell RNA-seq of the embryonic EP-enriched pancreatic epithelial cells

To time-resolve at the single cell level the molecular changes during endocrinogenesis, we performed high-throughput scRNA-seq analysis of pancreatic epithelial cells during the secondary transition (E12.5, E13.5, E14.5 and E15.5). To obtain the rare cell population enriched for EPs (expressing NVF), we first flow-sorted embryonic pancreatic cells using the fluorescence property of the Venus protein in homozygous *Ngn3*$^{Venus/Venus}$ pancreata. As we were specifically interested into how epithelial multipotent progenitors become lineage restricted into acinar and bipotent (ductal/endocrine) as well as unipotent progenitors, we isolated from the remaining cells that were negative for NVF (Venus^{-}) the pancreatic epithelial fraction by using the epithelial marker EpCAM. This allowed us to deplete non-epithelial cells and highly enrich for epithelial progenitor, ductal and acinar cells. A fraction of these EpCAM^{+}/Venus^{-} (NVF^{-}) cells were added to the corresponding EP cells (NVF^{+}) at each stage (2:1 ratio for NVF^{+}:NVF^{-}) (Fig. 2A). We used droplet-based scRNA-seq and transcriptionally profiled 10,790 single cells at E12.5, 5042 cells at E13.5, 9633 cells at E14.5 and 10,886 cells at E15.5 (in total 36,351 cells) (Fig. 2B). Of the total cells derived from four different stages, 7260 cells (~20%) expressed *Ngn3*. Unsupervised graph-based clustering revealed eight major cell clusters including multipotent pancreatic progenitors (MPCs), tip, trunk, acinar, ductal, EPs, Fev^{high} and endocrine cells (Fig. 2C; Table S1). These clusters represent distinct pancreatic lineages at different embryonic stages, when the pancreatic epithelium is composed of MPCs. The MPCs undergo step-wise lineage restrictions and segregation into two distinct tip and trunk domains, which further differentiate into acinar and duct/EPs, respectively (Nyeng et al., 2019; Zhou et al., 2007). EPs then differentiate into *Fev*^{high} cells that subsequently generate different types of endocrine hormone^{+} cells (Fig. 1D). *Fev*^{high} cells have been recently reported as a novel cluster of pancreatic cells (Byrnes et al., 2018). Clusters were annotated based on the expression of well-known marker genes with a described function during pancreas development and/or function, including *Dlk1* (MPCs) (Ramond et al., 2018); *Cpa1* and *Myc* (tip) (Zhou et al., 2007); *Notch2* (trunk) (Lee et al., 2005); *Ptf1a*, *Cpa1*, *Cel*, *Rbpjl* (acinar), *Sox9*, *Anxa2* and *Bicc1* (ductal) (Lemaire et al., 2016); *Ngn3* and *Hes6* (EPs) (Ahnfelt-Rønne et al., 2007); *Fev*, *Cck* and *Neurod1* (*Fev*^{high}) (Byrnes et al., 2018); and *Rbp4*, *Pyy* and *Chgb* (endocrine) (Fig. 2E, F). As the expression of Ngn3 is a well-described characteristic of EPs, we annotated *Ngn3*-expressing cells (except those expressing *Fev*) in the epithelial populations as EPs (see Materials and Methods). Our data revealed the expression of novel marker genes in each cluster that are uncharacterized or have not been associated with pancreatic cell development and/or function yet, e.g. *Mdk* and *Btf3* (MPCs); *Vtn* and *Jam3* (tip); *Cbx3*, *Hmgn1* and *Ybx1* (trunk);

Development (2019) 146, dev173849. doi:10.1242/dev.173849

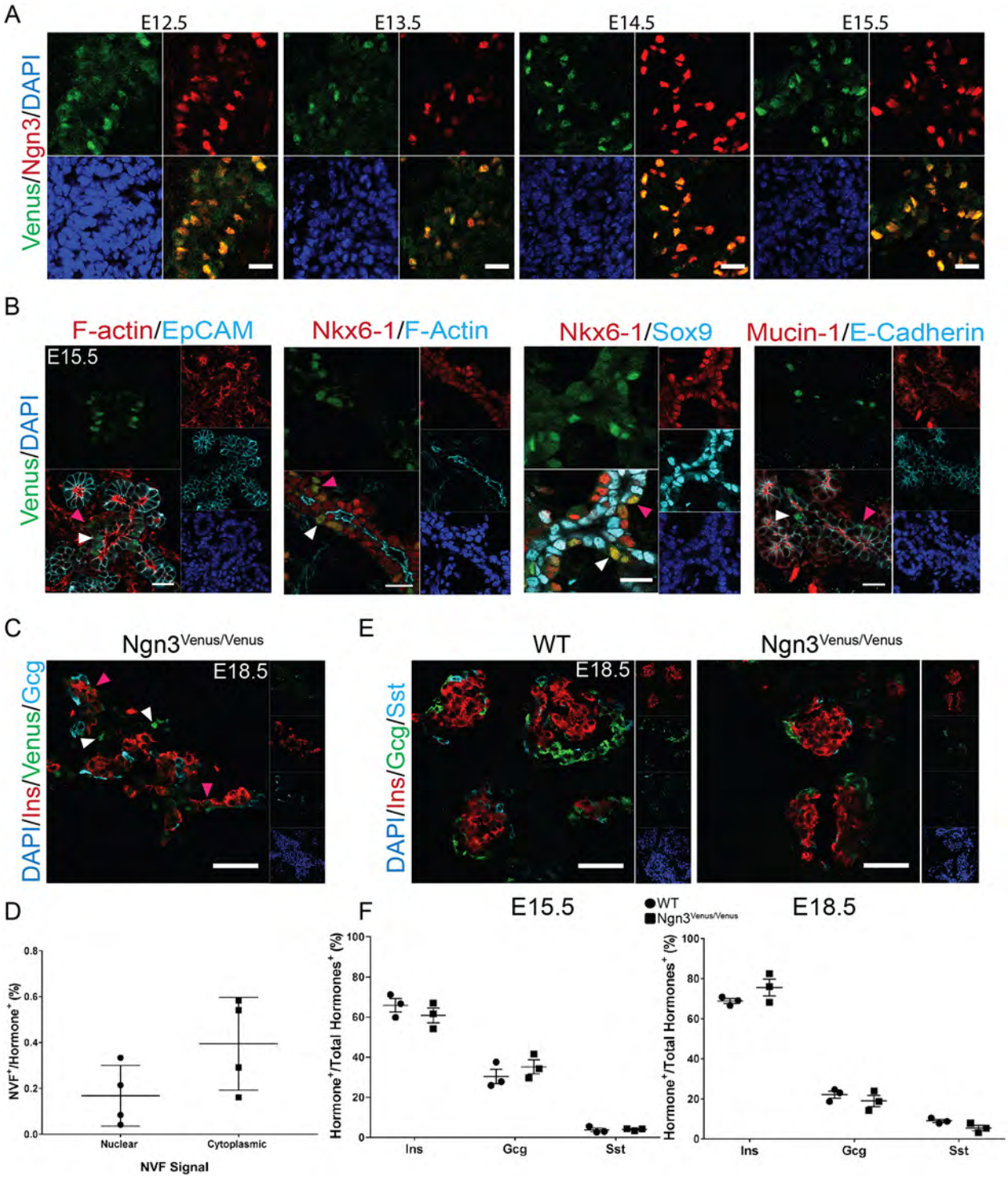

Fig. 1. Characterization of Ngn3-Venus fusion (NVF) reporter mouse line. (A) Immunohistochemical analysis indicates the same spatiotemporal expression pattern of NVF and endogenous Ngn3 expression in heterozygous NVF (*Ngn3*$^{+/Venus}$) pancreatic sections from E12.5 to E15.5. (B) Staining of specific markers of pancreatic tubular epithelium on E15.5 homozygous NVF (*Ngn3*$^{Venus/Venus}$) sections indicates the presence of NVF^{+} cells within (white arrowheads) and outside (pink arrowheads) the pancreatic epithelium. (C) Immunohistochemical analysis of co-expression of insulin and glucagon hormones with Venus in an E18.5 homozygous NVF section. White arrowheads indicate NVF^{+} hormone^{-} cells and pink arrowheads show low expression of Venus in hormone^{+} cells. (D) Quantification of the number of hormone-expressing endocrine cells that still express NVF at E18.5. (E) Immunostaining of insulin (Ins), glucagon (Gcg) and somatostatin (Sst) in E18.5 WT and homozygous NVF pancreatic sections. (F) Quantification of E15.5 and E18.5 homozygous NVF sections indicates normal endocrine cell formation compared with WT mice. Error bars represent s.d. Scale bars: 20 µm (A-C); 50 µm (E).

Reep5 (acinar); *Spp1* (duct); *Btbd17* and *Gadd45a* (EPs); *Vwa5b2* and *Tox3* (*Fev*^{high}); *Tmem97* and *Fam183b* (endocrine) (Fig. 2E,F). Thus, the identification of known markers for different clusters validated our scRNA-seq approach. Furthermore, we identified many novel and functionally uncharacterized genes at different steps of pancreatic and endocrine lineage allocation.

Development (2019) 146, dev173849. doi:10.1242/dev.173849

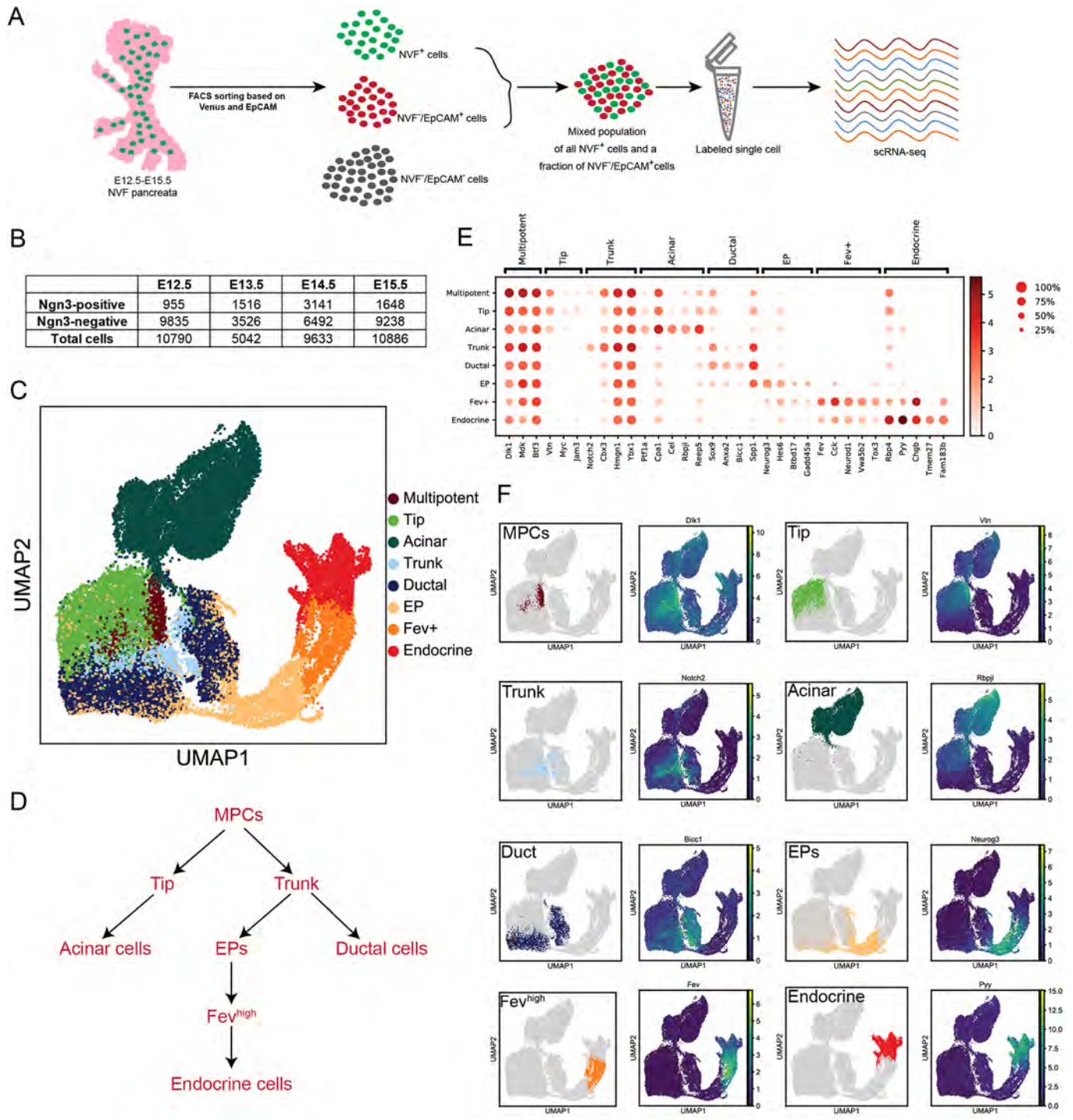

	E12.5	E13.5	E14.5	E15.5
Ngn3-positive	955	1516	3141	1648
Ngn3-negative	9835	3526	6492	9238
Total cells	10790	5042	9633	10886

Fig. 2. Identification of embryonic pancreatic epithelial populations at single cell resolution. (A) Scheme of the procedure of pancreatic epithelial cell isolation, sorting and single cell RNA sequencing. (B) The number of cells positive for Ngn3 (*Neurog3* expression >0) and negative for Ngn3 (no *Neurog3* expression, non-EP pancreatic epithelial populations) as well as the total number of cells used in single cell data of each stage. (C) UMAP plot of 36,351 profiled single cells from four distinct stages. Colors highlight clustering into eight main cell types that include all embryonic pancreatic epithelial populations. (D) Diagram of the lineage relationship between pancreatic cells at early embryonic stages. (E) Dot plot showing expression of known and uncharacterized cell type-specific gene sets of pancreatic epithelial populations. Color intensity indicates mean expression (normalized) in a cluster, dot size indicates the proportion of cells in a cluster expressing the gene. (F) Representative gene expression and distribution of known marker genes for each epithelial population in UMAP plots. Normalized expression values are shown.

Dynamic molecular changes of pancreatic progenitors during step-wise lineage allocation

To define the step-wise lineage restriction and allocation and to explore the dynamic heterogeneity of pancreatic progenitors, we performed stage-wise comparison of the molecular signatures of multipotent and bipotent progenitors as well as ductal, endocrine and acinar lineages. We found two subclusters of proliferating and non-proliferating cells for tip, trunk, acinar and ductal populations

Development (2019) 146, dev173849. doi:10.1242/dev.173849

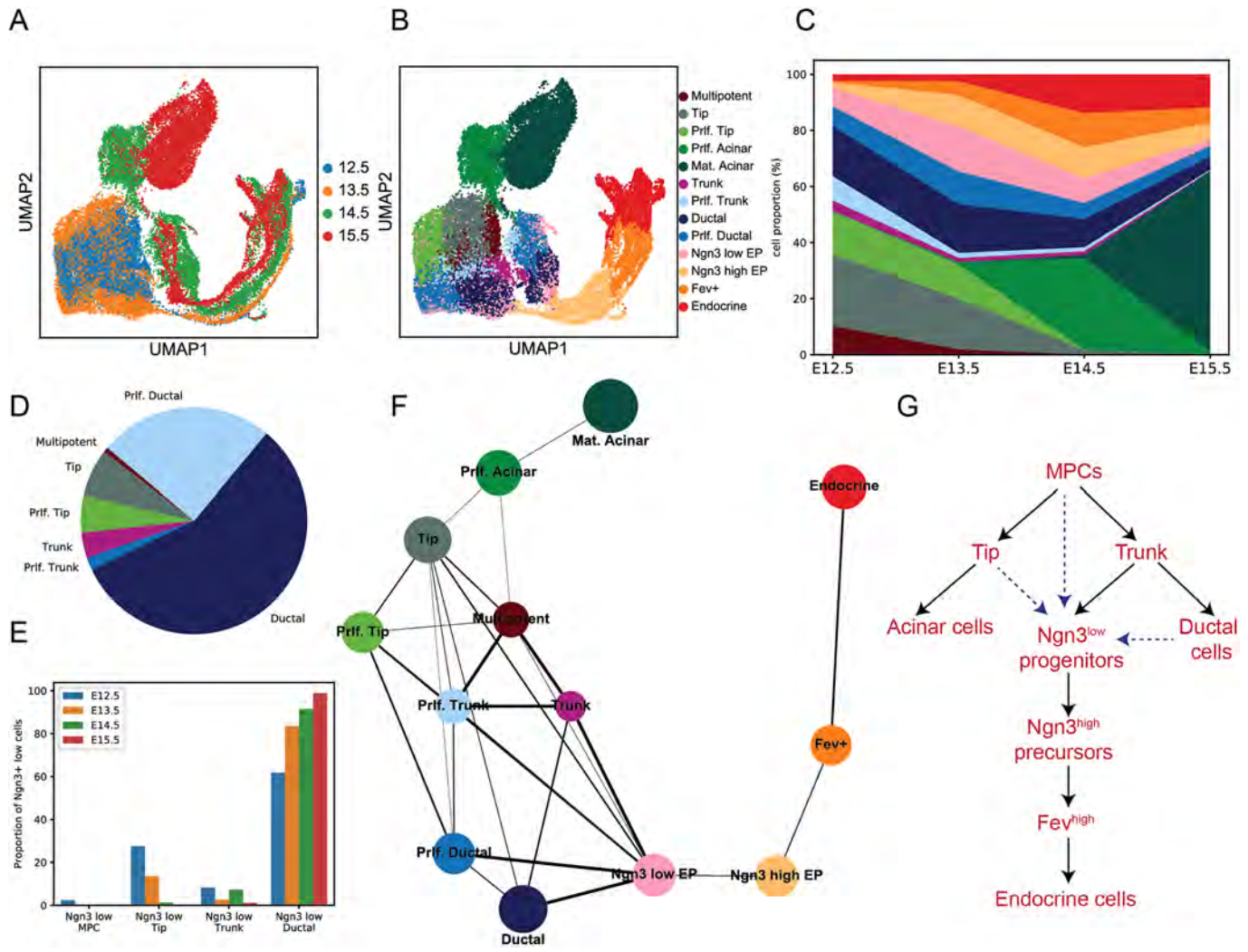

Fig. 3. Lineage segregation of early pancreatic epithelial cells. (A) UMAP plot of all pancreatic lineages from four different early stages of embryonic pancreas development. Cells from each stage are shown with different color codes. (B) UMAP plot showing the presence of proliferative and non-proliferative populations within acinar, tip, trunk and ductal clusters. (C) Area plot of pancreatic epithelial cell composition indicates rapid changes in different lineages during early pancreas development. The color codes are the same as in B. (D,E) The distribution of *Ngn3*^{low} progenitors within different pancreatic lineages (D) and by developmental stage (E). (F) Relationships of early pancreatic lineages inferred based on a measure for cluster connectivity using PAGA. Edges are weighted by significance. (G) *Ngn3*^{low} progenitors are generated from trunk bipotent progenitors. Dashed arrows indicate the possible contribution of MPCs, tip and ductal clusters to the generation of *Ngn3*^{low} progenitors. Mat., Mature; Prlf., Proliferative.

(Fig. 3A,B; Fig. S2A). MPCs were mainly evident at E12.5 and expressed the multipotent progenitor and acinar marker *Cpa1* at high levels, whereas the tip and trunk clusters were prominently found at E12.5 and E13.5. Ductal cells were present throughout all stages and acinar cells appeared mainly at E14.5 and E15.5 (Fig. 3C). EP cells showed different expression levels of *Ngn3* as has been previously described (Bechard et al., 2016) and were separated into *Ngn3*^{low} progenitors and *Ngn3*^{high} precursors (see Materials and Methods).

When looking for the origin of *Ngn3*^{low} progenitors, we found that they were scattered within the MPCs, tip, trunk and ductal progenitor clusters, suggesting multiple niches and birthplaces for these progenitors (Fig. 3D,E,G). The contribution of distinct epithelial clusters to *Ngn3*^{low} progenitor formation varied at different stages. *Ngn3*^{low} progenitors were found within the MPCs only at E12.5. The tip cluster also contained these progenitors from E12.5 to E14.5, but with rapidly decreasing numbers. The *Ngn3*^{low} progenitors were detected in the trunk domain mainly until E14.5. The presence of *Ngn3*^{low} progenitors from ductal cells was found at all stages and continuously increased from E12.5 to E15.5 (Fig. 3E). Thus, the MPCs and tip cells contain endocrine progenitors until E13.5, the existence of these cells within ductal cells persists until the end of the secondary transition. Moreover, the majority of *Ngn3*^{low} progenitors were derived from the ductal population (Fig. 3D,E), supporting the previous notion that this domain is the major epithelial source of endocrine progenitor-generating cells (Solar et al., 2009).

To infer the relationships between early pancreatic lineages, we performed partition-based graph abstraction (PAGA) analysis (Wolf et al., 2019) (see Materials and Methods). PAGA measures subgroup connectivity and draws a graph of possible differentiation paths. Consistent with the common belief (Sznurkowska et al., 2018; Zhou et al., 2007), we found that MPCs are mainly specified into tip and trunk domains. Tip cells then further connected to acinar cells, whereas trunk cells showed strong links to ductal cells. We found strong connections of *Ngn3*^{low} progenitors to the tip, trunk and ductal

Development (2019) 146, dev173849. doi:10.1242/dev.173849

cells, and a weaker connection of these progenitors with MPCs (Fig. 3F). This further supports the finding that all epithelial clusters contribute to *Ngn3*^{low} progenitor formation and that a lower number of *Ngn3*^{low} progenitors are derived from MPCs compared with other epithelial clusters. Taken together, these findings indicate that lineage restriction from multipotent to bipotent to unipotent fates occurs in a rapid step-wise manner during the secondary transition.

Identification of novel genes enriched in EPs

To obtain a dynamic and comprehensive picture of the molecular changes of the EP transcriptome during endocrinogenesis, we compared all Ngn3^{+} EPs (*Ngn3*^{low} and *Ngn3*^{high}) with all other (*Ngn3*$^{-}$) cells except acinar cells (Fig. 4A; see Materials and Methods). Differential expression analysis revealed several genes significantly regulated in the *Ngn3*$^{+}$ EPs (Fig. 4B,C; Table S2) and provided a list of EP-enriched genes. We found increased expression of genes with known function in EPs, such as the endocrine-specification factor *Amotl2* (Scavuzzo et al., 2018), the cell-cycle inhibitor *Cdkn1a* (Miyatsuka et al., 2011), the EP differentiation factor *Sox4* (Xu et al., 2015) and the Notch inhibitor *Mfng* (Svensson et al., 2009) among many others (Fig. 4B,C). In addition, we identified several other upregulated genes that have not been associated with pancreas development before, including the cell-cycle inhibitors *Gadd45a* and *Btg2* (Krentz et al., 2018), the protein phosphatase *Ppp1r14a* (also known as *Cpi17*), mitochondrial carrier homolog 1 (*Mtch1*), Numb-like protein (*Numbl*), and the *Hes1* repressor *Hes6* (Fig. 4B,C). Among those, *Numbl* and *Hes6* inhibit Notch signaling highlighting the requirement of efficient suppression of this pathway by multiple mechanisms during endocrine induction.

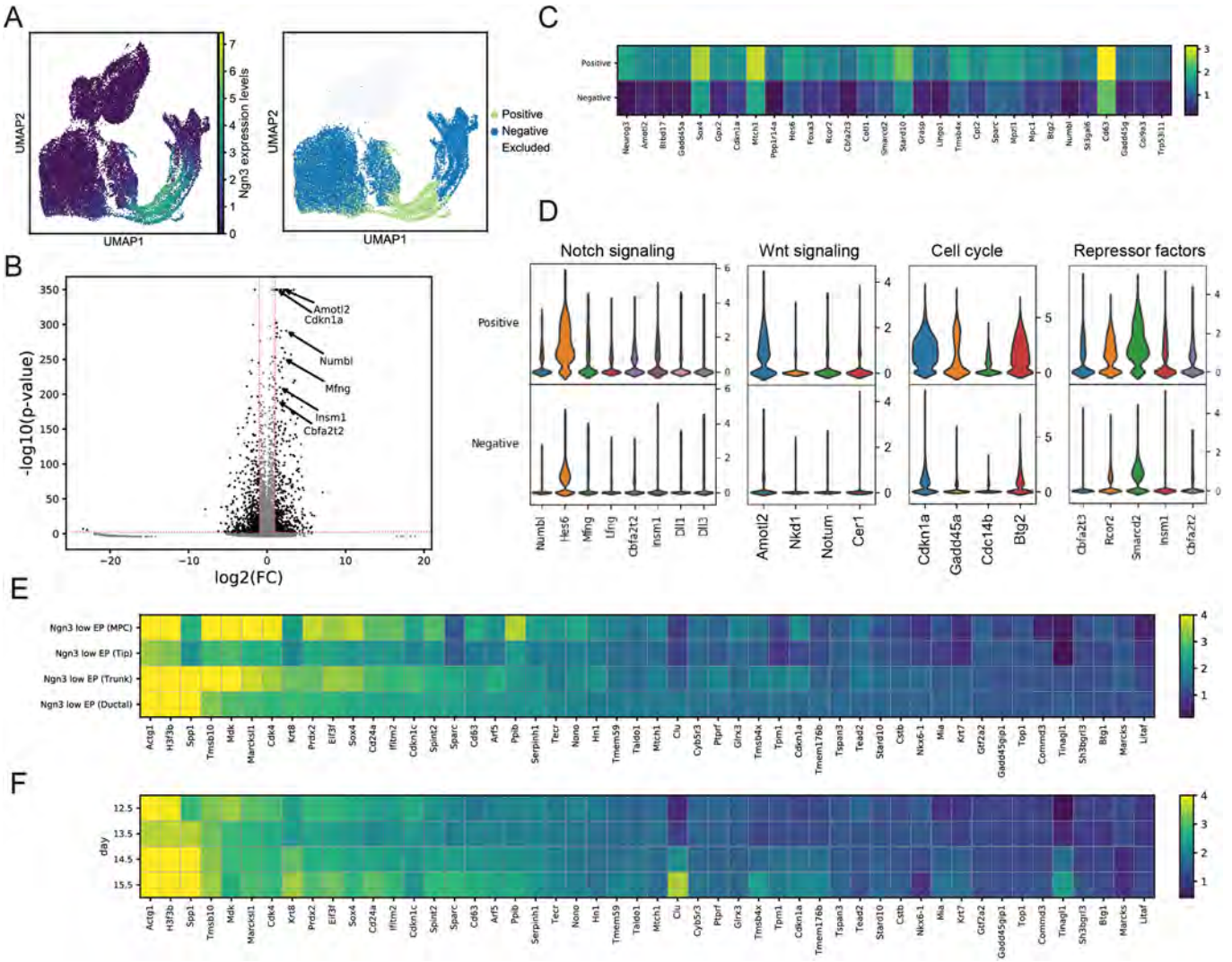

Fig. 4. Gene expression profiles of endocrine progenitors-precursors (EPs). (A) UMAP plots showing the distribution of cells considered as Ngn3^{+} cells. Left: *Neurog3* expression (normalized). Right: classification into *Ngn3*$^{+}$ and *Ngn3*$^{-}$ cells. Acinar cells were excluded here. (B) Volcano plot showing differential expression and its significance [–log$_{10}$(adjusted *P*-Value), limma] for each gene in *Ngn3*$^{+}$ EPs compared with *Ngn3*$^{-}$ cells. Red line indicates thresholds used for significance level and gene expression change, and regulated genes are highlighted in black. Selected relevant genes are annotated. (C) Heatmap showing the mean expression in *Ngn3*$^{+}$ and *Ngn3*$^{-}$ cells of the top 30 upregulated genes in *Ngn3*$^{+}$ from the data shown in B. Expression values are normalized and scaled to unit variance. (D) Pathway enrichment analyses indicate inhibition of Notch and Wnt signaling, increased expression of repressor factors and cell cycle exit in *Ngn3*$^{+}$ cells. Distributions of gene expression (normalized) in *Ngn3*$^{+}$ and *Ngn3*$^{-}$ of relevant genes of these pathways are shown as violin plots. (E,F) Heatmap showing the mean expression of genes that are highly enriched in *Ngn3*^{low} progenitors between progenitors derived from different pancreatic epithelial populations (E) and derived at different developmental stages (F). Genes displayed are the 50 genes showing the highest mean expression in *Ngn3*^{low} progenitors from the top 250 upregulated genes in *Ngn3*$^{+}$ cells from the data shown in B. Expression values are normalized.

Development (2019) 146, dev173849. doi:10.1242/dev.173849

To identify EP-specific signaling pathways and cellular processes, we analyzed the genes upregulated in *Ngn3*$^{+}$ cells and identified Notch and Wnt inhibitors, further suggesting that these pathways are negatively modulated in EPs (Fig. 4D). Interestingly, we found increased expression of the Hippo pathway components *Amotl2* and *Nkd1*, which are also antagonists of the Wnt pathway. This highlights that crosstalk between these pathways might be involved in regulation of endocrine cell formation. Furthermore, we found an upregulation of cell-cycle inhibitors in EPs (Fig. 4D), supporting the idea that endocrine differentiation leads to lengthening of the cell cycle. We identified several transcriptional repressors or co-repressors in the EP population, such as the co-repressor *Cbfa2t3*, the histone-modifying factor *Rcor2*, the chromatin remolding factor *Smarcd2*, the endocrine-specification factor *Insm1* (Liu et al., 2006; Osipovich et al., 2014) and the Notch repressor *Cbfa2t2* (Fig. 4D), that might be important for the suppression of non-EP gene programs.

Next, we investigated whether *Ngn3*^{low} progenitors derived from different epithelial clusters or from different developmental stages (E12.5-15.5) are transcriptionally heterogeneous. To this end, using the list of genes enriched in the total EP population (*Ngn3*^{low} and *Ngn3*^{high}) (Table S2), we first identified those genes that were highly expressed in *Ngn3*^{low} progenitors. Then, we compared the expression of these genes in *Ngn3*^{low} cells derived from MPCs, tip, trunk and ductal cells (Fig. 4E), as well as from different developmental stages (Fig. 4F). Some genes, such as *Spp1*, *Tmsb10*, *Mdk*, *Marcksl1*, *Cdk4* and *Sox4*, were differentially expressed in *Ngn3*^{low} progenitors; however, expression of these genes only reflect the origin of the *Ngn3*^{low} cells. For instance, *Ngn3*^{low} progenitors derived from trunk and ductal epithelium expressed high levels of *Spp1*, which is highly expressed in all trunk and ductal cells. In contrast, the expression of most of the highly enriched genes in *Ngn3*^{low} progenitors that could not be directly associated to their origin was not different between *Ngn3*^{low} progenitor populations derived from distinct epithelial clusters or from different stages (Fig. 4E,F).

Identification of transiently expressed EP-signature genes

During development, bipotent epithelial cells generate Ngn3^{low} mitotic progenitors that either reverse to a ductal fate or further generate Ngn3^{high} precursors (Bechard et al., 2016). Ngn3^{high} cells then differentiate into Fev^{high} cells that consequently produce hormone-expressing endocrine cells (Fig. 5A). Consistently, pseudotemporal ordering (Haghverdi et al., 2016) of the cells along this route, which was also inferred by PAGA (Fig. 3F), revealed a continuous differentiation trajectory (see Materials and Methods). Along this pseudotime *Ngn3* is transiently expressed as the levels of *Ngn3* increased from *Ngn3*^{low} to *Ngn3*^{high} cells and then decreased again in *Fev*^{high} cells (Fig. 5B,C). Next, we investigated whether there are other EP-specific signature genes that follow transient *Ngn3* expression in EPs. From the list of genes enriched in EPs we identified 58 genes (including *Ngn3*) that were expressed in EPs, but not or only at very low level in other pancreatic lineages (see Materials and Methods). Moreover, their expression was transient in EPs, i.e. their expression levels were gradually reduced upon differentiation of EPs into *Fev*^{high} cells (Fig. 5B; Fig. S2B). Among these genes were *Ppp1r14a*, the neuronal determination TF neurogenic differentiation factor 2 (*Neurod2*) (Gasa et al., 2008), sulfotransferase family cytosolic 2B member 1 (*Sult2b1*), uroplakin 3b-like protein 1 (*Upk3bl*), Ly6/neurotoxin-like protein 1 (*Lynx1*), the cell cycle regulator polo-like kinase 3 (*Plk3*), G protein γ subunit Gγ13 (*Gng13*), the Six1 transcriptional co-activator *Eya2*, regulator of G-protein signaling 16 (*Rgs16*), semaphorin 3G (*Sema3g*), the cancer-associated cell-surface antigen six-transmembrane epithelial antigen of the prostate 1 (*Steap1*), and the uncharacterized gene *Gm8773* (Fig. 5C; Fig. S2B). Notably, for most of these genes no function associated with pancreas development has been reported so far. However, genes such as *Neurod2*, *Sult2b1* and *Lynx1* are involved in neuronal development and function, which highlights the similarities of the developmental programs required for the formation of EPs and neuronal cells. We also found comparable expression levels of several of these signature genes in E15.5 pancreatic epithelial cells from WT and homozygous NVF pancreata, which further supports proper functioning of the fusion protein (Fig. S2C). Furthermore, scRNA-seq analysis of human fetal pancreatic cells has indicated the expression of some of these genes, including *EYA2* and *RGS16* in human endocrine progenitors (Ramond et al., 2018).

Next, from the list of genes enriched in the *Fev*^{high} population we extracted several genes that followed a similar expression pattern to that of *Fev*. The expression of these genes started in *Ngn3*^{high} precursors, reached maximum levels in *Fev*^{high} cells and then decreased again in hormone-expressing endocrine cells. Such *Fev*^{high}-enriched genes included *Neurod1*, von Willebrand factor A domain-containing protein 5B2 (*Vwa5b2*), the paired box protein *Pax4*, cholecystokinin (*Cck*), the cancer suppressor gene *Tox3*, solute carrier family 35 member D3 (*Slc35d3*), the Ngn3-regulated transcriptional co-repressor *Runx1t1* (*Cbfa2t1*) (Benitez et al., 2014) and the diabetes-associated protein voltage-dependent calcium channel subunit $\alpha_2\delta$-1 (*Cacna2d1*) (Mastrolia et al., 2017) and the uncharacterized gene transmembrane protein 185A (*BC023829*) (Fig. 5D,E; Fig. S2D). Among these, a high expression of *RUNX1T1* in *FEV*$^{+}$ cells has also been reported in human fetal pancreas (Ramond et al., 2018). Moreover, the expression of genes, such as chromogranin-A (*Chga*) and -B (*Chgb*), carboxypeptidase E (*Cpe*), *Pax6*, the ciliary-localized protein *Fam183b* (Stauber et al., 2017) and the neuroendocrine protein ProSAAS endopeptidase inhibitor (*Pcsk1n*) was turned on at the *Fev*^{high} stage and persisted in fully differentiated endocrine cells (Fig. S2D,E). Altogether, these data suggest that the development from EPs to fully differentiated endocrine cells occurs in a step-wise manner and involves the expression of unique molecular signatures at each stage (Fig. 5E).

To resolve further the dynamic changes in gene expression during the step-wise endocrine induction, specification and differentiation, we compared the transcriptional profiles of ductal bipotent (as the main source of *Ngn3*^{low} progenitors), *Ngn3*^{low}, *Ngn3*^{high} and *Fev*^{high} populations (Fig. S3A; Table S3). We identified a large number of differentially expressed genes between ductal bipotent and *Ngn3*^{low}, *Ngn3*^{low} and *Ngn3*^{high} as well as *Ngn3*^{high} and *Fev*^{high} cells (Fig. 5F). Ordering the cells along pseudotime supported a continuous developmental trajectory and revealed stage-specific induction or repression of genes involved in signaling pathways, cell-cycle control and organ morphogenesis during EP formation and differentiation. The low expression of *Ngn3* in EPs was accompanied by increased expression levels of genes involved in activation of cAMP, Rap1 and Ras/MAPK signaling as well as Notch inhibitors (Fig. 5F; Fig. S3B). Furthermore, compared with ductal bipotent cells, *Ngn3*^{low} progenitors expressed decreased levels of genes involved in Wnt signaling activation, suggesting the requirement of Wnt signaling inhibition during EP development. This was supported by upregulation of the secreted TGFβ and Wnt inhibitor *Cer1* (Piccolo et al., 1999) and Wnt-deacylation enzyme *Notum* (non-canonical inhibitor) (Kakugawa et al., 2015) in *Ngn3*^{low} progenitors compared with ductal bipotent cells (Fig. 5F).

Development (2019) 146, dev173849. doi:10.1242/dev.173849

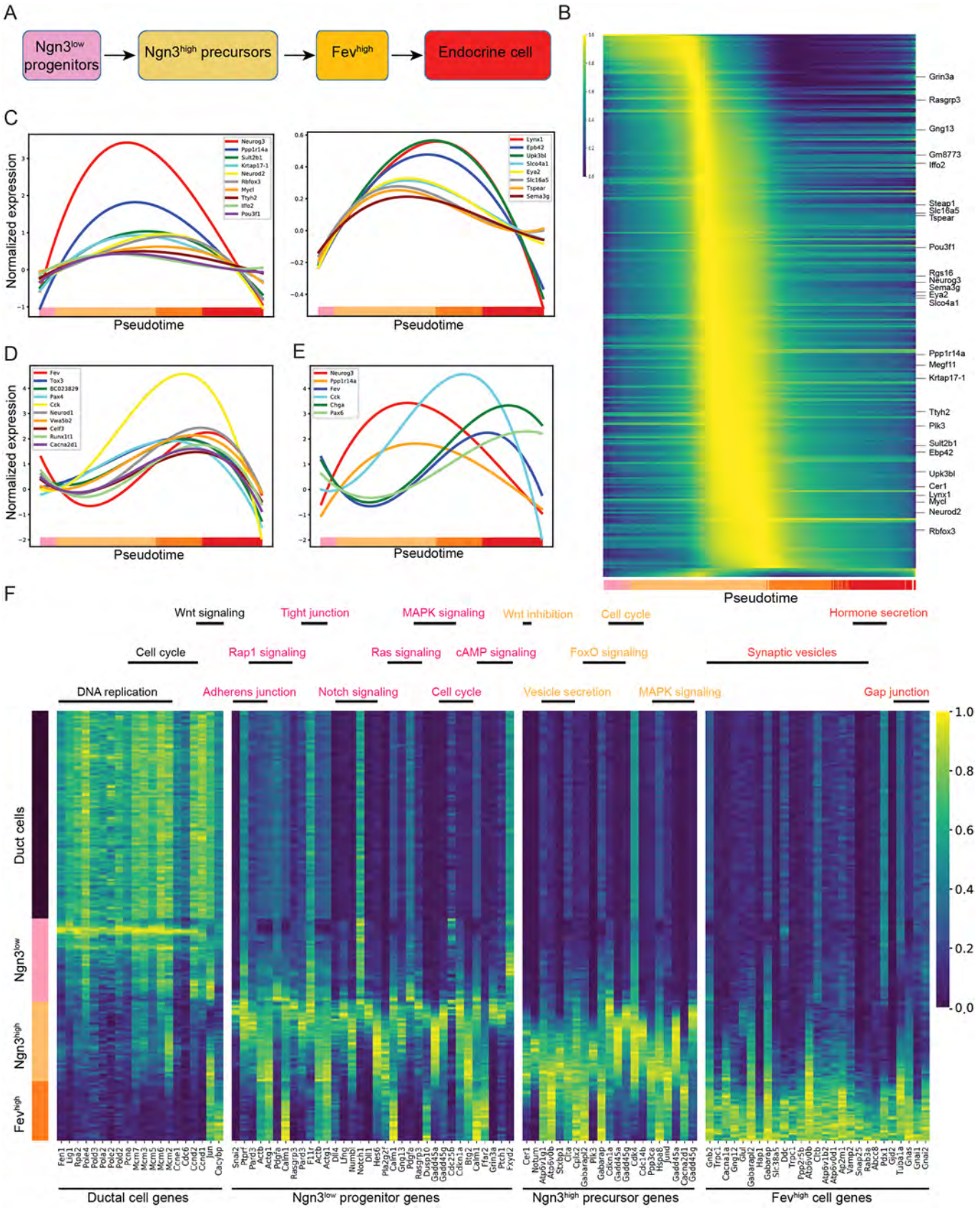

Fig. 5. See next page for legend.

Development (2019) 146, dev173849. doi:10.1242/dev.173849

Fig. 5. Distinct molecular signatures are expressed at different stages of endocrinogenesis. (A) Developmental scheme of differentiation of endocrine progenitors into endocrine cells. (B) Gene expression along a one-dimensional differentiation trajectory from *Ngn3*^{low} progenitors to endocrine cells. Each cell is assigned a value in diffusion pseudotime, which reflects the differentiation process. The top 250 genes upregulated in *Ngn3*$^{+}$ EPs are shown (Table S2) and selected EP signature genes highlighted. Expression is normalized and approximated by polynominal regression fits along pseudotime. Fitted values of each gene are then scaled to the range between 0 and 1. Cluster membership of the cells is indicated at the bottom. Color codes are as in A. (C-E) Gene expression changes along the pseudotime from endocrine progenitors to endocrine cells. Lines are polynominal regression fits of normalized expression data. Cluster membership of the cells is indicated at the bottom. Color codes are as in A. (C) Several EP-signature genes follow a transient expression pattern in EPs similar to that of *Ngn3*. For simplicity the representative genes are presented in two different graphs. (D) Expression profile of several *Fev*^{high}-enriched genes. The expression of these genes reaches its peak in *Fev*^{high} cells and is reduced upon differentiation into endocrine cells. (E) Gradual increase or decrease of several EP-, *Fev*^{high}- and endocrine-specific genes during endocrinogenesis. (F) Heatmap showing subtype-specific gene expression profiles of duct cells, *Ngn3*^{low} progenitors, *Ngn3*^{high} precursors and *Fev*^{high} cells. Cells are ordered along pseudotime rooted in the duct cell population. Cluster membership of the cells is indicated on the left. Pathways associated with the gene sets are highlighted at the top. Expression is normalized and shown as the running average over 80 cells scaled to the maximum observed level per gene. Several genes that are involved in different cellular processes or signaling pathways have been included in the heatmap repeatedly.

Additionally, alterations in cell adhesion molecules and activation of the Ras/Rap1 pathway in *Ngn3*^{low} progenitors likely drive cell morphological changes, suggesting that programs of morphogenesis are initiated at the progenitor level and continue while EPs delaminate from the pancreatic epithelium and differentiate into distinct endocrine cell types. Moreover, the expression of genes involved in cell-cycle exit was initiated in *Ngn3*^{low} progenitors and continued in *Ngn3*^{high} precursors. The high expression levels of *Ngn3* in EPs initiated the expression of the secretory machinery during differentiation towards slowly cycling hormone-expressing cells (Fig. 5F; Fig. S3B). The expression of secretory components was further increased in the *Fev*^{high} cells and at this stage cells expressed the hormone secretion machinery (Fig. 5F; Fig. S3B). Interestingly, *Fev*^{high} cells highly expressed neurotransmitters and synaptic vesicle genes (Fig. 5F; Fig. S3B), again highlighting the molecular and cellular similarities between endocrine and neuronal cells.

Stage-dependent heterogeneity of EPs defines endocrine cell allocation

Although all endocrine cells are derived from EPs, at which stage these cells become unipotent to produce distinct endocrine cell types remains largely unknown. It has been shown that mouse endocrine cells are generated in a step-wise manner, in which EPs are consecutively specified towards α-, β-, PP-, δ- and ε-cells during the secondary transition (Johansson et al., 2007). Indeed, the proportions of endocrine subtypes obtained at each time point reflected such a step-wise induction of endocrine cell fates. At E12.5, we only found α-cells, whereas β-, δ- and ε-cells appear between E13.5 and E14.5 (Fig. 6A). Interestingly, a portion of α-cells was also generated at later stages, suggesting that formation of these cells is not restricted to the primary transition (Fig. 6A; Fig. S4B,C). To investigate further the timing of endocrine specification, we estimated the RNA velocity of each cell (see Materials and Methods) (La Manno et al., 2018). RNA velocity is a proxy for the rate of pre-mRNA to mRNA processing and, therefore, is a vector in time that can be used to infer to which state a cell is moving in the high-dimensional transcriptome space. Thus, we can predict towards which endocrine subtype the EPs differentiate at a specific embryonic stage. As expected, we detected a movement of a portion of bipotent cells towards the endocrine lineage and a strong predicted directional flow from *Ngn3*^{low} to *Ngn3*^{high} to *Fev*^{high} cells. Interestingly, EPs and *Fev*^{high} cells at E12.5 and E13.5 pointed towards α-cells and to the few detected β-cells, whereas at E14.5 and E15.5 the majority of EPs showed a velocity towards β-cells (Fig. 6B). These data indicate that the α- and β-cell fate is specified in EPs mainly at early and late stages, respectively.

Furthermore, we found stage-dependent differential expression of several genes in differentiated α-cells (Fig. S4A). Genes such as *Arx* and *Slc38a5* showed similar expression levels in early (E12.5) and late (E15.5) differentiated α-cells (Fig. 6C), whereas *Sct*, *Mafb* and *Meis2* were differentially expressed. We found higher expression levels of *Sct* in early α-cells and higher expression levels of *Mafb* and *Meis2* in late α-cells (Fig. 6D,E). This differential gene expression of early and late α-cells might be related to the formation of these cells during the first and secondary transition. However, we could not find α-cells with a primary transition signature at E14.5 and E15.5 (Fig. S4B), suggesting that the α-cells derived from early stages either acquire a similar signature to the late-stage α-cells or they have been eliminated during pancreas development.

One of the proposed mechanisms for stage-dependent endocrine specification is a change in the epithelial status and the surrounding niche. In mouse, the formation of endocrine cells coincides with the ramification of epithelial plexus to a single-layer epithelial network that possibly exposes the EPs to different ECM components and defines their fate towards specific endocrine cell types (Bakhti et al., 2019; Bankaitis et al., 2015). However, it is unclear whether EP transcriptional heterogeneity also primes endocrine subtype specification. To this end, we compared the expression levels of the newly described EP-signature genes between EPs derived from different developmental stages. *Ngn3*^{low} progenitors derived from different stages showed low expression levels of most of the EP-signature genes and, except for a few genes, they expressed comparable levels of most of these genes (Fig. S4C). In contrast, we found differential expression of several signature genes in *Ngn3*^{high} precursors derived from different developmental stages (E12.5-15.5) (Fig. 7A). We discovered that several genes, including *Gng13*, *Steap1* and *Gm8773*, were expressed more highly in E12.5 *Ngn3*^{high} precursors compared with later stages, whereas other genes, including *Upk3bl*, *Sultb21* and *Neurod2*, showed clearly increased expression in E15.5 *Ngn3*^{high} precursors compared with earlier stages (Fig. 7B-D). These data were further supported experimentally by performing qPCR analysis of isolated cells from E13.5 and E15.5 pancreata (Fig. 7E). We speculated that the differential expression of these genes at early and late stages is related to a fate decision of EPs towards distinct endocrine subtypes. In such a scenario, early precursors that express genes such as *Gng13* and *Gm8773* might be specified towards α-cells, whereas late precursors that express genes such as *Upk3bl* and *Neurod2* might allocate to the β-cell fate. Indeed, PAGA analysis revealed that *Ngn3*^{high} precursors expressing high levels of *Gng13*, *Steap1* and *Gm8773* are highly connected to α-cells and *Ngn3*^{high} precursors expressing high levels of *Upk3bl*, *Sultb2l* and *Neurod2* are highly connected to β-cells (Fig. 7F). This finding is in line with a recent study showing that Ngn3^{+} cells that express Myt1 are biased toward β-cell fate (Liu et al., 2019). The balance between the expression of *Arx* and *Pax4* is the only currently known mechanism of endocrine cell subtype specification (Collombat et al., 2003, 2009). Although the expression of *Pax4* was started at late stages of

Development (2019) 146, dev173849. doi:10.1242/dev.173849

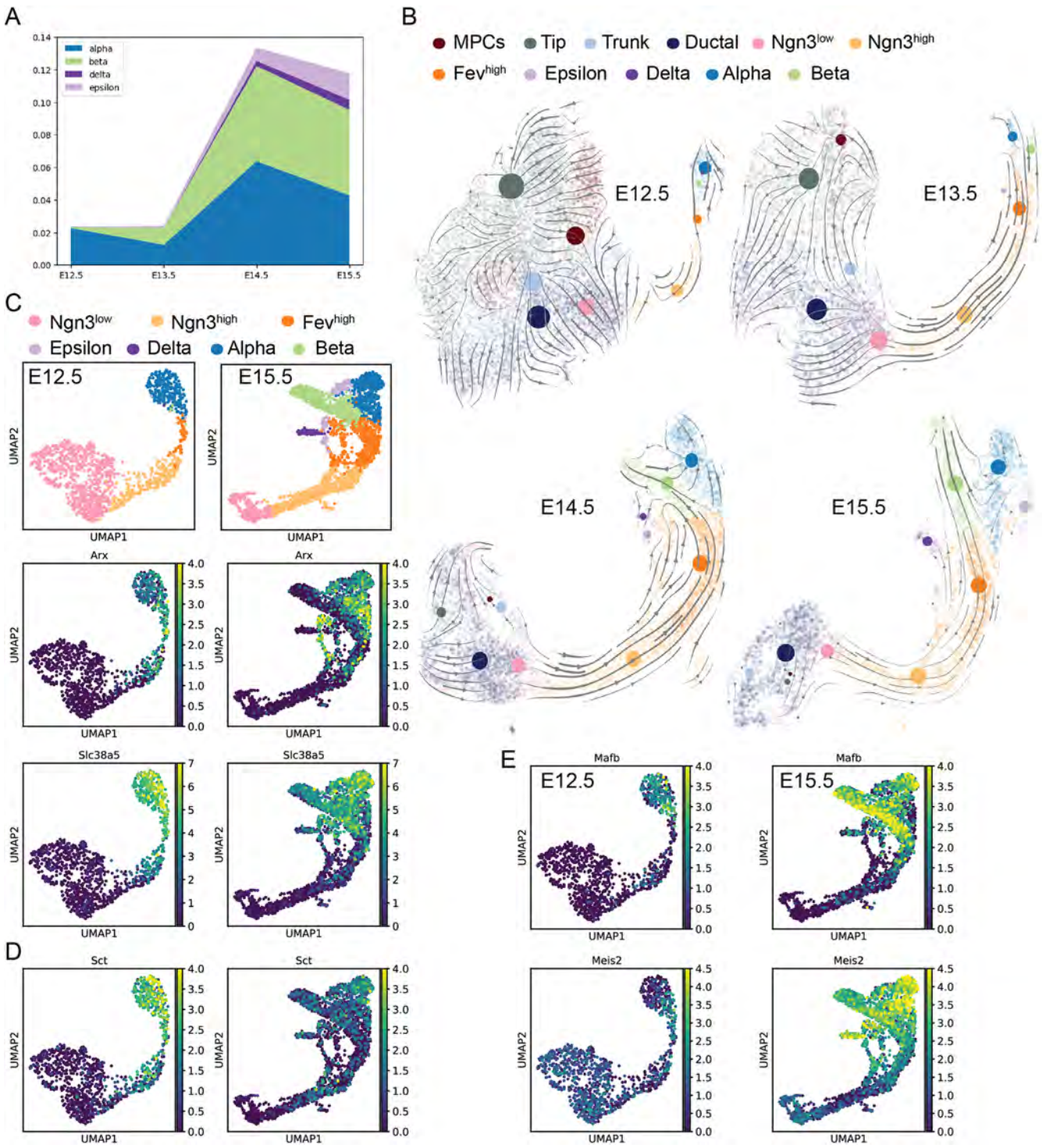

Fig. 6. Endocrine cells are produced at distinct developmental stages at different rates and with specific characteristics. (A) Area plot of endocrine cell type composition indicative of different differentiation rates of each cell type at distinct developmental stages. (B) Differentiation of EPs into endocrine subtypes at E12.5-E15.5. The direction of cell differentiation at each stage inferred from estimated RNA velocities are plotted as streamlines on the UMAP. Direction indicates transition towards the estimated future state of a cell. Dots are cluster centers of the indicated cell types. Dot size represents cluster size. Acinar clusters were removed from these analyses to better depict the endocrine lineage segregation. (C) Expression of different gene markers in primary (E12.5) and secondary (E15.5) α-cells. UMAP plots show that primary and secondary α-cells express comparable levels of *Arx* and *Slc38a5*. See also Fig. S4. (D) Primary α-cells (E12.5) express higher levels of *Sct* compared with the secondary α-cells (E15.5). (E) The expression levels of *Mafb* and *Meis2* is higher in secondary α-cells (E15.5) compared with the primary α-cells (E12.5). The UMAP plots in C-E are calculated and presented only for *Ngn3*^{low} progenitors until differentiated endocrine cells. Normalized expression values are shown.

Ngn3^{high} precursors, the expression of *Arx* was initiated only in *Fev*^{high} cells (Fig. S4D), suggesting that the *Pax4-Arx* axis is likely not established in *Ngn3*^{high} precursors but rather in the *Fev*^{high} cells. The fact that transcriptional heterogeneity of EPs exists in *Ngn3*^{high} precursors proposes that these cells might be already determined towards specific endocrine cell fates. Therefore, our findings,

Development (2019) 146, dev173849. doi:10.1242/dev.173849

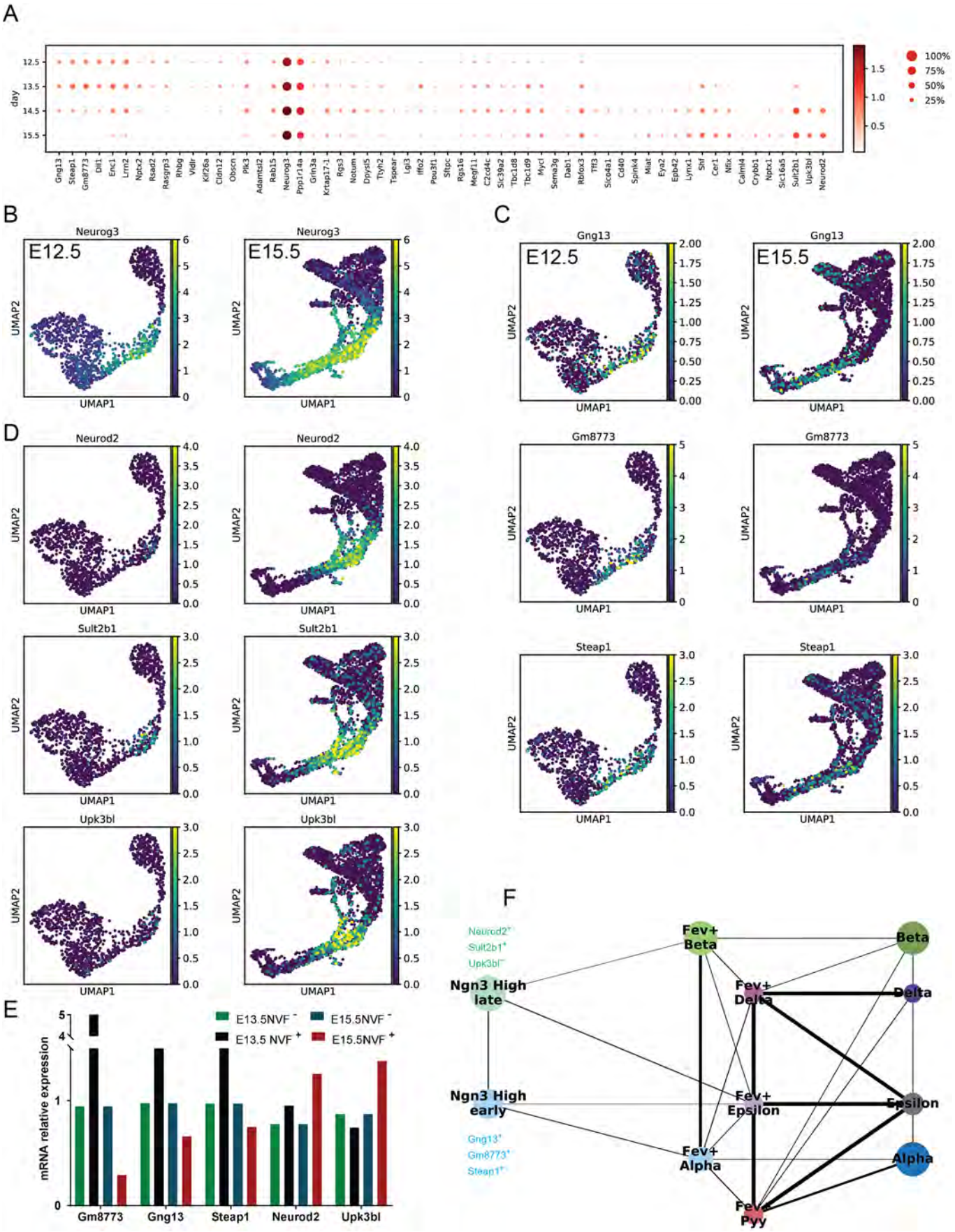

Fig. 7. See next page for legend.

Development (2019) 146, dev173849. doi:10.1242/dev.173849

Fig. 7. Stage-dependent heterogeneity of *Ngn3*^{high} precursors defines endocrine cell fate. (A) Dot plot of the expression levels of EP-signature genes in *Ngn3*^{high} precursors derived from different developmental stages. Although the expression levels of many of the EP-signature genes are comparable in cells derived from different stages, several genes show stage-dependent differential expression. Color intensity indicates mean expression (normalized) in a cluster, dot size indicates the proportion of cells in a cluster expressing the gene. (B) UMAP plots for the expression of *Ngn3* in the EP population at E12.5 and E15.5. Only clusters from *Ngn3*^{low} progenitors until differentiated endocrine cells are shown. (C) UMAP plots showing that expression levels of *Gng13*, *Gm8773* and *Steap1* are higher in E12.5 *Ngn3*^{high} precursors compared with those from E15.5. (D) UMAP plots indicating increased expression of *Neurod2*, *Sult2b1* and *Upk3bl* in E15.5 *Ngn3*^{high} precursors compared with those from E12.5. For B-D, normalized expression values are shown. (E) qPCR analysis of isolated cells from E13.5 and E15.5 homozygous NVF pancreata for several EP-signature genes (n=1 experiment derived from 8-10 embryos). (F) PAGA analysis indicating the association between the differential expressions of EP-signature genes in *Ngn3*^{high} precursors with their fate towards α- and β-cells. This analysis also shows two different *Fev*^{high} populations that are committed towards α- or β-cell fate.

together with other previous studies (Bechard et al., 2016; Desgraz and Herrera, 2009), support the idea that EPs are not unipotent progenitors at birth (Ngn3^{low}), but rather undergo cell-fate determination at the Ngn3^{high} state.

DISCUSSION

Improved therapy for diabetic patients could be achieved by islet cell replacement or *in vivo* regeneration of lost or dysfunctional β-cells. Both approaches rely on a detailed understanding of endocrinogenesis and the molecular programs driving endocrine lineage induction, specification and differentiation. Although gene regulatory networks and signaling cues that orchestrate endocrine cell differentiation have been well studied, the endogenous niche factors, morphogenetic cues and neighboring cell-type interactions priming endocrine cell specification are still only beginning to be understood. Uncovering mechanisms of endocrinogenesis is important for the generation of stem cell-derived islet-like clusters (ILCs) with defined cell composition and improved function (Bakhti et al., 2019).

NVF: a novel Ngn3 reporter mouse line

Here, we generated a novel NVF reporter mouse line, which accurately reflects the spatiotemporal protein expression and regulation of the endogenous Ngn3 protein. Previous Ngn3 reporter mouse lines have been generated either by the replacement of *Ngn3* by a fluorescent reporter gene (Lee et al., 2002) to generate heterozygous knock-in/knockout reporter mice or by transgenic expression of fluorescent proteins (FPs) regulated by the *Ngn3* promoter (Bechard et al., 2016; Kim et al., 2015; Mellitzer et al., 2004). Although the onset of expression of the transgenic reporter FPs reflects the expression of endogenous Ngn3 protein in these animals, the transient expression of the endogenous Ngn3 protein is not reflected due to the relatively high stability of the FPs. Therefore, analysis of EPs using such reporter mice is affected by the existence of a portion of differentiated endocrine cells that still express FPs but not Ngn3, undermining the efficiency and accuracy of EP labeling/tracking and their isolation. In addition, one of these mouse lines (Lee et al., 2002) can be used only in the heterozygous condition, which impacts endocrine formation and differentiation due to heterozygosity (Wang et al., 2010). In contrast, our NVF reporter mouse line shows no detectable endocrine phenotype even in the homozygous state and the fusion of Venus to Ngn3 results in a transient expression kinetic of NVF that is comparable to that of the endogenous Ngn3 protein. These properties enabled us to isolate a large number of early and late EPs to perform a high-throughput single cell transcriptomic analysis to decipher lineage relationships and molecular changes during endocrinogenesis.

Lineage relationship between embryonic pancreatic epithelial cells using scRNA-seq analysis

Using scRNA-seq during secondary transition, we identified eight main epithelial clusters and found the existence of *Ngn3*^{low} progenitors within MPCs, tip, trunk and ductal clusters. Among these, the presence of *Ngn3*^{low} progenitors within the MPCs and the tip cluster, although at lower numbers than in the ductal epithelial cells, was remarkable. Previously, a lineage-tracing study has shown that the pancreatic distal tip domain contains *Cpa1*$^{+}$ MPCs that at E12.5 are tripotent and are able to give rise to exocrine, duct and endocrine cells, but only generate exocrine cells after E13.5 (Zhou et al., 2007). Moreover, another study has shown that the tip domain cells retain their tripotency until E12.5 and afterwards become restricted towards the acinar fate (Sznurkowska et al., 2018). Lineage-tracing analysis using *Ptf1a*^{CreERTM} mice has also indicated contribution of MPCs to all three pancreatic lineages until E14.0, when the number of MPCs significantly declines (Pan et al., 2013). Therefore, our finding supports these previous reports on the contribution of tip cells to EP formation at early stages before tip cells become unipotent, i.e. fate restricted towards the acinar fate. Although our data provide evidence of the existence of endocrine progenitors within the MPCs and tip cluster, they do not show whether EP lineage-primed progenitor cells are physically located within the tip MPC domain. Along this line, a recent study not only reported the contribution of tip cells to the EP pool at E14.5, but also showed the existence of Ptf1a^{+} EPs within the distal domain of the epithelium (Scavuzzo et al., 2018). Therefore, this study may provide the first evidence of the existence of EPs that are physically positioned within the tip domain at early stages before the tip cells become unipotent acinar cells.

We found that the major portion of endocrine progenitors existed within the ductal cluster, supporting a lineage-tracing study using Hnf1β^{+} cells that demonstrated the appearance of EPs from the ductal epithelium until E16.5 (Solar et al., 2009). Furthermore, the appearance of high numbers of *Ngn3*^{low} progenitors at E15.5 indicates that the endocrine progenitor pool is not set at very early stages. Instead, it continues to be generated during secondary transition, as has been suggested previously (Bechard et al., 2016). It is important to note that we only detected *Ngn3*^{low} progenitors, but not *Ngn3*^{high} precursors, within the MPCs, tip, trunk and ductal clusters. Therefore, it still remains unclear whether all cells expressing low levels of *Ngn3* eventually differentiate into *Ngn3*^{high} precursors or if some of them differentiate back to the respective epithelial cells from which they are derived.

EP-enriched and -signature genes

The high number of isolated *Ngn3*$^{+}$ cells (7260) allowed us to obtain not only a high-confidence EP-enriched gene list (such as *Amotl2*, *Sox4* and *Hes6*), but also provided a unique set of endocrine signature genes (such as *Neurod2*, *Ppp1r14a*, *Gng13* and *Sult2b1*) with a similar expression kinetic as *Ngn3* in EPs. To our knowledge, this is the first study reporting the transient expression of several genes other than *Ngn3* in EPs. This unique EP-signature offers new markers for the labeling and/or tracking of these cells. Now, the important questions are whether the expression of these genes is controlled by Ngn3 and if they are upstream regulators or downstream effectors of Ngn3 activity. Interestingly, a recent time-resolved single cell study in the intestine identified several of

Development (2019) 146, dev173849. doi:10.1242/dev.173849

these endocrine-enriched and -signature genes, such as *Rcor2*, *Smarcd2*, *Sox4*, *Dll1*, *Eya2*, *Mycl* and *Neurod2* (Gehart et al., 2019). This data set together with our analysis further highlight significant similarities between the developmental programs for pancreatic and intestinal enteroendocrine cells. Remarkably, the *Ngn3*^{low} progenitors derived from different epithelial sources or at different developmental stages, did not show transcriptional heterogeneity in regard to the expression levels of EP-enriched and EP-signature genes. These data propose that, although in the Ngn3^{low}-state progenitors are biased towards an endocrine fate (Bechard et al., 2016), they might not yet be committed towards the endocrine fate and a specific endocrine subtype, leading us to question the unipotency of EPs at birth (Ngn3^{low}). In contrast, *Ngn3*^{high} precursors generated at different developmental stages expressed distinct levels of several EP-signature genes, such as *Neurod2*, *Sult2b1*, *Gng13* and *Gm8773*. Moreover, PAGA analysis revealed that the differential expression of these EP-signature genes associates with the fate of *Ngn3*^{high} precursors towards α- or β-cells. These findings indicate that *Ngn3*^{high} precursors are not a homogenous population on the transcriptional level and suggest that endocrine subtype specification likely occurs in the *Ngn3*^{high} precursor state. This conclusion supports the previous *in vivo* clonal study that has shown the unipotency of EPs expressing high levels of *Ngn3* (Desgraz and Herrera, 2009). Future work should address the function of those differentially expressed signature genes in early and late *Ngn3*^{high} precursors to provide deeper insights into the mechanisms underlying endocrine cell allocation. Such functional analysis might uncover the upstream cues defining the fate of endocrine cells through the establishment of the Arx-Pax4 axis. In addition, profound analysis of potential receptor-ligand interactions between EPs and endocrine subtypes could reveal unknown (feedback) cues from differentiated endocrine cells that further regulate induction of specific endocrine subtypes. Moreover, how many of those EP-signature genes are also expressed in human endocrine progenitors-precursors and whether they have a conserved function in endocrinogenesis deserves more attention. Finally, integration of real experimental time into pseudotime and trajectory inference can provide further insights into the dynamics of endocrine differentiation and the evolution of *Ngn3*^{high} precursors and their descendants over time (Fischer et al., 2019; Schiebinger et al., 2019). We anticipate that further development of computational methods to include large asynchronicity as found here will enable investigators to track back the differentiated endocrine subtypes to their origin and further elucidate their differentiation trajectories.

Fev^{high} population link endocrine precursors to endocrine cells

The Fev^{high} population has been recently reported as a novel endocrine cell state during pancreas development in mouse and human (Byrnes et al., 2018; Krentz et al., 2018; Ramond et al., 2018). These cells express low levels of *Ngn3* (declining after the *Ngn3*^{high} precursor state), but also several early endocrine TFs and marker genes, such as *Pax4*, *Neurod1* and *Chga/b*. Lineage-tracing analyses have indicated that these cells are derived from Ngn3^{+} EPs and differentiate into endocrine cells (Byrnes et al., 2018). This finding is supported by our PAGA and RNA velocity analysis indicating that differentiation of EPs into endocrine cells passes through a *Fev*$^{+}$ stage. Indeed, most of EP-signature genes, such as *Ppp1r14a*, *Sult2b1* and *Sema3g*, are still expressed (though with lower levels compared with that of EPs) in *Fev*^{high} cells, whereas the expression of many endocrine-specific genes, such as *Chga/b*, *Pax6* and *Cpe*, is initiated and increasing in these cells. This observation suggests that although each stage of endocrinogenesis involves the expression of a set of highly specific genes, the differentiation of EPs into endocrine cells does not occur through a rapid transcriptional switch but rather passes through gradual alterations in gene expression profiles (Fig. 5E). In addition, we found that the transcriptional heterogeneity of *Ngn3*^{high} EPs from different developmental stages is also partially reflected in *Fev*^{high} cells (data not shown), suggesting that similar to *Ngn3*^{high} precursors, *Fev*^{high} cells are also unipotent cells with a defined fate towards a specific endocrine subtype.

Conclusions

In summary, we provide here a comprehensive high-resolution single cell gene expression profile of distinct pancreatic and endocrine progenitors and lineages during secondary transition. This information can be used as a blueprint for the generation of ILCs from stem cells. We identified the formation of *Ngn3*^{low} progenitors from the heterogeneous populations of tip, trunk and ductal cells, suggesting that only a subset of specified pancreatic progenitors can be primed towards EPs. Defining this subpopulation and the involved pathways will help to expand adequate numbers of endocrine progenitors. Furthermore, our analysis indicated step-wise activation/suppression of different signaling pathways such as cAMP and Wnt signaling, as well as changes in morphogenesis programs during the induction and differentiation of EPs that will aid the efficient production of differentiated endocrine subtypes *in vitro*. Finally, we identified 58 transiently expressed endocrine signature genes that subdivide *Ngn3*^{high} precursors into distinct subpopulations. Such markers and factors might help to discriminate EP subpopulations and allow differentiation towards a specific endocrine cell fate thus improving current protocols to generate ILCs with defined cell-type composition. In addition, understanding how EPs differentiate towards non-β- and β-cells might uncover the molecular programs required for redifferentiation of dedifferentiated β-cells or transdifferentiation of non-β- into β-cells for regenerative diabetes therapy.

MATERIALS AND METHODS

Generation of the Ngn3-Venus fusion reporter mice

Mice were kept at the central facilities at Helmholtz Zentrum München German Research Center of Environmental Health in accordance with the German animal welfare legislation and acknowledged guidelines of the Society of Laboratory Animals (GV-SOLAS) and of the Federation of Laboratory Animal Science Associations (FELASA). Post-mortem examination of organs was not subject to regulatory authorization.

The Ngn3-Venus fusion (NVF) construct was generated as described previously (Petrezselyova et al., 2015). Mouse IDG3.2 embryonic stem cells were electroporated with pCAG195 Cas9v2D10A-bpA (encoding for the nickase Cas9), pbs-U6-chimericRNA and linearized targeting vector. Using geneticin treatment, positive Neo-resistant clones were selected and the targeting of Ngn3-Venus was assessed by PCR genotyping. Next, the NVF-positive clones were aggregated with CD1 morulae and the resulting chimeric mice passed the NVF allele through their germline cells. Finally, the Neo cassette flanked by LoxP sites was deleted by intercrossing with the ROSACre mouse line. The excision of the Neo cassette was confirmed by genotyping PCR. The mouse colony was maintained with a mixed background (C57BL/6J×129/SvJ). We named this mouse line the Ngn3-Venus fusion (NVF) reporter line. The mouse line will be available to the research community upon direct request to H.L.

Pancreata dissection and cell sorting

Embryonic pancreata from NVF homozygous mice were dissected and pooled together for each stage as follows: 29 pancreata from E12.5, 35

Development (2019) 146, dev173849. doi:10.1242/dev.173849

pancreata from E13.5, ten pancreata from E14.5 and seven pancreata from E15.5. Next, pancreata were kept in 0.25% Trypsin for 5 min on ice and then incubated at 37°C for 10 min. The single cell samples were then centrifuged at 1700 rpm (290 ***g***) for 5 min at 4°C. The supernatant was removed and cells were counted. 5 µl anti-mouse CD326 (EpCAM) PE (eBioscience, 12-5791-81) and rat IgG2a K isotype control (eBioscience, 12-4321-42) were used for 1×10^6 cells in 100 µl total volume. After staining for 30 min at 4°C, the cells were stained with DAPI to detect dead cells. The samples were then washed twice and resuspended in FACS buffer (PBS, 1% BSA, 0.5 mM EDTA) and loaded for FACS sorting. The gating strategy was as follows: main population>single cells>living cells (DAPI negative)>$Ngn3^+$ ($FITC^+$) and $EpCAM^+$ (PE^+) cells. The collected cells were enriched for $Ngn3^+$ (~2/3) and $EpCam^+$ cells (~1/3) in FACS buffer containing 1% BSA and 0.1 mM EDTA. Finally, cells were counted and the number of dead cells was identified by Trypan Blue staining. If less than 20% of the cells were dead, cells were processed for single cell RNA seq.

Single cell sequencing

Single cell libraries were generated using the Chromium Single Cell 3′ library and gel bead kit v2 (PN #120237) from 10x Genomics. Briefly, to reach a target cell number of 10,000 cells per sample 16,000 cells per sample were loaded onto a channel of the 10x chip to produce Gel Bead-in-Emulsions (GEMs). This underwent reverse transcription to barcode RNA before cleanup and cDNA amplification followed by enzymatic fragmentation and 5′adaptor and sample index attachment. Libraries were sequenced on the HiSeq4000 (Illumina) with 150 bp paired-end sequencing of read2.

Quantitative PCR (qPCR)

qPCR was performed using TaqMan probes and 25 ng cDNA per reaction. Each reaction consisted of 4.5 µl cDNA in nuclease-free water, 5 µl TaqMan Advanced master mix (Life Technologies) and 0.5 µl TaqMan probe. The qPCR was performed using Viia7 (Thermo Fisher Scientific). C_t-values were normalized among samples, transformed to linear expression values, normalized to reference genes and to control samples, i.e. relative expression (gene)=$(2^{Ct(\text{mean genes})-Ct(\text{gene})})/(2^{Ct(\text{mean references})-Ct(\text{reference})})$, and normalized expression (gene)=relative expression (gene)/relative $\text{expression}_{\text{control}}$ (gene).

See supplementary Materials and Methods for details of the probes used.

Immunohistochemistry and microscopy

Embryonic pancreata were dissected and fixed in 4% paraformaldehyde (PFA) in PBS overnight at 4°C. The tissues were equilibrated in 10% and 30% sucrose-PBS solutions at RT (2 h each solution) followed by 1:1 tissue-freezing medium:30% sucrose overnight at 4°C. Afterwards, they were embedded in cryoblocks using tissue-freezing medium (Leica, 14020108926) and sections of 20 µm were cut. Next, samples were permeabilized (0.1% Triton X-100, 0.1 M glycin) for 15 min and incubated in blocking solution (10% fetal calf serum, 3% donkey serum, 0.1% BSA and 0.1% Tween-20 in PBS) for 1 h at room temperature (RT). Primary antibodies were diluted in blocking solution and incubated with the samples overnight at 4°C. After washing with PBS, samples were stained with secondary antibodies diluted in the blocking solution for 3-5 h at RT. The samples were then incubated with 4′, 6-diamidin-2-phenylindol, followed by three washes with PBS and embedded in commercial medium ProLong Gold (Life Technologies). All images were obtained with a DMI 6000Leica microscope using LAS AF software. Images were analyzed using LAS AF and ImageJ software programs. See supplementary Materials and Methods for details of the antibodies used.

Islet isolation

The isolation of islets was performed using collagenase P (Roche) digestion of adult pancreas as described previously (Bastidas-Ponce et al., 2017b). See supplementary Materials and Methods for further details.

Glucose-stimulated insulin secretion (GSIS)

For GSIS analysis, the isolated islets were cultured overnight before transferring to a 96-well plate containing modified Krebs Ringer phosphate Hepes (KRPH) buffer with 1 mM glucose for 1 h. Different glucose concentrations (2.8 and 16.8 mM) were added to the islets (1 h for each). The supernatants were collected and used for insulin measurement. At the end, the islets were lysed for DNA measurements. Insulin concentrations were measured and quantified using an ultrasensitive insulin ELISA kit (CristalChem). The analysis was performed using a standard curve, and the data were normalized to the DNA content.

Blood glucose level measurement

Mice were maintained in standard conditions, and were starved 4 h before the measurements. Blood glucose values were determined from venous blood using an automatic glucose monitor (Glucometer Elite, Bayer).

Analysis of single cell RNA-seq data

The following data processing and computational analyses of single cell data were used: preprocessing of droplet-based single cell RNA-seq data, low dimensional embedding, visualization and clustering, marker gene identification and subtype characterization, cell cycle classification, reconstruction of lineage relationships and differentiation trajectories, directionality of endocrine differentiation using RNA velocity estimation and software specifications. See supplementary Materials and Methods for further details of each analysis.

Statistical analysis

Data are presented as mean±s.d. Two-tailed unpaired *t*-tests were used to analyze the data.

Acknowledgements

We thank Jessica Jaki, Bianca Vogel, Kerstin Diemer and Julia Beckenbauer for technical support. We thank Maike Sander and Helena Edlund for providing Ngn3 antibodies.

Competing interests

The authors declare no competing or financial interests.

Author contributions

Conceptualization: M.B., H.L.; Methodology: A.B.-P., K.S., M.T.-M., C.S., S.S., I.B., A.B., M.B.; Software: F.J.T., S.T., L.D.; Validation: M.B., H.L., F.J.T., A.B.-P., S.T., L.D.; Investigation: M.B., H.L., A.B.-P., S.T., L.D.; Resources: H.L., F.J.T.; Data curation: M.B., F.T., A.B.-P., S.T., L.D.; Writing - original draft: M.B., H.L., A.B.-P., S.T.; Writing - review & editing: M.B., H.L., F.J.T., A.B.-P., S.T., L.D., K.S., M.T.-M., C.S., S.S., I.B., A.B.; Visualization: M.B., A.B.-P., S.T.; Supervision: M.B., H.L., F.J.T.; Project administration: M.B., H.L.; Funding acquisition: M.B., H.L., F.J.T.

Funding

This work was supported by the Helmholtz-Gemeinschaft (Helmholtz Portfolio Theme ‘Metabolic Dysfunction and Common Disease), Deutsche Forschungsgemeinschaft (DFG) (Collaborative Research Centre 1243, Subproject A17) and Deutsches Zentrum für Diabetesforschung (DZD). This project is supported by DZD NEXT Grant funding. H.J.T. acknowledges financial support by the Chan Zuckerberg Initiative Donor-Advised Fund (DAF) (grant 182835). S.T. is supported by a DFG Fellowship through the Graduate School of Quantitative Biosciences Munich (QBM). L.D. is supported by the Graduate Program of the International Max Planck Research School for Translational Psychiatry (IMPRS-TP).

Data availability

scRNA-seq data have been deposited in Gene Expression Omnibus under accession number GSE132188. All code to reproduce the results from this data as well as fully processed and annotated count matrices are available at http://github.com/theislab/pancreatic-endocrinogenesis.

Supplementary information

Supplementary information available online at
http://dev.biologists.org/lookup/doi/10.1242/dev.173849.supplemental

References

Ahnfelt-Rønne, J., Hald, J., Bødker, A., Yassin, H., Serup, P. and Hecksher-Sørensen, J. (2007). Preservation of proliferating pancreatic progenitor cells by Delta-Notch signaling in the embryonic chicken pancreas. *BMC Dev. Biol.* **7**, 63. doi:10.1186/1471-213X-7-63

Apelqvist, A., Li, H., Sommer, L., Beatus, P., Anderson, D. J., Honjo, T., de Angelis, M. H., Lendahl, U. and Edlund, H. (1999). Notch signalling controls pancreatic cell differentiation. *Nature* **400**, 877-881. doi:10.1038/23716

Arda, H. E., Benitez, C. M. and Kim, S. K. (2013). Gene regulatory networks governing pancreas development. *Dev. Cell* **25**, 5-13. doi:10.1016/j.devcel.2013.03.016

Azzarelli, R., Hurley, C., Sznurkowska, M. K., Rulands, S., Hardwick, L., Gamper, I., Ali, F., McCracken, L., Hindley, C., McDuff, F. et al. (2017). Multi-site Neurogenin3 phosphorylation controls pancreatic endocrine differentiation. *Dev. Cell* **41**, 274-286.e5. doi:10.1016/j.devcel.2017.04.004

Bakhti, M., Böttcher, A. and Lickert, H. (2019). Modelling the endocrine pancreas in health and disease. *Nat. Rev. Endocrinol.* **15**, 155-171. doi:10.1038/s41574-018-0132-z

Bankaitis, E. D., Bechard, M. E. and Wright, C. V. E. (2015). Feedback control of growth, differentiation, and morphogenesis of pancreatic endocrine progenitors in an epithelial plexus niche. *Genes Dev.* **29**, 2203-2216. doi:10.1101/gad.267914.115

Bankaitis, E. D., Bechard, M. E., Gu, G., Magnuson, M. A. and Wright, C. V. E. (2018). ROCK-nmMyoII, Notch and *Neurog3* gene-dosage link epithelial morphogenesis with cell fate in the pancreatic endocrine-progenitor niche. *Development* **145**, dev162115. doi:10.1242/dev.162115

Bastidas-Ponce, A., Scheibner, K., Lickert, H. and Bakhti, M. (2017a). Cellular and molecular mechanisms coordinating pancreas development. *Development* **144**, 2873-2888. doi:10.1242/dev.140756

Bastidas-Ponce, A., Roscioni, S. S., Burtscher, I., Bader, E., Sterr, M., Bakhti, M. and Lickert, H. (2017b). Foxa2 and Pdx1 cooperatively regulate postnatal maturation of pancreatic β-cells. *Mol. Metab.* **6**, 524-534. doi:10.1016/j.molmet.2017.03.007

Bechard, M. E., Bankaitis, E. D., Hipkens, S. B., Ustione, A., Piston, D. W., Yang, Y.-P., Magnuson, M. A. and Wright, C. V. E. (2016). Precommitment low-level neurog3 expression defines a long-lived mitotic endocrine-biased progenitor pool that drives production of endocrine-committed cells. *Genes Dev.* **30**, 1852-1865. doi:10.1101/gad.284729.116

Benitez, C. M., Qu, K., Sugiyama, T., Pauerstein, P. T., Liu, Y., Tsai, J., Gu, X., Ghodasara, A., Arda, H. E., Zhang, J. et al. (2014). An integrated cell purification and genomics strategy reveals multiple regulators of pancreas development. *PLoS Genet.* **10**, e1004645. doi:10.1371/journal.pgen.1004645

Byrnes, L. E., Wong, D. M., Subramaniam, M., Meyer, N. P., Gilchrist, C. L., Knox, S. M., Tward, A. D., Ye, C. J. and Sneddon, J. B. (2018). Lineage dynamics of murine pancreatic development at single-cell resolution. *Nat. Commun.* **9**, 3922. doi:10.1038/s41467-018-06176-3

Collombat, P., Mansouri, A., Hecksher-sørensen, J., Serup, P., Krull, J., Gradwohl, G. and Gruss, P. (2003). Opposing actions of Arx and Pax4 in endocrine pancreas development. *Genes Dev.* **17**, 2591-2603. doi:10.1101/gad.269003

Collombat, P., Xu, X., Ravassard, P., Sosa-Pineda, B., Dussaud, S., Billestrup, N., Madsen, O. D., Serup, P., Heimberg, H. and Mansouri, A. (2009). The Ectopic Expression of Pax4 in the Mouse Pancreas Converts Progenitor Cells into α and Subsequently β Cells. *Cell* **138**, 449-462. doi:10.1016/j.cell.2009.05.035

Cortijo, C., Gouzi, M., Tissir, F. and Grapin-Botton, A. (2012). Planar cell polarity controls pancreatic beta cell differentiation and glucose homeostasis. *Cell Rep.* **2**, 1593-1606. doi:10.1016/j.celrep.2012.10.016

Desgraz, R. and Herrera, P. L. (2009). Pancreatic neurogenin 3-expressing cells are unipotent islet precursors. *Development* **136**, 3567-3574. doi:10.1242/dev.039214

Fischer, D. S., Fiedler, A. K., Kernfeld, E. M., Genga, R. M. J., Bastidas-Ponce, A., Bakhti, M., Lickert, H., Hasenauer, J., Maehr, R. and Theis, F. J. (2019). Inferring population dynamics from single-cell RNA-sequencing time series data. *Nat. Biotechnol.* **37**, 461-468. doi:10.1038/s41587-019-0088-0

Gasa, R., Mrejen, C., Lynn, F. C., Skewes-Cox, P., Sanchez, L., Yang, K. Y., Lin, C.-H., Gomis, R. and German, M. S. (2008). Induction of pancreatic islet cell differentiation by the neurogenin-neuroD cascade. *Differentiation* **76**, 381-391. doi:10.1111/j.1432-0436.2007.00228.x

Gehart, H., van Es, J. H., Hamer, K., Beumer, J., Kretzschmar, K., Dekkers, J. F., Rios, A. and Clevers, H. (2019). Identification of enteroendocrine regulators by real-time single-cell differentiation mapping. *Cell* **176**, 1158-1173.e16. doi:10.1016/j.cell.2018.12.029

Gouzi, M., Kim, Y. H., Katsumoto, K., Johansson, K. and Grapin-Botton, A. (2011). Neurogenin3 initiates stepwise delamination of differentiating endocrine cells during pancreas development. *Dev. Dyn.* **240**, 589-604. doi:10.1002/dvdy.22544

Gradwohl, G., Dierich, A., LeMeur, M. and Guillemot, F. (2000). Neurogenin3 is required for the development of the four endocrine cell lineages of the pancreas. *Proc. Natl. Acad. Sci. USA* **97**, 1607-1611. doi:10.1073/pnas.97.4.1607

Gu, G., Dubauskaite, J. and Melton, D. A. (2002). Direct evidence for the pancreatic lineage: NGN3+ cells are islet progenitors and are distinct from duct progenitors. *Development* **129**, 2447-2457.

Haghverdi, L., Büttner, M., Wolf, F. A., Buettner, F. and Theis, F. J. (2016). Diffusion pseudotime robustly reconstructs lineage branching. *Nat. Methods* **13**, 845-848. doi:10.1038/nmeth.3971

Johansson, K. A., Dursun, U., Jordan, N., Gu, G., Beermann, F., Gradwohl, G. and Grapin-Botton, A. (2007). Temporal control of Neurogenin3 activity in pancreas progenitors reveals competence windows for the generation of different endocrine cell types. *Dev. Cell* **12**, 457-465. doi:10.1016/j.devcel.2007.02.010

Kakugawa, S., Langton, P. F., Zebisch, M., Howell, S. A., Chang, T.-H., Liu, Y., Feizi, T., Bineva, G., O'Reilly, N., Snijders, A. P. et al. (2015). Notum deacylates Wnt proteins to suppress signalling activity. *Nature* **519**, 187-192. doi:10.1038/nature14259

Kim, Y. H., Larsen, H. L., Rué, P., Lemaire, L. A., Ferrer, J. and Grapin-Botton, A. (2015). Cell cycle–dependent differentiation dynamics balances growth and endocrine differentiation in the pancreas. *PLoS Biol.* **13**, e1002111. doi:10.1371/journal.pbio.1002111

Kopp, J. L., Dubois, C. L., Schaffer, A. E., Hao, E., Shih, H. P., Seymour, P. A., Ma, J. and Sander, M. (2011). Sox9+ ductal cells are multipotent progenitors throughout development but do not produce new endocrine cells in the normal or injured adult pancreas. *Development* **138**, 653-665. doi:10.1242/dev.056499

Krentz, N. A. J., van Hoof, D., Li, Z., Watanabe, A., Tang, M., Nian, C., German, M. S. and Lynn, F. C. (2017). Phosphorylation of NEUROG3 links endocrine differentiation to the cell cycle in pancreatic progenitors. *Dev. Cell* **41**, 129-142. doi:10.1016/j.devcel.2017.02.006

Krentz, N. A. J., Xu, E. E., Lynn, F. C., Sasaki, S., Lee, M. Y. Y., Maslova, A. and Sproul, S. L. J. (2018). Single-cell transcriptome profiling of mouse and hESC-derived pancreatic progenitors. *Stem Cell Rep.* **11**, 1551-1564. doi:10.1016/j.stemcr.2018.11.008

La Manno, G., Soldatov, R., Zeisel, A., Braun, E., Hochgerner, H., Petukhov, V., Lidschreiber, K., Kastriti, M. E., Lönnerberg, P., Furlan, A. et al. (2018). RNA velocity of single cells. *Nature* **560**, 494-498. doi:10.1038/s41586-018-0414-6

Lee, C. S., Perreault, N., Brestelli, J. E. and Kaestner, K. H. (2002). Neurogenin 3 is essential for the proper specification of gastric enteroendocrine cells and the maintenance of gastric epithelial cell identity. *Genes Dev.* **16**, 1488-1497. doi:10.1101/gad.985002

Lee, K. M., Yasuda, H., Hollingsworth, M. A. and Ouellette, M. M. (2005). Notch2-positive progenitors with the intrinsic ability to give rise to pancreatic ductal cells. *Lab. Investig.* **85**, 1003-1012. doi:10.1038/labinvest.3700298

Lemaire, L. A., Goulley, J., Kim, Y. H., Carat, S., Jacquemin, P., Rougemont, J., Constam, D. B. and Grapin-Botton, A. (2016). Bicaudal C1 promotes pancreatic NEUROG3+ endocrine progenitor differentiation and ductal morphogenesis. *Development* **142**, 858-870. doi:10.1242/dev.114611

Liu, W.-D., Wang, H.-W., Muguira, M., Breslin, M. B. and Lan, M. S. (2006). INSM1 functions as a transcriptional repressor of the neuroD/β2 gene through the recruitment of cyclin D1 and histone deacetylases. *Biochem. J.* **397**, 169-177. doi:10.1042/BJ20051669

Liu, J., Banerjee, A., Herring, C. A., Attalla, J., Hu, R., Xu, Y., Shao, Q., Simmons, A. J., Dadi, P. K., Wang, S. et al. (2019). Neurog3-independent methylation is the earliest detectable mark distinguishing pancreatic progenitor identity. *Dev. Cell* **48**, 49-63.e7. doi:10.1016/j.devcel.2018.11.048

Löf-Öhlin, Z. M., Nyeng, P., Bechard, M. E., Hess, K., Bankaitis, E., Greiner, T. U., Ameri, J., Wright, C. V. and Semb, H. (2017). EGFR signalling controls cellular fate and pancreatic organogenesis by regulating apicobasal polarity. *Nat. Cell Biol.* **19**, 1313-1325. doi:10.1038/ncb3628

Mastrolia, V., Flucher, S. M., Obermair, G. J., Drach, M., Hofer, H., Renström, E., Schwartz, A., Striessnig, J., Flucher, B. E. and Tuluc, P. (2017). Loss of α2d-1 calcium channel subunit function increases the susceptibility for diabetes. *Diabetes* **66**, 897-907. doi:10.2337/db16-0336

Mellitzer, G., Martín, M., Sidhoum-Jenny, M., Orvain, C., Barths, J., Seymour, P. A., Sander, M. and Gradwohl, G. (2004). Pancreatic islet progenitor cells in neurogenin 3-yellow fluorescent protein knock-add-on mice. *Mol. Endocrinol.* **18**, 2765-2776. doi:10.1210/me.2004-0243

Miyatsuka, T., Kosaka, Y., Kim, H. and German, M. S. (2011). Neurogenin3 inhibits proliferation in endocrine progenitors by inducing Cdkn1a. *Proc. Natl. Acad. Sci. USA* **108**, 185-190. doi:10.1073/pnas.1004842108

Nyeng, P., Heilmann, S., Löf-Öhlin, Z. M., Pettersson, N. F., Hermann, F. M., Reynolds, A. B. and Semb, H. (2019). p120ctn-mediated organ patterning precedes and determines pancreatic progenitor fate. *Dev. Cell* **49**, 31-47.e9. doi:10.1016/j.devcel.2019.02.005

Osipovich, A. B., Long, Q., Manduchi, E., Gangula, R., Hipkens, S. B., Schneider, J., Okubo, T., Stoeckert, C. J., Takada, S. and Magnuson, M. A. (2014). Insm1 promotes endocrine cell differentiation by modulating the expression of a network of genes that includes Neurog3 and Ripply3. *Development* **141**, 2939-2949. doi:10.1242/dev.104810

Pan, F. C. and Wright, C. (2011). Pancreas organogenesis: from bud to plexus to gland. *Dev. Dyn.* **240**, 530-565. doi:10.1002/dvdy.22584

Pan, F. C., Bankaitis, E. D., Boyer, D., Xu, X., Van de Casteele, M., Magnuson, M. A., Heimberg, H. and Wright, C. V. E. (2013). Spatiotemporal patterns of multipotentiality in Ptf1a-expressing cells during pancreas organogenesis and injury-induced facultative restoration. *Development* **140**, 751-764. doi:10.1242/dev.090159

Petrezselyova, S., Kinsky, S., Truban, D., Sedlacek, R., Burtscher, I. and Lickert, H. (2015). Homology arms of targeting vectors for gene insertions and CRISPR/Cas9 technology: Size does not matter; Quality control of targeted clones does. *Cell. Mol. Biol. Lett.* **20**, 773-787. doi:10.1515/cmble-2015-0047

Piccolo, S., Agius, E., Leyns, L., Bhattacharyya, S., Grunz, H., Bouwmeester, T. and De Robertis, E. M. (1999). The head inducer cerberus is a multifunctional

antagonist of Nodal, BMP and Wnt signals. *Nature* **397**, 707-710. doi:10.1038/17820

Ramond, C., Beydag-Tasöz, B. S., Azad, A., van de Bunt, M., Petersen, M. B. K., Beer, N. L., Glaser, N., Berthault, C., Gloyn, A. L., Hansson, M. et al. (2018). Understanding human fetal pancreas development using subpopulation sorting, RNA sequencing and single-cell profiling. *Development* **145**, dev165480. doi:10.1242/dev.165480

Scavuzzo, M. A., Hill, M. C., Chmielowiec, J., Yang, D., Teaw, J., Sheng, K., Kong, Y., Bettini, M., Zong, C., Martin, J. F. et al. (2018). Endocrine lineage biases arise in temporally distinct endocrine progenitors during pancreatic morphogenesis. *Nat. Commun.* **9**, 3356. doi:10.1038/s41467-018-05740-1

Schiebinger, G., Shu, J., Tabaka, M., Cleary, B., Subramanian, V., Solomon, A., Gould, J., Liu, S., Lin, S., Berube, P. et al. (2019). Optimal-transport analysis of single-cell gene expression identifies developmental trajectories in reprogramming. *Cell* **176**, 928-943. doi:10.1016/j.cell.2019.01.006

Seymour, P. A., Freude, K. K., Tran, M. N., Mayes, E. E., Jensen, J., Kist, R., Scherer, G. and Sander, M. (2007). SOX9 is required for maintenance of the pancreatic progenitor cell pool. *Proc. Natl. Acad. Sci. USA* **104**, 1865-1870. doi:10.1073/pnas.0609217104

Sharon, N., Chawla, R., Mueller, J., Vanderhooft, J., Whitehorn, L. J., Rosenthal, B., Gürtler, M., Estanboulieh, R. R., Shvartsman, D., Gifford, D. K. et al. (2019). A peninsular structure coordinates asynchronous differentiation with morphogenesis to generate pancreatic islets. *Cell* **176**, 790-804.e13. doi:10.1016/j.cell.2018.12.003

Shih, H. P., Kopp, J. L., Sandhu, M., Dubois, C. L., Seymour, P. A., Grapin-Botton, A. and Sander, M. (2012). A Notch-dependent molecular circuitry initiates pancreatic endocrine and ductal cell differentiation. *Development* **139**, 2488-2499. doi:10.1242/dev.078634

Solar, M., Cardalda, C., Houbracken, I., Martín, M., Maestro, M. A., De Medts, N., Xu, X., Grau, V., Heimberg, H., Bouwens, L. et al. (2009). Pancreatic exocrine duct cells give rise to insulin-producing beta cells during embryogenesis but not after birth. *Dev. Cell* **17**, 849-860. doi:10.1016/j.devcel.2009.11.003

Stanescu, D. E., Yu, R., Won, K.-J. and Stoffers, D. A. (2016). Single cell transcriptomic profiling of mouse pancreatic progenitors. *Physiol. Genomics* **49**, 105-114. doi:10.1152/physiolgenomics.00114.2016

Stauber, M., Weidemann, M., Dittrich-Breiholz, O., Lobschat, K., Alten, L., Mai, M., Beckers, A., Kracht, M. and Gossler, A. (2017). Identification of FOXJ1 effectors during ciliogenesis in the foetal respiratory epithelium and embryonic left-right organiser of the mouse. *Dev. Biol.* **423**, 170-188. doi:10.1016/j.ydbio.2016.11.019

Svensson, P., Bergqvist, I., Norlin, S. and Edlund, H. (2009). MFng is dispensable for mouse pancreas development and function. *Mol. Cell. Biol.* **29**, 2129-2138. doi:10.1128/MCB.01644-08

Sznurkowska, M. K., Hannezo, E., Azzarelli, R., Rulands, S., Nestorowa, S., Hindley, C. J., Nichols, J., Göttgens, B., Huch, M., Philpott, A. et al. (2018). Defining lineage potential and fate behavior of precursors during pancreas development. *Dev. Cell* **46**, 360-375.e5. doi:10.1016/j.devcel.2018.06.028

Wang, S., Yan, J., Anderson, D. A., Xu, Y., Kanal, M. C., Cao, Z., Wright, C. V. E. and Gu, G. (2010). Neurog3 gene dosage regulates allocation of endocrine and exocrine cell fates in the developing mouse pancreas. *Dev. Biol.* **339**, 26-37. doi:10.1016/j.ydbio.2009.12.009

Wolf, F. A., Hamey, F. K., Plass, M., Solana, J., Dahlin, J. S., Göttgens, B., Rajewsky, N., Simon, L. and Theis, F. J. (2019). PAGA: graph abstraction reconciles clustering with trajectory inference through a topology preserving map of single cells. *Genome Biol.*. **20**, 59. doi:10.1186/s13059-019-1663-x

Xu, E. E., Krentz, N. A. J., Tan, S., Chow, S. Z., Tang, M., Nian, C. and Lynn, F. C. (2015). SOX4 cooperates with neurogenin 3 to regulate endocrine pancreas formation in mouse models. *Diabetologia* **58**, 1013-1023. doi:10.1007/s00125-015-3507-x

Yu, X.-X., Qiu, W.-L., Yang, L., Li, L.-C., Zhang, Y.-W. and Xu, C.-R. (2018). Dynamics of chromatin marks and the role of JMJD3 during pancreatic endocrine cell fate commitment. *Development* **145**, dev163162. doi:10.1242/dev.163162

Yu, X.-X., Qiu, W.-L., Yang, L., Zhang, Y., He, M.-Y., Li, L.-C. and Xu, C.-R. (2019). Defining multistep cell fate decision pathways during pancreatic development at single-cell resolution. *EMBO J.* **38**, e100164. doi:10.15252/embj.2018100164

Zhou, Q., Law, A. C., Rajagopal, J., Anderson, W. J., Gray, P. A. and Melton, D. A. (2007). A multipotent progenitor domain guides pancreatic organogenesis. *Dev. Cell* **13**, 103-114. doi:10.1016/j.devcel.2007.06.001

Supplementary materials and methods

Quantitative PCR (qPCR) probes

The used qPCR probes were from Life Technologies and listed as follow; Mm00440465_g1 for Neurod2, Mm00435565_m1 for Pdx1, Mm01950294_s1 for Insulin 1, Mm00731595_Gh for Insulin 2, Mm01269055_m1 for Glucagon, Mm00436671_m1 for Somatostatin, Mm01946604_s1 for Neurod1, Mm00545903_m1 for Arx, Mm01159036_m1 for Pax4, Mm00450550_m1 for Sult2b1, Mm01208248_m1 for Upk3bl, Mm01269371_m1 for Shf, Mm03053598_s1 for Mycl, Mm00459097_m1 for Steap1, Mm00803317_m1 for Rgs16, Mm04239638_m1 for Gm8773 and Mm00458153_g1 for Gng13.

Antibody list for immunohistochemistry

The following primary antibodies were used for staining: rabbit anti-Sox9 (Millipore, Cat. Nr: AB5535, Batch Nr: 3107073, dilution 1:300) (Carrasco et al., 2012), goat anti-Nkx6.1 (R&D systems, Cat. Nr: AF5857, dilution 1:300) (Bastidas-Ponce et al., 2017), rat anti-E-Cadherin (DECMA-1, a generous gift from Kremmer, dilution 1:500) (Bastidas-Ponce et al., 2017), rat anti-EpCAM (DSHB Hybridoma, Cat. Nr: 4G1, dilution 1:300), goat anti-Pancreatic polypeptide (Novus, Cat. Nr: NB100-1793, 1:300), hamster anti-Mucin-1(Invitrogen, Cat. Nr: HM1630P0, Batch Nr: 022017, dilution 1:100), guinea pig anti-glucagon (TAKARA, Cat. Nr: M182, dilution 1:3500) (Bastidas-Ponce et al., 2017), chicken anti-GFP (to detect Venus; Aves Labs, Cat. Nr: 1020, dilution 1:1000) (Bastidas-Ponce et al., 2017), rabbit anti-insulin (Cell signaling, Cat. Nr: 3014, dilution 1:300) (Bastidas-Ponce et al., 2017), rabbit anti-Ngn3 (a generous gift from Helena Edlund, dilution 1:800), guinea pig anti-Ngn3 (a generous gift from Maike Sander, dilution 1:1000) and rat anti-somatostatin (Invitrogen, Cat. Nr: MA5-16987, Batch Nr: 75739969, dilution 1:300). The secondary antibodies used were from Dianova and Invitrogen, (dilution 1:800) and Phalloidin Alexa Fluor 546 was from Invitrogen (Cat. Nr: A22283, dilution 1:200).

Islet isolation

The isolation of islets was performed using collagenase P (Roche) digestion of adult pancreas. First, 3 mL of collagenase P (1 mg/mL) was injected into the bile duct, then the perfused pancreas was dissected and placed into other 3 mL collagenase P for 15 min at 37 °C. To stop the digestion, 10 mL of G-solution (HBSS + 1% BSA) were added followed by centrifugation at 1600 rpm (421 *g*) at 4 °C. After another washing step with G-solution, the pellets were re-suspended in 5.5 mL of gradient solution (5 mL 10% RPMI + 3 mL 40% Optiprep/per sample), and placed on top of 2.5 mL of the same solution. To form a 3-layers gradient, 6 mL of G-solution were added on top of the abovementioned layers. Samples were then centrifuged at 1700 rpm (475 *g*). Finally, the interphase between the upper and the middle

layer of the gradient was recovered and filtered through a 70 µm Nylon filter, washed with G-solution and the islets were handpicked under the microscope.

Analysis of single cell RNAseq data

Preprocessing of droplet-based single-cell RNAseq data

Demultiplexing of raw base call (BCL) files, alignment, read filtering, barcode and UMI counting were performed using the CellRanger analysis pipeline (Version 2.1.1) provided by 10X Genomics. High quality barcodes were selected based on the overall UMI distribution using the standard CellRanger cell detection algorithm. All further analyses were run using the python-based Scanpy API (Wolf et al., 2018) except stated otherwise (for software specifications and code availability see below and in Materials and Methods). To further remove low quality cells, we filtered cells with a high fraction of counts from mitochondrial genes (20% or more) indicating stressed or dying cells, and cells expressing less than 1200 genes. In addition, genes with expression in less than 20 cells were excluded. Cell by gene count matrices of all samples were then concatenated to a single matrix and values log transformed. To account for differences in sequencing depth or cell size UMI counts were normalized using quantile normalization as previously described (Weinreb et al., 2018). Briefly, each cell is normalized by the total UMI count in the cell of genes that account for less than 5% of the total UMI counts across all cells. The top 4000 variable genes were selected based on normalized dispersion as described in (Zheng et al., 2017). This output matrix was input to all further analyses except for differential expression testing where all genes were used.

Low dimensional embedding, visualization and clustering

A single-cell neighborhood graph was computed on the 50 first principal components that sufficiently explain the variation in the data using 15 nearest neighbors. Uniform Manifold Approximation and Projection (UMAP) (Mcinnes and Healy, 2018) was run for visualization. For clustering and cell type identification louvain-based clustering (Blondel et al., 2008) at varying resolution in different parts of the data manifold was used as implemented in louvain-igraph (https://github.com/vtraag/louvain-igraph) and adopted by Scanpy. Cell types were annotated based on the expression of known marker genes. Clusters were merged if only reflecting further heterogeneity within a cell type not discussed in this manuscript. For the exact steps of clustering and annotation and the parameters used consult the available code. We removed clearly distinct clusters of cells highly expressing immune cell or mesenchymal marker genes, respectively. In addition, we found a major cluster and a small endocrine subcluster expressing a mixture of gene expression profiles of other cell types but no specific marker genes suggesting that these cells are doublets. We further checked this hypothesis and calculated a doublet score signifying the probability of being a doublet for each cell using the doublet detection package Scrublet (Wolock et al., 2019) using *scr.compute_doublet_scores* function with parameters as recommended in the Scrublet tutorial (min_counts = 2, min_cells = 3, vscore_percentile = 85, n_pc = 50, expected_doublet_rate = 0.08, sim_doublet_ratio = 3, n_neighbors = 15). Indeed, the majority of

these cells were predicted to be doublets even when setting a high threshold for the doublet score and we therefore removed these two clusters from further analyses. In all other subtypes we found only a small proportion of predicted doublet cells that did not form a separate cluster or misleadingly connect two clusters. We did not remove these cells as downstream analyses were not strongly influenced by them. In different figures varying resolutions of subtype clustering are shown. EP, Pre-endocrine and α-cell subtypes were annotated based on marker gene expression as well as the developmental stages they existed. For the specification of *Ngn3*^{low} progenitors we referred to the expression of *Neurog3* and picked all cells with expression > 0 in the multipotent, tip, trunk and ductal cluster. Proliferating subtypes were annotated using the cell cycle classification described below.

Marker gene identification and subtype characterization

Characteristic gene signatures were identified by testing for differential expression of a subgroup against all other cells or between two subgroups as outlined in the text using a t-test with overestimated variance implemented in the *tl.rank_genes_groups* function of Scanpy. Testing was performed on the log-transformed quantile normalized data to account for confounding differences in sequencing depth between samples. It has been shown that a simple t-test performs comparable to differential expression tools adopting more complex models in a simple set-up as here (no additional confounding factors) (Soneson and Robinson, 2018). Gene set enrichment was performed with the gseapy (v0.9.3) implementation of EnrichR. To identify genes enriched in EPs, *Ngn3*$^{+}$ cells (*Ngn3*^{low} progenitors and *Ngn3*^{high} precursors) were compared against all other cells except for acinar cells. Top 250 upregulated genes were considered (Table S2). From this list, EP signature genes that are transiently expressed in EPs similar to Ngn3 but not or only lowly expressed in other populations were extracted by computing the mean expression of all 250 genes in each cell type after scaling the data from 0 to 1. All genes that showed a mean expression > 0.04 in *Ngn3*^{high} precursors, < 0.04 in all other non-endocrine progenitor-precursor clusters and < 0.18 in *Fev*^{high} cells were defined as EP signature genes. Expression thresholds were chosen based on the mean expression levels of *Neurog3*. For characterization of the EP subtypes we compared ductal cells against *Ngn3*^{low} progenitors, *Ngn3*^{low} progenitors against ductal cells, *Ngn3*^{high} precursors against *Ngn3*^{low} progenitors and *Fev*^{high} against *Ngn3*^{high} precursors to identify genes changing along the differentiation trajectory.

Cell cycle classification

To classify cells into cell cycle phases we used a cell scoring function as described by (Satija et al., 2015) and implemented in the *tl.score_genes_cell_cycle* function in Scanpy with default parameters. Shortly, the score is the average expression of the gene set subtracted with the average expression of a randomly sampled background set with expression values within the same range. Cell cycle genes as defined in (Tirosh et al., 2016) were used to distinguish between S, G2/M and G1 phase cells.

Reconstruction of lineage relationships and differentiation trajectories

To infer lineage relationships between clusters and predict potential routes of differentiation partition-based graph abstraction (PAGA) was performed (Wolf et al., 2019) using the *tl.paga* function of Scanpy with a threshold on edge significance of 0.11 for all subtypes and 0.1 for the endocrine lineage. Edge weights represent the confidence of a connection calculated based on a measure for connectivity. Paths in the PAGA graph signify cluster relationships indicating potential differentiation paths. To infer a pseudotemporal ordering of the cells along the predicted routes in the PAGA graph, diffusion pseudotime (dpt) (Haghverdi et al., 2016) was used as implemented in Scanpy (*tl.dpt*) setting a root cell within the starting population. Dpt is designed to learn such continuous cellular differentiation trajectories and projects the differentiating cells to a one-dimensional developmental trajectory. Before dpt inference the single cell neighborhood-graph and diffusion map was recalculated for the represented subset of cells. To test whether cell cycle effects mask other biological processes and affect the pseudotemporal ordering, dpt was recomputed after linearly regressing out S and G2M cell scores (using *sc.pp.regress_out*; data not shown). Removal of cell cycle effects did not considerably change the ordering of the cells. Also, the expression of genes described in the manuscript figures was not affected except for, as expected, genes involved in DNA replication and cell cycle.

Directionality of endocrine differentiation using RNA velocity estimation

To infer directionality of endocrine differentiation we performed RNA velocity estimation (La Manno et al., 2018) implemented as a stochastic version in the scVelo python package (https://github.com/theislab/scvelo). We extracted spliced and unspliced reads using the velocyto pipeline (http://velocyto.org), which generated a loompy file. The file was read into an AnnData object for downstream analysis with Scanpy. All analysis related to RNA velocity such as estimating velocities and obtaining the RNA velocity projection were done using scVelo. Here, we followed the recommended procedures described in scVelo, consisting of four main steps: preprocessing, computing first- and second-order moments, estimating velocities, and constructing a velocity graph. That is, we filtered genes with less than 10 spliced and 10 unspliced counts and normalized unspliced and spliced reads by their initial counts and log transformed the data. Then, for each stage separately, we recomputed the neighborhood graph on the represented cell subset using 15 neighbors and the 50 first PCs that sufficiently explain the variation in the data, and the UMAP embedding. Next, first-order and second-order moments for each cell were computed across its nearest neighbors. Velocities were estimated using a stochastic model of transcriptional dynamics, whereby we used a 95% quantile fit for more conservative velocity estimates. Finally, the velocity graph was obtained by computing the correlations between potential cell transitions and the predicted cell state change given by the velocity vector. Only genes with an $r^2 > 0.1$ were considered. The graph was then used to project the velocities into the low dimensional UMAP embedding.

Software specifications

All analyses from UMI count matrices were run with python 3 with the Scanpy API v.1.3.2 to v.1.3.4 and anndata v.0.6.11 (https://github.com/theislab/scanpy). Versions of packages required by Scanpy that might influence numerical results are indicated in the custom scripts. Unspliced and spliced reads were extracted using velocyto v0.17.7 and loompy v2.0.12 (http://velocyto.org). Velocities were calculated with scVelo v0.1.16 (https://github.com/theislab/scvelo). All figures were plotted with matplotlib and seaborn and data was exported to excel-sheets with xlsxwriter. Custom scripts of code for all analyses will be made available upon publication.

Supplementary references

Bastidas-Ponce, A., Roscioni, S. S., Burtscher, I., Bader, E., Sterr, M., Bakhti, M. and Lickert, H. (2017). Foxa2 and Pdx1 cooperatively regulate postnatal maturation of pancreatic β-cells. *Mol. Metab.* **6**, 524–534.

Blondel, V. D., Guillaume, J. L., Lambiotte, R. and Lefebvre, E. (2008). Fast unfolding of communities in large networks. *J. Stat. Mech. Theory Exp.* **10**, P10008.

Carrasco, M., Delgado, I., Soria, B., Martín, F. and Rojas, A. (2012). GATA4 and GATA6 control mouse pancreas organogenesis. *J. Clin. Invest.* **122**, 3504–3515.

Haghverdi, L., Büttner, M., Wolf, F. A., Buettner, F. and Theis, F. J. (2016). Diffusion pseudotime robustly reconstructs lineage branching. *Nat. Methods* **13**, 845–8.

La Manno, G., Soldatov, R., Zeisel, A., Braun, E., Hochgerner, H., Petukhov, V., Lidschreiber, K., Kastriti, M. E., Lönnerberg, P., Furlan, A., et al. (2018). RNA velocity of single cells. *Nature* 560, 494–498.

Mcinnes, L. and Healy, J. (2018). UMAP : Uniform Manifold Approximation and Projection for Dimension Reduction. *arXiv:1802.03426* 1–18.

Satija, R., Farrell, J. A., Gennert, D., Schier, A. F. and Regev, A. (2015). Spatial reconstruction of single-cell gene expression data. *Nat. Biotechnol.* **33**, 495–502.

Soneson, C. and Robinson, M. D. (2018). Bias, robustness and scalability in single-cell differential expression analysis. *Nat. Methods* **15**, 255–261.

Tirosh, I., Izar, B., Prakadan, S. M., Wadsworth, M. H., Treacy, D., Trombetta, J. J., Rotem, A., Rodman, C., Lian, C., Murphy, G., et al. (2016). Dissecting the multicellular ecosystem of metastatic melanoma by single-cell RNA-seq. *Science (80-.).* **352**, 189–96.

Weinreb, C., Wolock, S. and Klein, A. M. (2018). SPRING: A kinetic interface for visualizing high dimensional single-cell expression data. *Bioinformatics* **34**, 1246–1248.

Wolf, F. A., Angerer, P. and Theis, F. J. (2018). SCANPY: Large-scale single-cell gene expression data analysis. *Genome Biol.* **19**, 15.

Wolf, F. A., Hamey, F., Plass, M., Solana, J., Dahlin, J. S., Gottgens, B., Rajewsky, N., Simon, L. and Theis, F. J. (2019). PAGA: graph abstraction reconciles clustering with trajectory inference through a topology preserving map of single cells. *Genome Biol.* **20**, 59.

Wolock, S. L., Lopez, R. and Klein, A. M. (2019). Scrublet: Computational Identification of Cell Doublets in Single-Cell Transcriptomic Data. *Cell Syst.* **8**, 281–291.e9.

Zheng, G. X. Y., Terry, J. M., Belgrader, P., Ryvkin, P., Bent, Z. W., Wilson, R., Ziraldo, S. B., Wheeler, T. D., McDermott, G. P., Zhu, J., et al. (2017). Massively parallel digital transcriptional profiling of single cells. *Nat. Commun.* **8**, 14049.

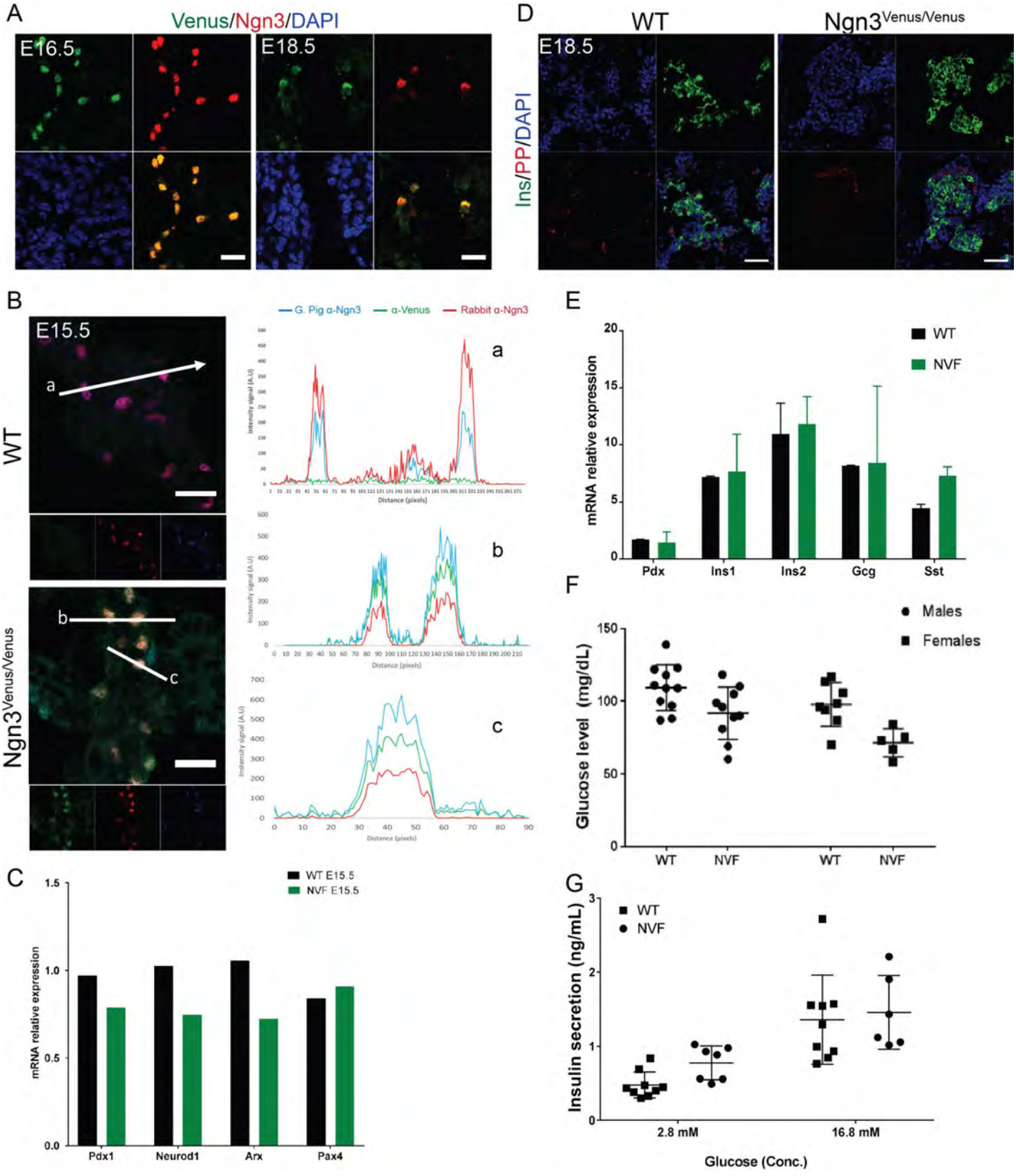

Figure S1. Characterization of endocrine cell formation and function in NVF mice. (A) Immunohistochemical analysis shows similar spatio-temporal expression pattern of NVF and endogenous Ngn3 expression at E16.5 and E18.5 heterozygous NVF pancreatic section. Scale bar, 20 µm. (B) Plot profile of Venus staining together with two different antibodies against endogenous Ngn3 in WT and homozygous NVF pancreatic sections. No Venus signal was detected in the WT sample. Scale bar, 20 µm. (C) qPCR analysis of isolated cells from E15.5 WT and homozygous NVF pancreata for expression of Ngn3 target genes (N= 1 experiment derived from 8-10 embryos). (D) Staining of PP-cells in E18.5 pancreatic sections from WT and homozygous NVF mice show no significant difference in the formation of these cells. Scale bar, 50 µm. (E) qPCR analysis of key pancreatic hormones from isolated islets from 3-month-old WT and homozygous NVF mice (N = 3). (F) Normoglycemic levels in 3-month-old homozygous NVF mice compared to WT. (G) Glucose-stimulated insulin secretion test shows no differences in insulin secretion from isolated islets from 3-month-old homozygous NVF and WT mice.

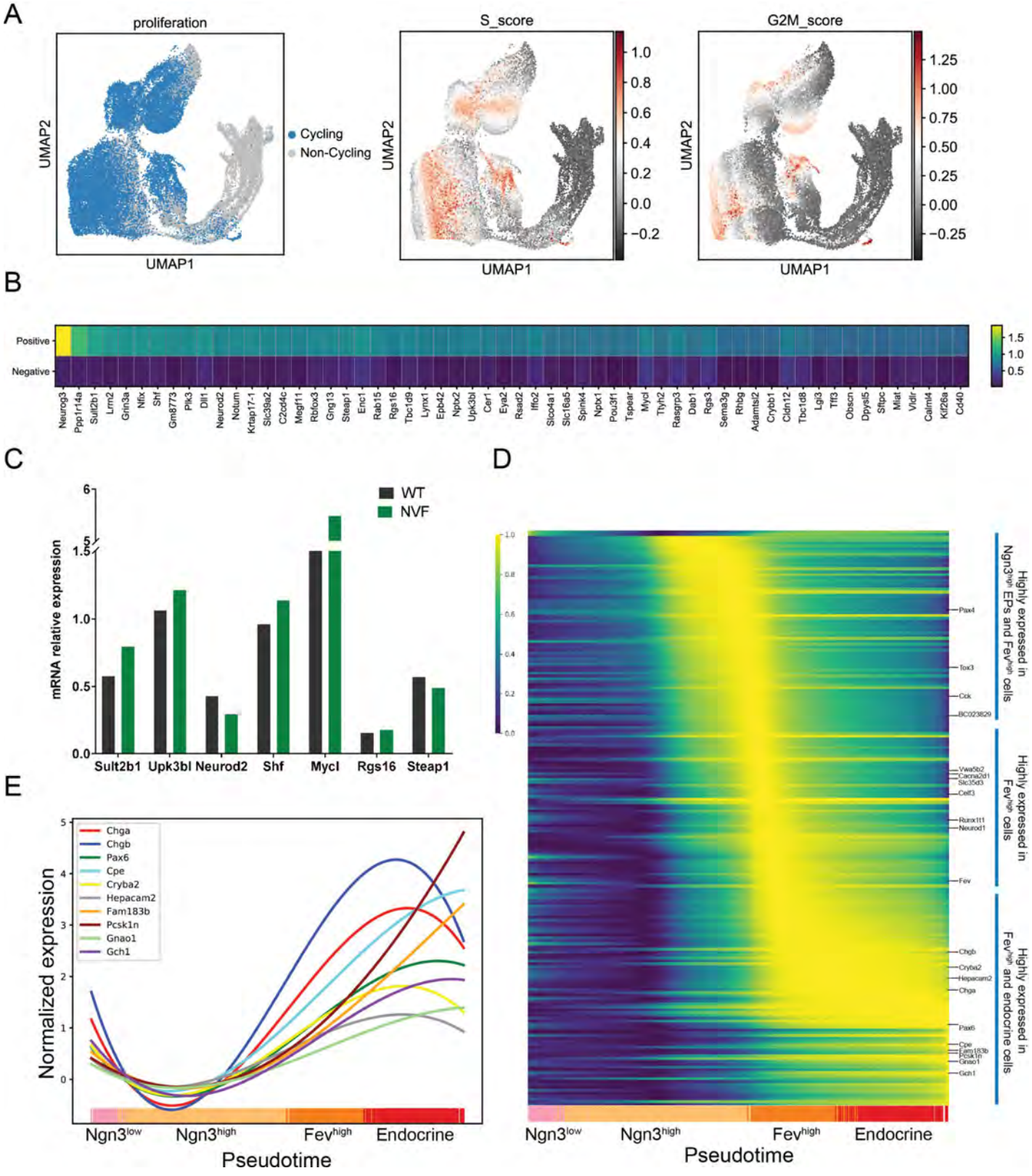

Figure S2. Cell cycle classification and *Fev*^{high} cell-enriched genes. (A) UMAP plots of proliferative status of all pancreatic epithelial populations. Classification into cycling and non-cycling cells (left) based on cell score levels for cell cycles phases S and G2/M calculated based on the expression of a set of genes involved in cell cycle progression (right). (B) Heatmap showing the mean expression in *Ngn3*$^{+}$ and *Ngn3*$^{-}$ cells of the 58 EP-signature genes. Expression values are normalized and scaled to unit variance. (C) qPCR analysis of E15.5 isolated pancreatic epithelial cells indicates no significant changes in the expression levels of several EP-signature genes in WT and homozygous NVF mice (N= 1 experiment derived from 8-10 embryos). (D) Gene expression along pseudotime from *Ngn3*^{low} progenitors to endocrine cells. The top 200 genes enriched in *Fev*^{high} cells are shown (Table S3) and selected genes highlighted. Expression is normalized and approximated by polynominal regression fits along pseudotime. Fitted values of each gene are then scaled to the range between 0 and 1. Cluster membership of the cells is indicated at the bottom. (E) Gene expression along pseudotime of selected genes starting expression in *Fev*^{high} cells and continuously expressed in differentiated endocrine cells. Lines are polynominal regression fits of normalized data. Cluster membership of the cells is indicated at the bottom.

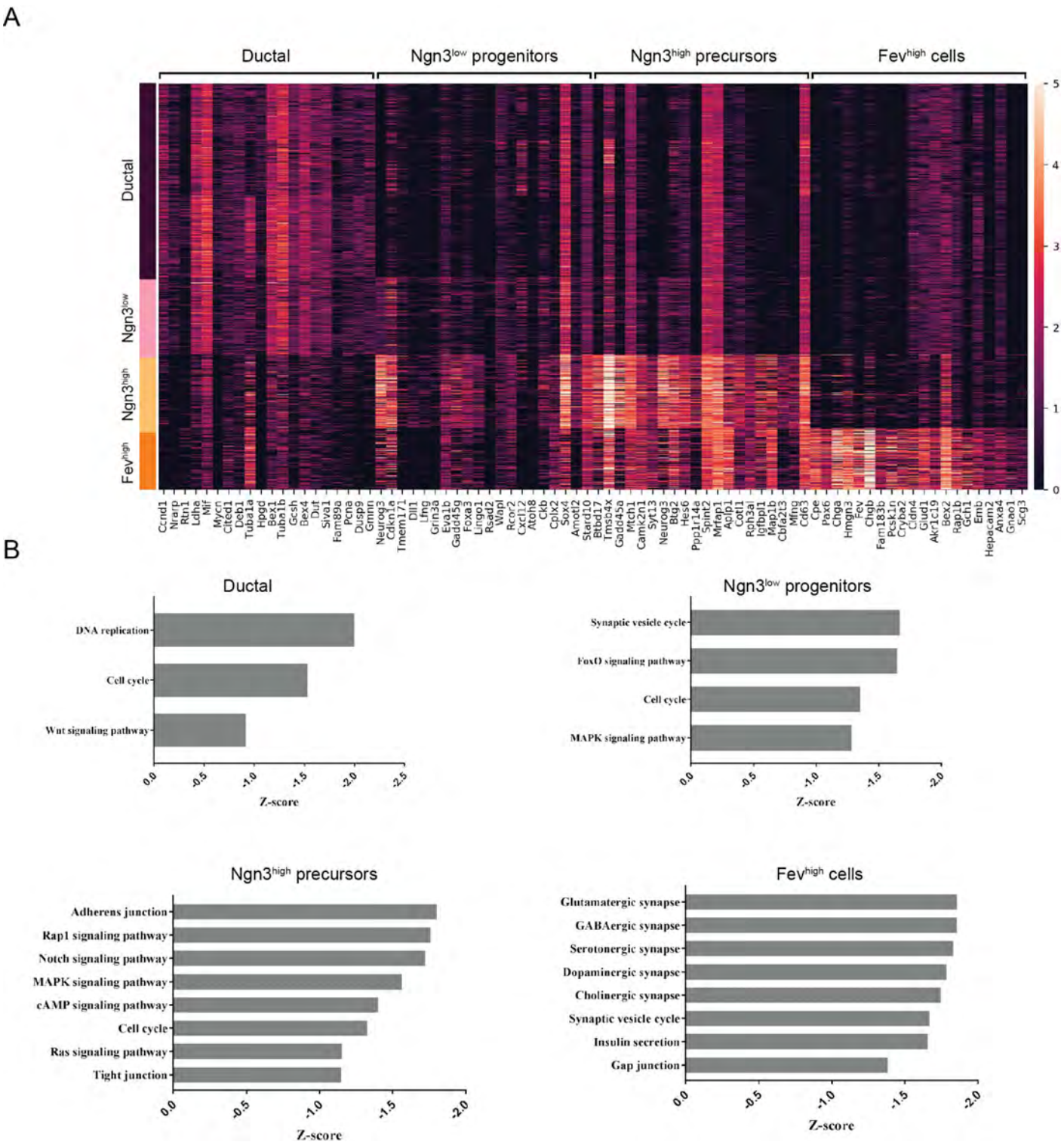

Figure S3. Pathway analysis of EPs and *Fev*^{high} cells. (A) Heatmap showing the top 20 genes of subtype-specific expression profiles of ductal, *Ngn3*^{low} progenitor, *Ngn3*^{high} precursor and *Fev*^{high} cells. Normalized expression values are shown. (B) GO-term enrichment analysis of gene sets specific to ductal, *Ngn3*^{low} progenitors, *Ngn3*^{high} precursors and *Fev*^{high} populations.

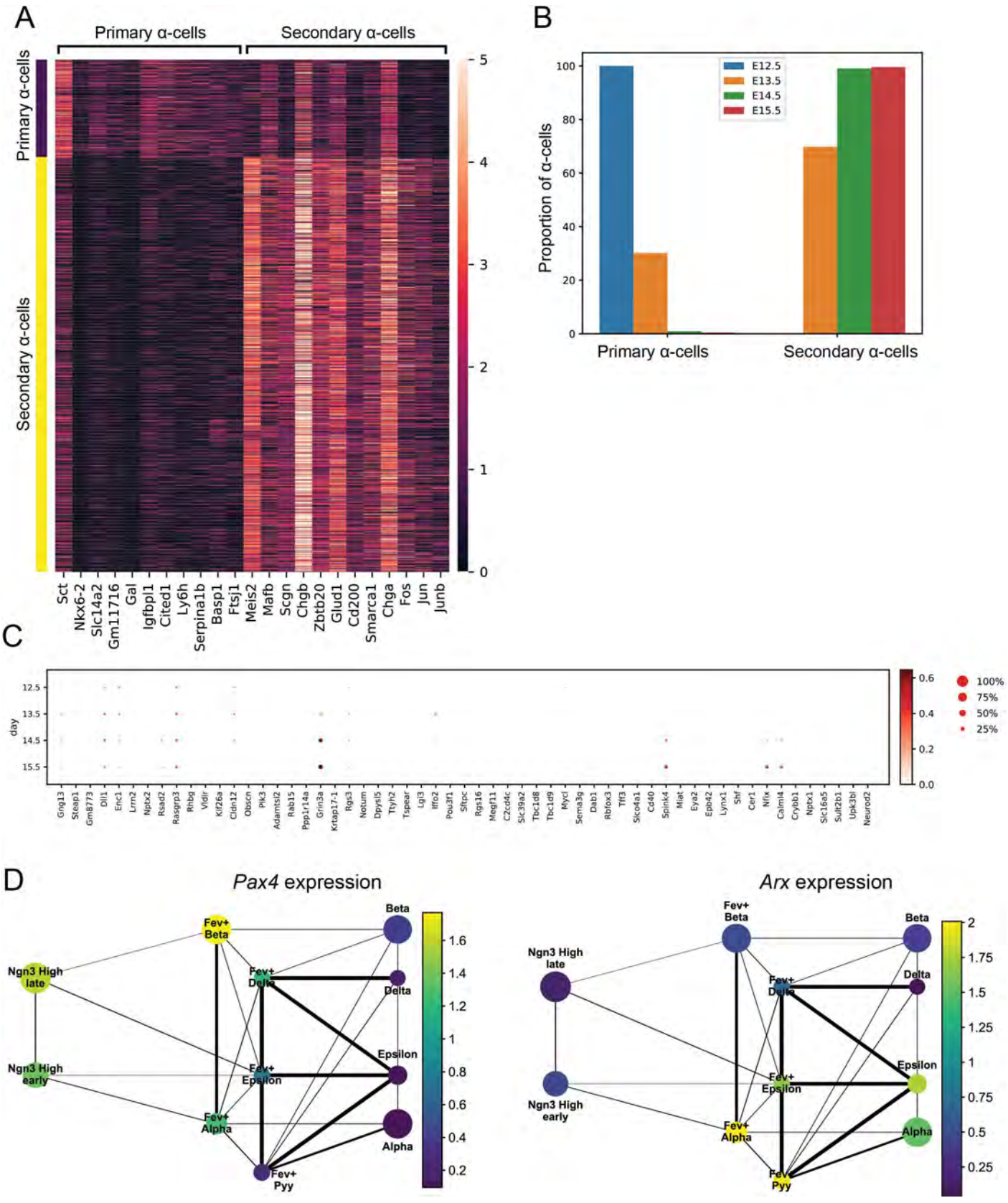

Figure S4. Early and late α-cells are transcriptionally heterogeneous. (A) Expression of selected differentially expressed genes between primary and secondary α-cells indicates stage-dependent α-cell heterogeneity. Normalized expression values are shown. (B) Proportion of primary and secondary α-cells from E12.5 to E15.5 developmental stages. (C) Dotplot of the expression levels of EP-signature genes in *Ngn3*^{low} progenitors derived from different developmental stages. (D) The expression of *Pax4* and *Arx* in different pancreatic clusters overlaid onto the PAGA graph. The expression of *Pax4* starts in late *Ngn3*^{high} precursors, while the expression of *Arx* is mainly evident in *Fev*^{high} alpha cells. Mean of normalized expression per cluster is shown.

Table S1. Marker genes of pancreatic epithelial populations. Differential gene expression analysis of 8 main pancreatic epithelial clusters from E12.5-E15.5 mouse embryonic pancreas. List of genes that are differentially upregulated in each cluster compared to all other clusters. This list is related to Figure 2.

Click here to Download Table S1

Table S2. Gene expression profile of *Ngn3*+ EPs. List of upregulated and downregulated genes in EPs (*Ngn3*^{low} progenitors and *Ngn3*^{high} precursors) compared to non-EP clusters. This list is related to Figure 4 and 5.

Click here to Download Table S2

Table S3. Gene expression changes during early endocrinogenesis. Differentially expressed genes by comparison of ductal cluster to Ngn3^{low} progenitors, *Ngn3*^{low} progenitors to ductal cluster, *Ngn3*^{high} precursors to *Ngn3*^{low} progenitors and *Fev*^{high} cells to *Ngn3*^{high} precursors. This list is related to Figure 5 and Figure S3.

Click here to Download Table S3

Original Article

MOLECULAR METABOLISM

Foxa2 and Pdx1 cooperatively regulate postnatal maturation of pancreatic β-cells

Aimée Bastidas-Ponce [1,2,4], Sara S. Roscioni [1,2], Ingo Burtscher [1,2,4], Erik Bader [1,2], Michael Sterr [1,2], Mostafa Bakhti [1,2,4], Heiko Lickert [1,2,3,4,*]

ABSTRACT

Objective: The transcription factors (TF) Foxa2 and Pdx1 are key regulators of beta-cell (β-cell) development and function. Mutations of these TFs or their respective cis-regulatory consensus binding sites have been linked to maturity diabetes of the young (MODY), pancreas agenesis, or diabetes susceptibility in human. Although Foxa2 has been shown to directly regulate Pdx1 expression during mouse embryonic development, the impact of this gene regulatory interaction on postnatal β-cell maturation remains obscure.

Methods: In order to easily monitor the expression domains of Foxa2 and Pdx1 and analyze their functional interconnection, we generated a novel double knock-in homozygous ($FVFPBF^{DHom}$) fluorescent reporter mouse model by crossing the previously described Foxa2-Venus fusion (FVF) with the newly generated Pdx1-BFP (blue fluorescent protein) fusion (PBF) mice.

Results: Although adult PBF homozygous animals exhibited a reduction in expression levels of Pdx1, they are normoglycemic. On the contrary, despite normal pancreas and endocrine development, the $FVFPBF^{DHom}$ reporter male animals developed hyperglycemia at weaning age and displayed a reduction in Pdx1 levels in islets, which coincided with alterations in β-cell number and islet architecture. The failure to establish mature β-cells resulted in loss of β-cell identity and trans-differentiation towards other endocrine cell fates. Further analysis suggested that Foxa2 and Pdx1 genetically and functionally cooperate to regulate maturation of adult β-cells.

Conclusions: Our data show that the maturation of pancreatic β-cells requires the cooperative function of Foxa2 and Pdx1. Understanding the postnatal gene regulatory network of β-cell maturation will help to decipher pathomechanisms of diabetes and identify triggers to regenerate dedifferentiated β-cell mass.

Keywords Foxa2; Pdx1; β-Cell maturation; β-Cell identity; Trans-differentiation

1. INTRODUCTION

The pancreatic and duodenal homeobox 1 (Pdx1) transcription factor plays an essential role in the proper expansion and specification of pancreatic lineages during development [1–3]. In rodents, Pdx1 is expressed in the entire pancreatic epithelium during early development, and null mice do not develop a pancreas and die within a few days after birth [4,5]. During the formation of endocrine cells, an increase in Pdx1 levels is crucial for the commitment and differentiation of pancreatic β-cells [1,6,7]. In adulthood, Pdx1 ultimately becomes restricted to β- and δ-cells in the islets, where it maintains β-cell identity and function through the regulation of genes involved in glucose homeostasis [8,9], such as insulin, glucose transporter 2 (GLUT-2), and glucokinase (GK) [10]. Therefore, mice heterozygous for *Pdx1* develop diabetes in adulthood with glucose unresponsiveness and increased β-cell apoptosis [11–13]. Moreover, a mutation in the human *PDX1* locus generates MODY4 (Maturity onset diabetes of the young 4), which results in early diabetes occurrence without any signs of insulin resistance [14].

Another recently emerging player predisposing for diabetes is *FOXA2*, which belongs to the forkhead family of TFs. This protein is a pioneer transcription factor, which opens compact chromatin and allows DNA binding of other TFs in a higher-order gene regulatory network [15]. Although at earlier development stages Foxa2 is detectable in all pancreatic progenitor cells, the protein becomes upregulated and progressively restricted to endocrine progenitors during secondary transition and has lower expression levels in the exocrine and ductal lineages [16]. Foxa2 is not only essential for pancreas development and endocrine differentiation [7] but also for the maintenance of adult β-cell function [17,18]. Therefore, deletion of Foxa2 specifically in β-cells causes a hyperinsulinemic hypoglycemic phenotype through the misregulation of the insulin secretion machinery [19]. In line with this, a recent genetic fine mapping and genomic annotation study has revealed an association of type 2 diabetes risk alleles with FOXA2-bound enhancers in human [20].

Foxa2 and Pdx1 share several important functions, such as regulation of insulin production and modulation of the function of other transcription factors [10,21,22]. In diabetic models, the levels of both TFs

[1]Institute of Diabetes and Regeneration Research, Helmholtz Zentrum München, Germany [2]Institute of Stem Cell Research, Helmholtz Zentrum München, Germany [3]Technical University of Munich, Germany [4]German Center for Diabetes Research (DZD), Germany

*Corresponding author. Helmholtz Zentrum München, Parkring 11, D-85748, Garching, Germany. Fax: +49 89 31873761. E-mail: heiko.lickert@helmholtz-muenchen.de (H. Lickert).

Received January 20, 2017 • Revision received March 16, 2017 • Accepted March 21, 2017 • Available online 25 March 2017

http://dx.doi.org/10.1016/j.molmet.2017.03.007

appeared to be reduced in dedifferentiated β-cells, suggesting that these TFs act alone or in combination to induce or maintain β-cell identity [23,24]. Furthermore, mice heterozygous for both *Pdx1* and *Foxa2* display altered islet architecture and loss of β-cell identity resulting in severe distortion in insulin secretion and blood glucose regulation [2]. Foxa2 binds directly to *Pdx1* enhancer elements during development and deletion of Foxa1 and Foxa2 in the Pdx1 lineage leads to pancreas agenesis [7]. Although Foxa2-driven Pdx1 expression has also been reported in differentiating β-cells [25], the biological significance of this interconnection regarding postnatal β-cell maturation has not been thoroughly addressed.

To follow the expression domains of Foxa2 and Pdx1 easily and study the functional link between these two TFs in detail, we have generated knock-in reporter fluorescent protein (FP) fusion mouse lines, a previously reported Foxa2-Venus fusion (FVF) strain [15], and, for this study, a Pdx1-BFP fusion (PBF) model. Both single homozygous knock-in reporter mice were viable and fertile with normal glycemic condition. Surprisingly, the FVFPBF^{DHom} reporter mice developed hyperglycemia at the weaning age although they were vital and healthy immediately after birth, with no obvious alteration in pancreas organogenesis and islet formation. Remarkably, the elevated blood glucose levels were only detected in male animals and coincided with significantly reduced levels of Pdx1. In addition, β-cells from FVFPBF^{DHom} male mice did not induce a proper maturation program, lost their identity, and possibly transdifferentiated towards the α- and δ-cell fates. Analysis of ChIP-seq datasets showed that Foxa2 and Pdx1 co-occupy a substantial number of *cis*-regulatory regions of genes involved in β-cell development, maturation, and function. Strikingly, the expression of key players in establishing and maintaining β-cell maturation were impaired in the FVFPBF^{DHom} male mice, suggesting the interference of the fused FPs with the cooperative binding and/or transactivation of these crucial factors. These results suggest that Foxa2 and Pdx1 genetically interact and cooperatively regulate a gene regulatory network of postnatal β-cell maturation.

2. MATERIAL AND METHODS

2.1. Generation of Pdx1 BFP fusion (PBF) reporter mouse line

2.1.1. Production of the Pdx1 BFP targeting construct

The Pdx1 BFP targeting construct was designed as shown in Supplementary Figure 1A. The 5′ and 3′ homology regions (HR) for the Pdx1 gene were amplified by PCR using EP-1015/1016 and EP-1017/1018 primer pairs, respectively. We used C57BL/6 BAC (RPCI22−254-G2) as the template DNA. HRs were cloned by restriction enzymes AscI, HindIII, and BamHI into the PL-254 vector [26−28]. From the same BAC, a 9.5 kb fragment was recovered using gap repair via homologous recombination in EL350 bacteria as described previously [26], resulting in the production of pL254-Pdx1. BamHI and XbaI were used as single cutters for linearization prior to the gap repair. For cloning of the knock-in cassette, the 5′ HR (EP-1006, 1007) and 3′HR (EP-1008, 1009) from exon 2 of Pdx1 were amplified by PCR using the previously described BAC as template and subcloned via NotI, XbaI, HindIII, or XhoI into the pBluescript KS- (pBKS-), respectively, to generate the pBKS-Ex2 HR. The BFP sequence (Evrogen) with translational stop codon was amplified (EP-25, 1010) and subcloned between the homology regions of the pBKS-Ex2 HR via XbaI and SpeI, resulting in the generation of pBKS-Ex2 HR BFP. Next, the neomycin resistance gene, which is driven by PGK promoter and is flanked by LoxP sites, was cloned from the PL452 [27] vector via EcoRI and BamHI into the downstream of the BFP sequence resulting in the formation of pBKS-Ex2 HR-BFP-Neo. Afterwards, the mini-targeting cassette was released by digestion with NotI and KpnI and introduced into the pL254-Pdx1 via bacterial homologous recombination in EL250 bacteria, resulting in the generation of the final targeting construct (pL-254 Pdx1-BFP Fusion targeting vector, see Supplementary Figure 1A), which was confirmed by sequencing.

2.1.2. Cell culture and homologous recombination in ES-Cells

Mouse ES cells were cultured as previously described [29]. The AscI-linearized pL-254 Pdx1-BFP fusion (PBF) targeting vector was electroporated into the IDG3.2 ES cells [30]. 300 mg/mL of G418 (Invitrogen, 50 mg/mL) were used to select the neo-resistant clones. Homologous recombination at the Pdx1 locus was evaluated by southern blot analysis of the BamHI-digested genomic DNA using the Pdx1 3′ probe located outside the targeting vector (3′ (EP1013, 1014) was subcloned into and later released by PstI and HindIII digestion from pBKS). Through the southern blot analysis, three positive clones were identified out of 110 total selected clones (Supplementary Figure 1B). The homologous recombined-clones were aggregated with CD1 morulae and the resulting chimeric mice passed the Pdx1BFPneo allele through their germline cells. Finally, by intercrossing with the ROSA-Cre mouse line, the Neo cassette flanked by LoxP sites was deleted. The excision of the Neo cassette was confirmed through the genotyping PCR using the primers EP-536, 1189, and 1193, generating a 339 bp product for the Pdx1$^{BFP\ Neo}$ allele and a 421 bp product for the Pdx1BFPdelta Neo allele (Supplementary Figure 1C). To genotype the homozygous and heterozygous PBF mice, the primers EP 1188, 1189, and 1193 were used. The WT mice generated a 211 bp PCR product, distinguished from the 421 bp band of the homozygous animals. Two products of 211 and 421 bp were identified for the heterozygous mice (Supplementary Figure 1D). The mouse line described here will be available to the research community upon acceptance of this manuscript.

2.2. Western blot analysis

Western blot analysis was performed according to the standard protocols. Briefly, lysates from embryonic pancreata or isolated islets from adult mice were prepared as described [31] and subjected to the SDS-PAGE electrophoresis and transferred to the nitrocellulose membranes. After blocking, the membranes were incubated with the appropriate primary antibodies (Supplementary Table 2) overnight followed by incubation with HRP-conjugated secondary antibodies. The signals were detected by enhanced chemiluminescence (Thermo Scientific).

2.3. Immunostaining and imaging

2.3.1. Whole-mount staining

Mouse embryos were fixed using 2% PFA in PBS for 20 min. After permeabilization (0.1% Triton, 0.1 M Glycin) for 15 min, they were subjected to the blocking solution (10% FCS, 3% Donkey serum, 0.1% BSA and 0.1% Tween-20 in PBS) for 1 h at room temperature (RT). Next, the primary antibodies (Supplementary Table 2) diluted in the blocking solution were added to the samples overnight at 4 °C. After extensive washing with PBST (0.1% Tween-20 in PBS), the embryos were stained by secondary antibodies diluted in the blocking solution for 3−5 h at RT. The samples were then incubated with 4′,6-diamidin-2-phenylindol (DAPI), followed by washing with PBST and embedding in the commercial medium (Life Tech., ProLong Gold).

2.3.2. Pancreas section staining

Embryonic or adult pancreata were dissected and fixed in 4% PFA in PBS for 2 h at 4 °C. The tissues were merged in 7.5, 15 and 30% sucrose-PBS solutions at RT (2 h incubation for each solution). Afterwards, they were embedded in cryoblocks using tissue-freezing medium (Leica 14020108926). Next, sections of 20 μm thickness were cut from each sample and subjected to immunostaining as described for Whole-mount staining. All images were obtained with a Leica microscope of the type DMI 6000 using the LAS AF software. Images were analyzed using ImageJ and Imaris imaging software programs.

2.4. Islet isolation

The isolation of islets was performed by collagenase P (Roche) digestion of the adult pancreas. Briefly, 3 mL of collagenase P (1 mg/mL) was injected into the bile duct and the perfused pancreas was consequently dissected and placed into another 3 mL collagenase P for 15 min at 37 °C. 10 mL of G-solution (HBSS + 1% BSA) was added to the samples followed by centrifugation at 1600 rpm at 4 °C. After another washing step with G-solution, the pellets were re-suspended in 5.5 mL of gradient preparation (5 mL 10% RPMI + 3 mL 40% Optiprep/per sample), and placed on top of 2.5 mL of the same solution. To form a 3-layers gradient, 6 mL of G-solution was added on the top. Samples were then incubated for 10 min at RT before subjecting to centrifugation at 1700 rpm. Finally, the interphase between the upper and the middle layers of the gradient was harvested and filtered through a 70 μm Nylon filter and washed with G-solution and the islets were handpicked under the microscope.

2.5. RNA isolation and amplification

RNA isolation was performed using the miRNA micro kit (Qiagen) according to the manual. On a column, DNase I treatment was applied to degrade DNA. 14 μl of nuclease-free water were added to elute the RNA fractions, which were used immediately or stored at −80 °C. Due to the low amounts of RNA, RNA amplification was carried out using the Ovation® PicoSL WTA SystemV2 (Nugen). The amplification process was done according to the manual using 50 ng total RNA.

2.6. Quantitative PCR (qPCR)

The qPCR was carried out using TaqMan™ probes (Life Technologies) (Supplemental Table 3) and the Viia7 Real Time PCR System (Thermo Fisher Scientific). Each reaction contained 25 ng of cDNA. For analysis, the C_t-values were transformed to the linear expression values and normalized to the reference genes and to the control samples.

2.7. Glucose-stimulated insulin secretion (GSIS)

For GSIS analysis, the isolated islets were cultured overnight before transferring to a 96-well plate containing modified Krebs Ringer phosphate Hepes (KRPH) buffer with 2 mM glucose for 1 h. Different glucose concentrations (2 and 16.5 mM) were added to the islets (2 h for each). The supernatant were used for insulin measurement. At the end, the islets were lysed in RIPA buffer and samples were kept at −20 °C. Insulin concentrations were measured and quantified using an ultrasensitive insulin ELISA kit (Cristal Chem). The analysis was performed using a standard curve, and the data were normalized to the total insulin content. The islet insulin content was obtained by normalizing the insulin content to the total protein content in the islets.

2.8. Blood glucose level measurement

Mice were maintained in standard conditions and starved 6 h before the measurement. Blood glucose values were determined from venous blood using an automatic glucose monitor (Glucometer Elite, Bayer).

2.9. ChIP-seq dataset analysis

Raw reads from Foxa2 ChIP-seq (GSM1306337) and Pdx1 ChIP-seq (GSM1824088) were obtained from public databases and subsequently processed with Trimmomatic (0.35) to remove low quality bases and adapter contamination. Next, reads were aligned to mm10 genome using bowtie2 (2.2.6) with very-sensitive option and duplicate reads were removed using samtools (1.3). Binding sites were then called using GEM [32] and filtered after visual inspection using a q value cut-off of 10^{-4} and 10^{-12} for Pdx1 and Foxa2, respectively. For pathway analysis, binding sites within 20 kb of a TSS or within a gene body were mapped to the respective gene using bedtools (2.18). Pathway enrichment analysis was performed using HOMER [33].

2.10. Statistical analysis

All data are presented as Means ± Standard Deviation. The data were analyzed using a two-tailed unpaired *t*-test.

3. RESULTS

To circumvent development of MODY4 due to *Pdx1* haploinsufficiency [34], we generated a PBF reporter mouse line by removing the translational stop codon and fusing *BFP* in frame with *Pdx1* (Supplementary Figure 1A). Southern blot analysis with a 3′ probe revealed a targeting efficiency of 2.72% at the *Pdx1* locus (Supplementary Figure 1B). We generated chimeric mice and removed the *LoxP*-flanked neomycin selection cassette by Cre recombinase-mediated excision in the germ line (Supplementary Figure 1C). Genotyping of the offspring from heterozygous intercrosses revealed normal Mendelian distribution, suggesting that the Pdx1-BFP fusion protein does not interfere with pancreas development (Supplementary Figure 1D and data not shown). Western blot analysis of embryonic day (E) 14.5 pancreata and adult islets confirmed the endogenous expression of both Pdx1 and Pdx1-BFP fusion protein in heterozygous animals. Furthermore, a reduction in Pdx1 and PBF levels was observed in both heterozygous and homozygous PBF mice compared to the WT animals during development and adulthood (Supplementary Figure 1E and F).

Next, we assured that the PBF mirrors the endogenous Pdx1 expression patterns during primary and secondary transitions of pancreas development. Using whole-mount staining of embryos, we confirmed that PBF is expressed in a spatio-temporal manner as endogenous Pdx1 during primary transition (E9.0—11.5) (Figure 1A—D). During the secondary transition, the expression of Pdx1 is restricted to the endocrine lineage [35]. Analysis of the E13.5—15.5 pancreata indicated that the PBF expression becomes gradually limited to a subpopulation of pancreatic cells (Supplementary Figure 1G—I). In addition, immunostaining of E15.5 pancreatic sections using endocrine and exocrine markers revealed the expression of PBF in the endocrine compartment (Figure 1E—H). Furthermore, we showed that β- but not α-cells exhibit PBF reporter activity (Figure 1I). Finally, we found that PBF expression is restricted to β- and δ-cells in adult islets (Figure 1J). Collectively, these data indicate that the PBF protein resembles the spatio-temporal expression pattern of endogenous Pdx1 during development and in adulthood. Moreover, PBF homozygous mice are viable and fertile and do not show any signs of MODY4.

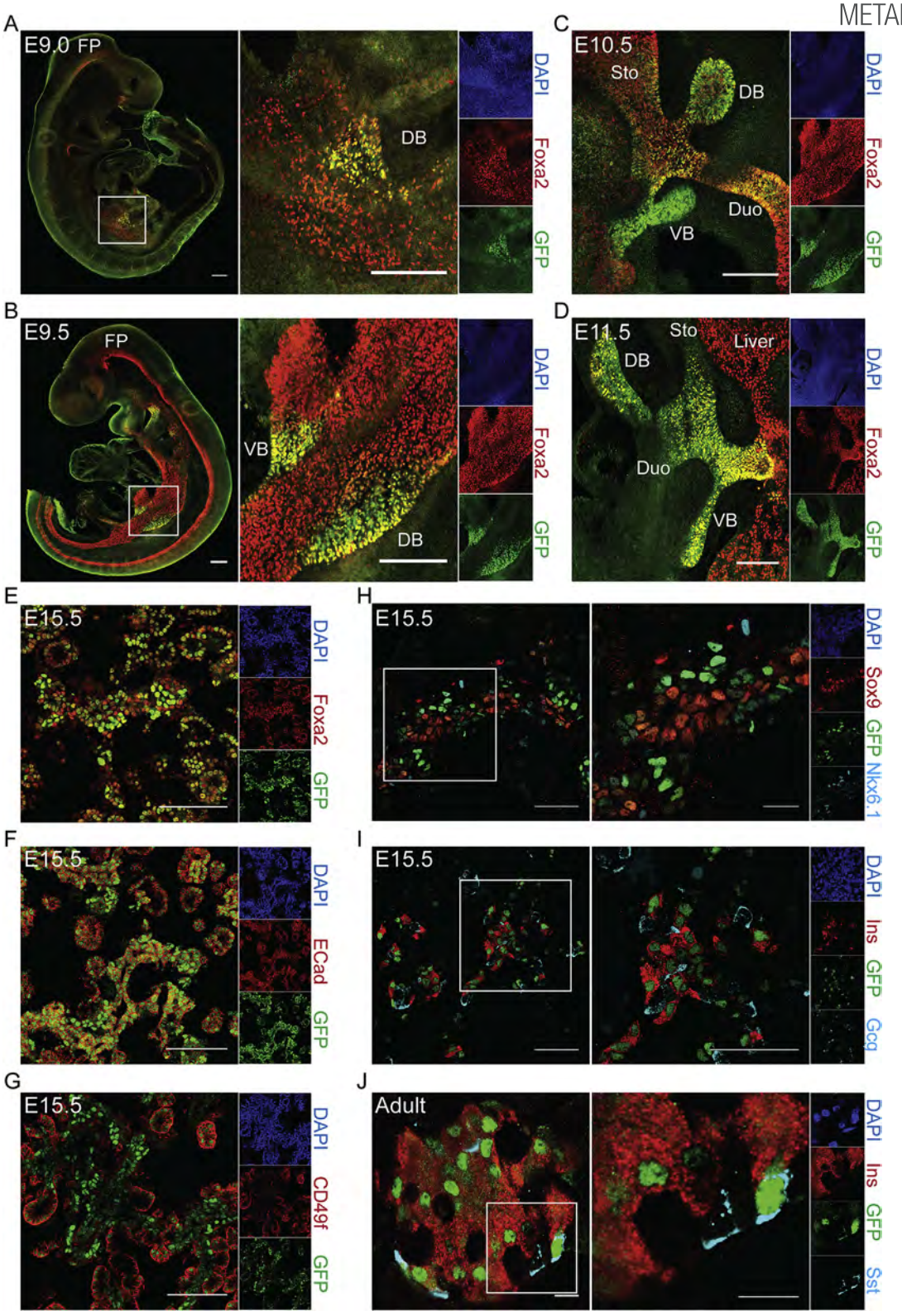

Figure 1: PBF is expressed in a spatio-temporal pattern as endogenous Pdx1 during pancreas development and in adulthood. (A, B) Whole-mount immunostaining of embryos indicating the expression of PBF during early stages of pancreas organogenesis at E9.0 and E9.5. Whereas the BFP signal is detected at the dorsal buds at E9.0, it is visible at both ventral and dorsal buds at E9.5. (C, D) The expansion of the BFP-positive buds through the primary transition of pancreas development, indicating the similar expression pattern of PBF and the endogenous Pdx1 protein. (E, F) Immunostaining of pancreata for Foxa2 and E-Cadherin suggesting the endocrine identity of the PBF^{+} cells at E15.5. (G) Co-staining of the PBF and CD49f (*α6 integrin* subunit), as a marker for exocrine cells, excludes the exocrine characteristics of PBF^{+} cells. (H) PBF-positive cells are negative for Sox9 and positive for Nkx6.1, which mark ductal epithelial and a subpopulation of endocrine cells, respectively. (I) Co-staining of PBF with insulin and glucagon indicating the β- but not α-cells identity of the PBF^{+} cells. (J) Immunostaining of PBF mice-derived isolated islets showing the expression of Pdx1-BFP in insulin^{+} β- and somatostatin^{+} δ-cells in adulthood. All analyses have been performed using heterozygous animals. Scale bars, A-D, 200 μm; E-G, 100 μm; H and I, 50 μm; J, 10 μm. FP, floor plate; DB, dorsal bud; VD, ventral bud; Sto, stomach; Duo, duodenum; ECad, E-Cadherin; Ins, Insulin; Gcg, Glucagon and Sst, Somatostatin.

To analyze the functional link between Foxa2 and Pdx1 in detail, we created FVF and PBF double homozygous knock-in (FVFPBF^{DHom}) animals. Early postnatal FVFPBF^{DHom} mice were viable and healthy with normal pancreas development and growth when compared to WT, FVF homozygous, and PBF homozygous mice. However, further analysis of 3-month-old animals revealed remarkably high blood glucose levels (>450 mg/dL) in males FVFPBF^{DHom} (Figure 2A), but only slightly increased levels of 130 mg/dL in females, suggesting that females are protected from developing diabetes (Supplementary Figure 2A). In comparison, PBF single homozygous animals were normoglycemic. For this study, we focused on understanding the pathomechanisms of developing diabetes in the FVFPBF^{DHom} male animals. First, we analyzed gene expression by qPCR in isolated isles from 3-month-old FVFPBF^{DHom} and controls, which indicated a reduction in the expression of *Pdx1* but not in *Foxa2* mRNA (Figure 2B). This was further confirmed by western blot analysis in isolated islets from FVFPBF^{DHom} mice, in which we found no change in Foxa2 but a notable decrease in Pdx1 protein levels (Figure 2C and D). Moreover, whereas PBF homozygous mice exhibited a reduction in Pdx1 levels, the FVF single homozygous animals expressed normal levels of this protein (Figure 2C and D and Supplementary Figure 2B). Finally, immunostaining of isolated islets from FVFPBF^{DHom} mice also revealed a reduction in the Pdx1, but not in Foxa2 levels (Figure 2E and F). These results confirm the upstream function of Foxa2 on Pdx1 in a gene regulatory network [7] and the presence of an autoregulatory, positive feedback loop of Pdx1 [36]. Therefore, the fusion of the FPs to these TFs impacts the expression levels of Pdx1 but not of Foxa2.

To assess whether the reduction in the Pdx1 levels in FVFPBF^{DHom} mice leads to impaired β-cell function [9], we measured the mRNA levels of the downstream *Ins1* gene. We found a striking reduction in the expression of this gene at mRNA level in islets from 3-month-old FVFPBF^{DHom} mice (Figure 3A). Furthermore, enzyme-linked immunosorbent assay (ELISA) of total islet-precipitated protein indicated a significant reduction in insulin content in the FVFPBF^{DHom} animals compared to the controls (Figure 3B). In line with this, glucose-stimulated insulin secretion (GSIS) of pancreatic islets from FVFPBF^{DHom} animals showed a significant decreased insulin release upon high glucose when compared to control islets (Figure 3C). These changes in islet insulin content and GSIS coincided with remarkable alterations in islet morphology. We observed that islets from FVFPBF^{DHom} mice lose their typical spherical shape and exhibit the presence of α-cells intermingled with β-cells in the islet core (Figure 3D). Finally, we analyzed the maturation status of β-cells by analyzing the maturation markers Urocortin 3 (Ucn3) [37] and MafA [38] and found an almost complete lack of expression in 3-month-old FVFPBF^{DHom} male animals when compared to controls (Figure 3E and F). Taken together, these data suggest that the combined defect in FVF and PBF activity results in impaired β-cell maturation and function.

To better understand if β-cells lose their identity or fail to mature, we monitored the newly born β-cells in control and FVFPBF^{DHom} mice from postnatal day 9 (P9) until 1.5 months of age. We selected these time points to cover the postnatal maturation period of β-cells. In mice, β-cells undergo two major steps of maturation, postnatally. The first step occurs at P14 and is marked by the expression of Ucn3 [37], whereas

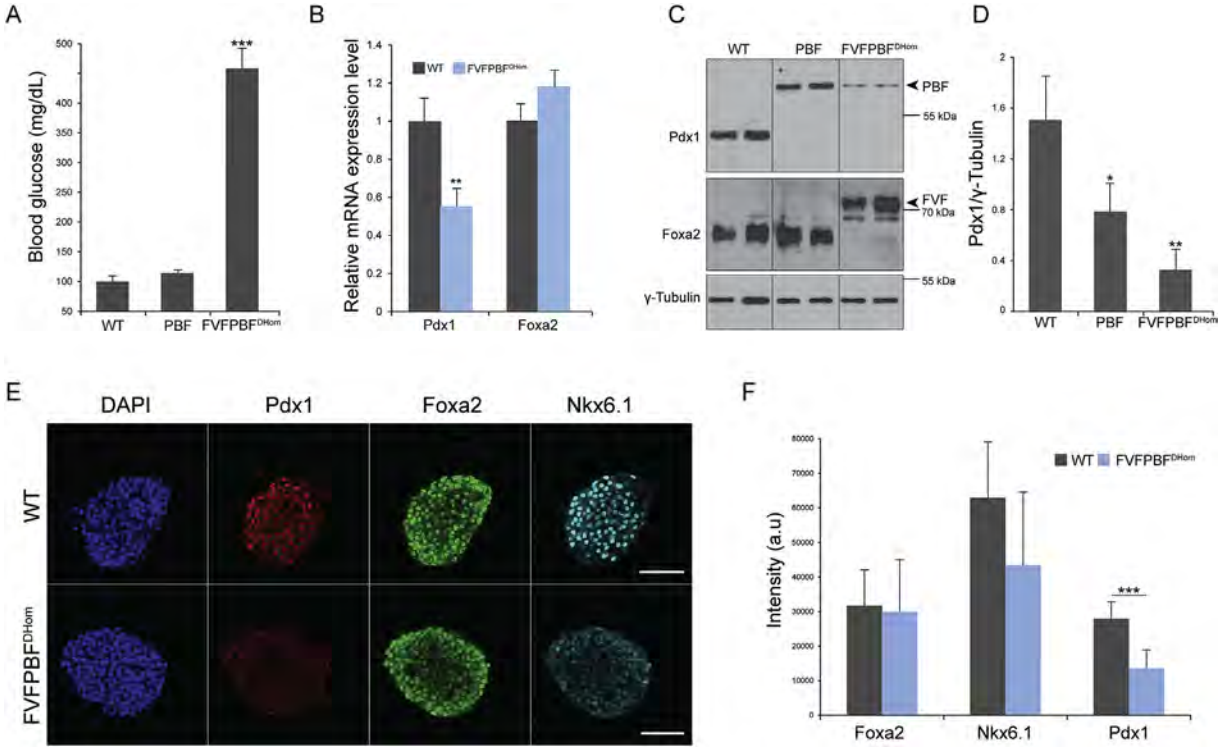

Figure 2: FVFPBF^{DHom} male mice exhibit reduction in Pdx1 levels postnatally and develop hyperglycemia at the weaning age. (A) Fasted blood glucose levels (mg/dL) for 3-month-old male FVFPBF^{DHom}, PBF, and WT mice (n = 3, ***P < 0.001). (B) qPCR analysis for *Foxa2* and *Pdx1* of isolated islets from 3-month-old male WT and FVFPBF^{DHom} mice. Data were normalized according to 18S. (n = 4 for WT and 3 for FVFPBF^{DHom}, **P < 0.01). (C, D) Expression of Foxa2 and Pdx1 proteins using western blot analysis from isolated adult islets. (n = 3 for, *P < 0.05; **P < 0.01) (E) Immunostaining of isolated islets exhibits a significant reduction in the expression levels of Pdx1 but not Foxa2 in the male FVFPBF^{DHom} mice compared to the controls. (F) Quantification of signal density of Foxa2, Nkx6.1, and Pdx1 in the FVFPBF^{DHom} and WT islets (n = 3, ***P < 0.001). Scale bars, 50 μm.

the second step takes place when the animal changes from a high-fat milk diet from the mother to a high-carbohydrate chow after weaning (around P25) [39]. Blood glucose levels were comparable between controls and FVFPBF^{DHom} mice at P9 and P14, but significantly increased from P25 onwards in FVFPBF^{DHom} animals. Remarkably, this elevation in blood glucose levels was not affected by the diet change and increase in metabolic demands during weaning, suggesting that the genetic predisposition rather than environmental factors causes β-cell dysfunction (Figure 4A). When we quantified the endocrine composition of islets, we found a significant reduction in β-cells along with an increase in α-cell number in 1.5-month-old FVFPBF^{DHom} mice. However, at P14 the number of both cell types remained unaffected (Figure 4B and Supplementary Figures 3A and B), suggesting that normal number of endocrine cells are formed during development. We could also detect subtle but not significant changes in the δ-cell number in the FVFPBF^{DHom} mice (Supplementary Figure 3B). Next, we investigated the expression of β-cell maturation marker and found that FVFPBF^{DHom} animals exhibited lower levels of Ucn3 at P14, and almost no expression at P25 and 1.5 months. Importantly, the switch from high-fat milk diet to carbohydrate-enriched chow did not prevent the loss of Ucn3, indicating that the failure in β-cell maturation occurs before the weaning age (Figure 4C). Furthermore, we analyzed the expression levels of Ucn3 in isolated islets from FVF and PBF single homozygous mice and found normal levels of this proteins compared to the WT islets (Figure 4D). The changes in Ucn3 levels in FVFPBF^{DHom} mice were accompanied by sporadic appearance of insulin-glucagon and insulin-somatostatin double-positive cells within the islets (Figure 4E and F), suggesting that β-cells lose their identity and transdifferentiate towards other endocrine cell types as previously reported [8]. This phenotype was not detected in the FVF and PBF single homozygous islets (Supplementary Figure 3C).

Since Foxa2 and Pdx1 induce several similar target genes in β-cells, it is possible that they function, cooperatively. To identify Pdx1 and Foxa2 binding sites in β-cell-specific enhancers and promoters, we analyzed the ChIP-seq dataset from mouse pancreatic β-cell lines [40,41]. In agreement to previous results [42], we found 5976 sites to be co-

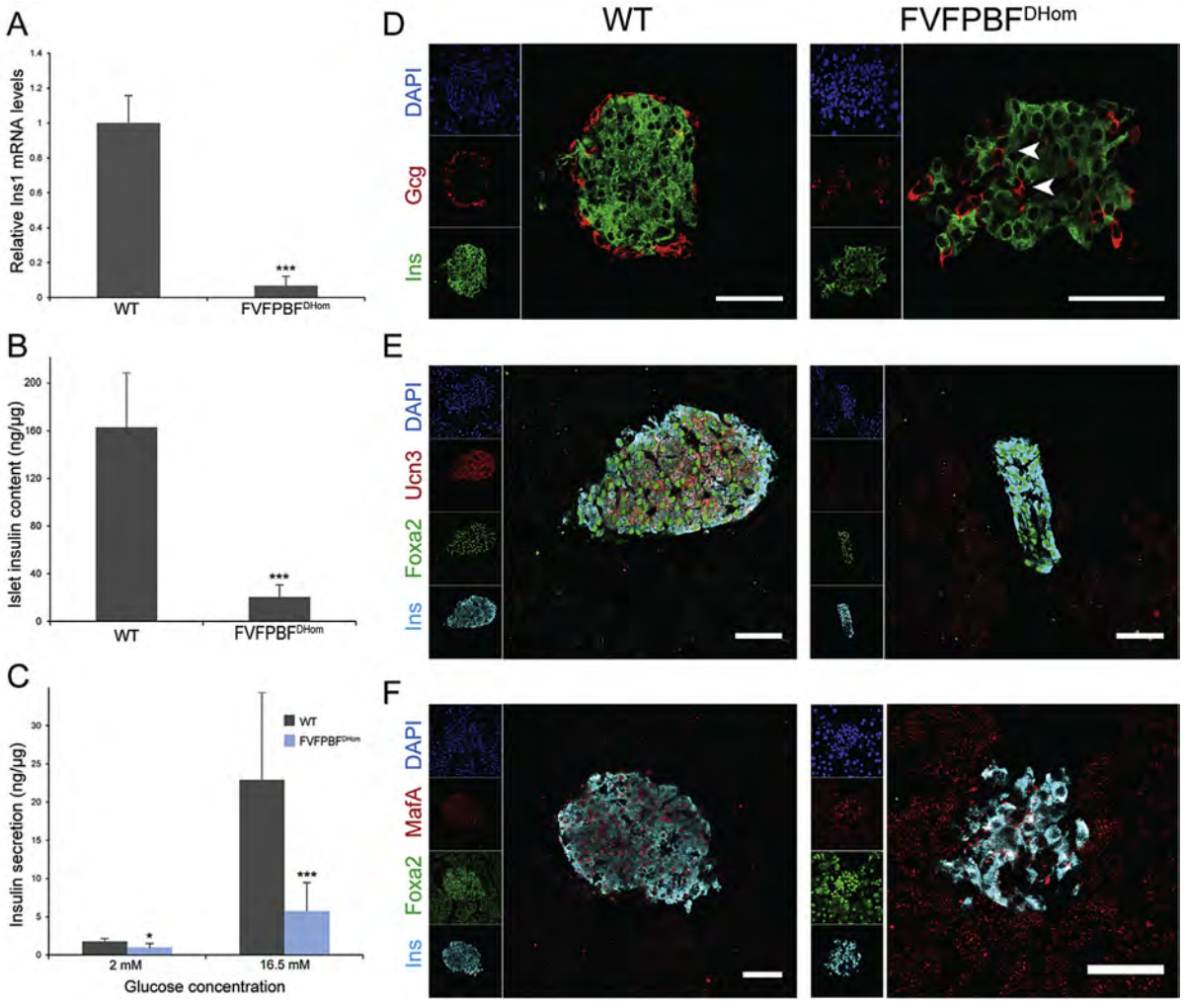

Figure 3: Impairment in insulin biosynthesis and release coincides with loss of islet architecture integrity in adult FVFPBF^{DHom} mice. (A) qPCR analysis for *Ins1* levels in isolated islets from male FVFPBF^{DHom} and WT mice (n = 4 for WT and 3 for FVFPBF^{DHom}, ***P < 0.001). (B) Measurement of total insulin content normalized to protein content from isolated islets from 3-month-old male FVFPBF^{DHom} and control animals (n ≥ 3, ***P < 0.001). (C) Quantification of insulin secretion in response to low (2 mM) and high (16 mM) glucose concentrations determined by GSIS assay in islets from adult male FVFPBF^{DHom} and WT mice (n ≥ 3, ***P < 0.001). (D) Immunostaining of pancreatic sections showing the disturbed islet structure in the FVFPBF^{DHom} male compared to the WT mice. (E) Ucn3 staining in islets from 3-month-old male FVFPBF^{DHom} and WT mice. (F) Immunostaining of MafA in male FVFPBF^{DHom} and WT adult islets. Scale bars, 50 µm.

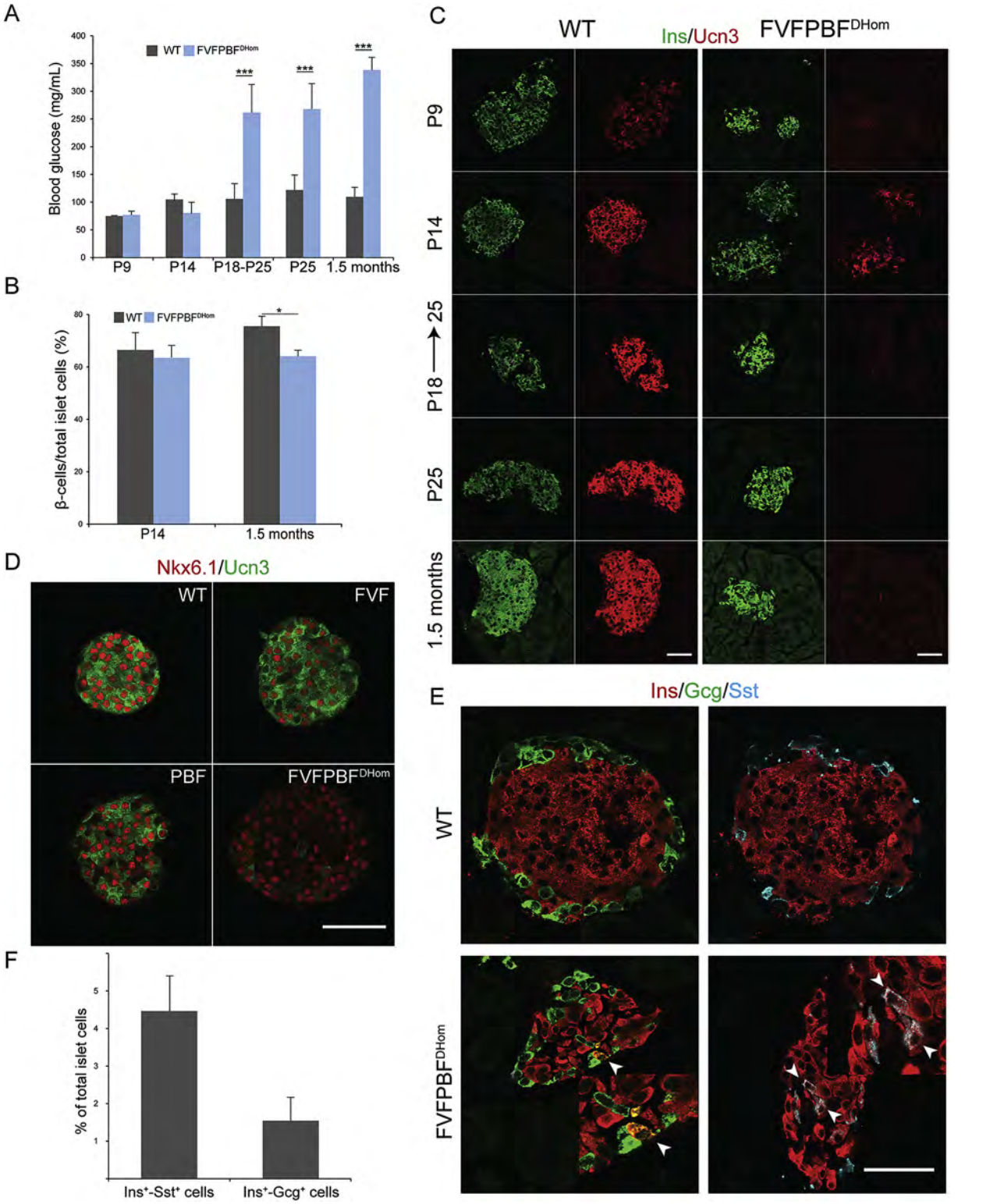

Figure 4: FVFPBF^{DHom} β-cells fail to induce maturation step and consequently lose their identity. (A) Fasted blood glucose levels (mg/dL) from animals of age P9 through 1.5 months old ($n \geq 3$, ***$P < 0.001$). (B) Quantification of β-cell number in islets from the male FVFPBF^{DHom} and WT mice ($n = 3$, *$P < 0.05$). (C) FVFPBF^{DHom} male mice show a gradual reduction in the Ucn3 expression levels starting from P25 till 1.5 months. (D) Ucn3 staining of isolated islets from 1.5 month single homozygous FVF and PBF mice shows normal levels of this protein compared to the WT control. (E) Islets derived from the FVFPBF^{DHom} male mice exhibit the presence of poly-hormonal cells within the islet core. (F) Quantification of poly-hormonal cells within the islet from the male FVFPBF^{DHom} animals ($n = 3$). Scale bars, 50 μm.

occupied by Foxa2 and Pdx1, suggesting that a substantial number of β-cell-specific enhancers and promoters are co-occupied by both TFs (Figure 5A). More general, genes with co-occupied sites are involved in insulin secretion, β-cell development and function, and can be related to diabetes susceptibility (Figure 5B). This suggests that the cooperative action of Foxa2 and Pdx1 is critical to maintain β-cell maturation and identity (Figure 5C). Furthermore, genes nearby these co-occupied sites also included those important for mature β-cell function, such as MafA, Slc2a2, and Ins1. To test whether these co-occupied genes are indeed directly regulated by Foxa2 and Pdx1, we next performed qPCR analysis and found a significant reduction in the levels of MafA, Slc2a2, and Ucn3 in the islets from the FVFPBF^{DHom} mice when compared to WT. Interestingly, we found a striking increase in the levels of MafB in the FVFPBF^{DHom} islets, suggesting that failure to switch from MafB to MafA impairs β-cell maturation (Figure 5D) [38]. Another β-cell signature gene is glucose transporter, Glut2 (also known as Slc2a2), which is essential for glucose sensing of mature β-cells [43]. Immunostaining for Glut2 revealed failure of synthesis of this protein in the FVFPBF^{DHom} islets supporting the loss of β-cell maturation and function in these mice (Figure 5E).

4. DISCUSSION

The Pdx1 and Foxa2 TFs are two crucial players during multiple stages of pancreas development and are also important for adult β-cell function; however, their role in early postnatal maturation of β-cells is

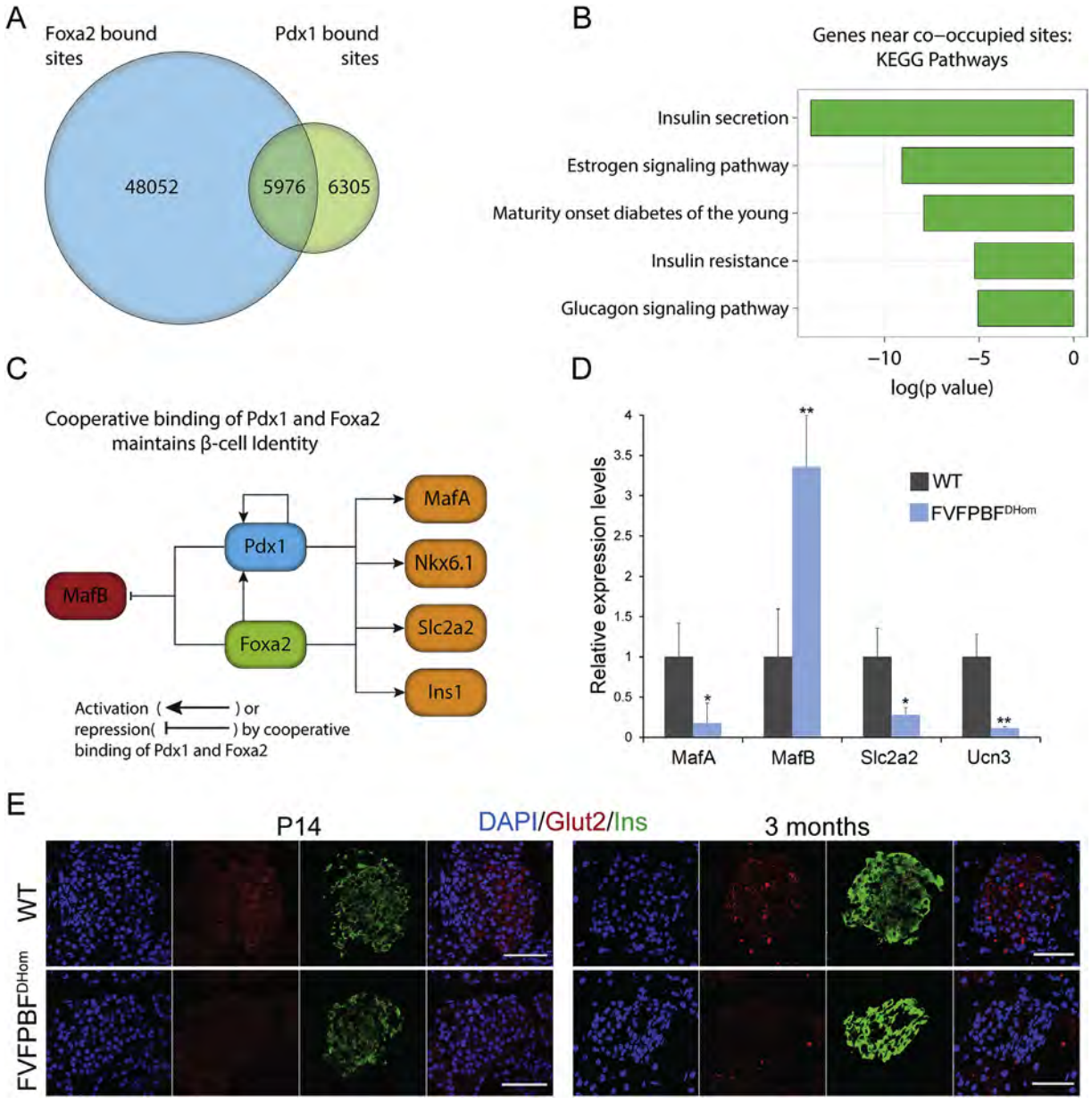

Figure 5: Cooperative function of Foxa2 and Pdx1 regulates β-cell maturation. Foxa2 and Pdx1 target genes were identified using raw reads from Foxa2 ChIP-seq (GSM1306337) and Pdx1 ChIP-seq (GSM1824088) obtained from pancreatic β-cell lines [40,41]. (A) Venn diagram representing the co-occupation of 5976 enhancer and promoter sites by Foxa2 and Pdx1. (B) KEGG ontology pathway of gene category near to the co-binding sites of Foxa2 and Pdx1. (C) Cooperative binding of Foxa2 and Pdx1 regulates expression of key genes involved in β-cell maturation and function. (D) qPCR analysis of crucial genes regulating β-cell maturation in the FVFPBF^{DHom} and WT islets. (n = 4 for WT and 3 for FVFPBF^{DHom}. *P < 0.05; **P < 0.01). (E) Immunostaining of Glut2 in P14 and 3-month-old islets from FVFPBF^{DHom} and WT mice. Scale bars, 50 μm.

less well studied. The synergistic effect of these TFs in pancreatic islets has been demonstrated in mice heterozygous for both Pdx1 and Foxa2 [2]. Although the results so far point to a combinatorial effect of both TFs on β-cell function, the precise functional relationship between these two TFs during postnatal β-cell maturation is not well understood. Therefore, we generated a double reporter knock-in mouse line to easily track the expression domains and investigate the functional interconnection between Foxa2 and Pdx1 in adult islets. In these mice, FVF and PBF proteins mirror the expression of endogenous Foxa2 and Pdx1, respectively. Whereas, the single homozygous reporter mice did not show blood glucose alterations, the male FVFPBF^{DHom} homozygous mice developed hyperglycemia, postnatally. Furthermore, they displayed a reduction in the Pdx1 levels which coincided with alteration in β-cell number and islet architecture.

It is well known that the expression of several endocrine-specific TFs, including Nkx6.1, Pax6, Nkx2.2, and Pdx1, is driven by Foxa1 and Foxa2 (Foxa1/2) during development [7]. Therefore, the absence of obvious defects in early pancreas development in the FVFPBF^{DHom} animals is likely due to the compensatory function of Foxa1 [44]. To regulate the Pdx1 expression, Foxa1/2 bind to multiple *cis*-regulatory elements, which precisely regulate and maintain the expression levels of Pdx1 gene [7,45]. This enhancer domain consists of a proximal region close to the transcriptional start site called Area I—II—III and a distal district termed Area IV, containing binding sequences for different *trans*-acting factors, including Foxa1/2 [45—52]. Although, the interaction of Foxa1/2 with Pdx1 enhancer domain increases during development, the increase is more robust for Foxa2 than for Foxa1 [7]. Thus, it is tempting to speculate that the fusion of Venus to Foxa2 perhaps reduces DNA binding or cooperative binding with other TF and cofactors to the Pdx1 enhancer elements that consequently decreases the expression levels of Pdx1. This might explain why the FVFPBF^{DHom} mice exhibit a severe postnatal phenotype when Foxa2 plays a major role in regulating Pdx1 levels [7]. In addition, it has been shown that by binding to *cis*-regulatory elements (Area I and IV), Pdx1 regulates its own expression through an autoregulatory positive feedback loop [36,47,53]. Therefore, it is possible that the fusion of the bulky BFP to Pdx1 reduces the autoregulatory function of this TF in a similar manner as described above for FVF and contributes to the reduction of Pdx1 levels. This is also supported by the finding of reduced Pdx1 levels in PBF homozygous mice.

We found almost normal blood glucose levels in the female FVFPBF^{DHom} compared to the male mice, which can be due to the gender difference in diabetes susceptibility and has been reported previously [54]. This sexual dimorphism has been attributed to the protective role of hormones, specifically estrogen, in the development of diabetes [55—57]. Recently, Foxa2 has been shown to dictate sexual dimorphism in liver cancer by opposing interactions with the androgen and estrogen receptors [58]. Of note, genes acting in the estrogen signaling pathway showed significant enhanced Foxa2 and Pdx1 binding in their enhancer and promoter regions (Figure 5B). However, the interaction of Foxa2 (and Pdx1) with sex hormones in pancreatic islets and its potential role in diabetes need further investigation.

Even though the FVFPBF^{DHom} male mice showed normal pancreas morphogenesis, they developed hyperglycemia at weaning age, suggesting either the involvement of diet-induced metabolic changes or failure in generating or maintaining functional mature β-cells. When we pre-weaned the mice at P18 and compared them to those that remained on high-fat milk diet, we could not distinguish any differences regarding blood glucose homeostasis, indicating that the observed phenotype is due to genetic predisposition to develop diabetes rather than environmental factors. Indeed, we found a massive reduction in the levels of the β-cell maturation marker Ucn3 in the FVFPBF^{DHom} male mice before and at weaning age independent from the diet switch. These data indicate that β-cells not only undergo a poor maturation process but also fail to maintain and preserve their maturation program in FVFPBF^{DHom} mice.

The defect in β-cell maturation concurred with the appearance of poly-hormonal endocrine cells within the islets from the FVFPBF^{DHom} mice. In particular, we could detect a significant number of insulin-glucagon and insulin-somatostatin double-positive cells in the FVFPBF^{DHom} islets. In addition, immunostaining analysis revealed an increase in the α-cell number in the FVFPBF^{DHom} mice. It has been shown that *Insulin*-Cre-induced Pdx1 removal in β-cells during development results in increase in the ratio of glucagon-positive to insulin-expressing cells [9,59]. Moreover, β-cell-specific deletion of Pdx1 leads to hyperglycemia through the reprograming of these cells towards α-cells [8]. This occurs because Pdx1 is not only required for preserving β-cell identity but also for repressing a α-cell program [8]. This is supported by the finding that Pdx1 converts perinatal α-cells into β-cells through a glucagon-insulin double positive state, upon forced expression in the embryonic endocrine progenitors [60]. Furthermore, Pdx1 represses the *MafB* and *glucagon* genes in β-cells. Therefore, in Pdx1-depleted β-cells, this inhibitory function is removed, leading to the formation of cells exhibiting ultrastructural and physiological features of endogenous α-cells [8]. The fact that the levels of *MafB* are increased in the FVFPBF^{DHom} mice suggests that β-cells undergo the trans-differentiation towards the α-cells partially through the derepression of this gene. Thus, trans-differentiation of β-cells might be the main mechanism reducing the number of these cells in the FVFPBF^{DHom} islets. We detected no cleaved caspase3 signal in the FVFPBF^{DHom} mice (Supplementary Figure 3D), proposing a minor contribution of cell death to the decreased number of β-cells. This is also supported by the absence of apoptotic cells in the Pdx1-depleted β-cells [8]. Therefore, the impairment in β-cell maturation along with hyperglycemia in FVFPBF^{DHom} mice likely leads to reduction in β-cell number through loss of identity and trans-differentiation towards other endocrine cells.

Because Foxa2 and Pdx1 activate many similar genes in β-cells, it is likely that they trigger their targets, cooperatively. Indeed, using ChIP-seq analysis, 5976 loci were identified to be co-occupied by both Foxa2 and Pdx1 in the islets. Among these, were those involved in insulin secretion, estrogen signaling pathway, MODY, insulin resistance, and the glucagon signaling pathway. This cooperative function is highly tissue-specific, and in the islets, it regulates several target genes involved in β-cell maturation and function, such as *MafA*, *Ins1*, and *Slc2a2*. The expression of these genes that are important for mature β-cell function is impaired in the FVFPBF^{DHom} islets. Furthermore, the function of Foxa2 and Pdx1 in preserving β-cell maturation and identity is partially through the repression of genes necessary for the α-cell fate, such as *MafB*, which is up-regulated in the FVFPBF^{DHom} mice. Therefore, it is possible that the fused bulky fluorescence tags prevent the co-binding of Foxa2 and Pdx1 to the regulatory elements of their target genes through the steric hindrance. Notably, the binding of FOXA2 and PDX1 to *cis* regulatory elements has also been identified in human. For instance, both TFs occupy a sequence acting as a developmental enhancer of *PTF1A* in hESC-derived pancreatic progenitors. The binding of FOXA2 and PDX1 is eliminated upon mutations in this *cis*-regulatory enhancer region and leads to isolated pancreatic agenesis [61].

In summary, we generated a FVFPBF^{DHom} reporter mouse line that develops hyperglycemia postnatally. This phenotype occurs due to the failure to generate and preserve mature β-cells, which ultimately undergo trans-differentiation towards other endocrine cells, mainly α- and δ-cells. The reduction in Pdx1 levels along with the possible destruction of the cooperative function of this TF with Foxa2 are the responsible mechanisms underlying loss of β-cell maturation, identity, and function.

AUTHOR CONTRIBUTIONS

A.B. and S.R. researched data, contributed to discussion and reviewed/edited manuscript. I.B., E.B. and M.S. researched data and reviewed/edited manuscript. M.B. researched data and wrote the manuscript. H.L. wrote the manuscript and conceived the work. H.L. is the guarantor of this work and takes full responsibility for the work as a whole. The authors declare no conflicts of interest.

ACKNOWLEDGMENTS

We thank Marta Tarquis Medina, Anne Theis, Bianca Vogel, and Christiana Polydorous (Helmholtz Zentrum München) for technical support. The work was supported by the European Research Council (ERC) Starting Grant (to H.L.) and the HumEn project from the European Union's Seventh Framework Program for Research, Technological Development and Demonstration under grant agreement No. 602587 (http://www.hum-en.eu/). We thank the Helmholtz Society, Helmholtz Portfolio Theme 'Metabolic Dysfunction and Common Disease, German Research Foundation, and German Center for Diabetes Research (DZD e.V.) for financial support.

CONFLICT OF INTEREST

None declared.

APPENDIX A. SUPPLEMENTARY DATA

Supplementary data related to this article can be found at http://dx.doi.org/10.1016/j.molmet.2017.03.007.

REFERENCES

[1] Pan, F.C., Wright, C., 2011. Pancreas organogenesis: from bud to plexus to gland. Developmental Dynamics 240(3):530—565.

[2] Shih, H.P., Wang, A., Sander, M., 2013. Pancreas organogenesis: from lineage determination to morphogenesis. Annual Review of Cell and Developmental Biology 29:81—105.

[3] Edlund, H., 2002. Pancreatic organogenesis—developmental mechanisms and implications for therapy. Nature Reviews. Genetics 3(7):524—532.

[4] Jonsson, J., Carlsson, L., Edlund, T., Edlund, H., 1994. Insulin-promoter-factor 1 is required for pancreas development in mice. Nature 371:606—609.

[5] Holland, A.M., Hale, M.A., Kagami, H., Hammer, R.E., MacDonald, R.J., 2002. Experimental control of pancreatic development and maintenance. Proceedings of the National Academy of Sciences of the United States of America 99(19):12236—12241.

[6] Bernardo, A.S., Hay, C.W., Docherty, K., 2008. Pancreatic transcription factors and their role in the birth, life and survival of the pancreatic beta cell. Molecular and Cellular Endocrinology 294:1—9.

[7] Gao, N., LeLay, J., Vatamaniuk, M.Z., Rieck, S., Friedman, J.R., Kaestner, K.H., 2008. Dynamic regulation of Pdx1 enhancers by Foxa1 and Foxa2 is essential for pancreas development. Genes and Development 22(24):3435—3448.

[8] Gao, T., McKenna, B., Li, C., Reichert, M., Nguyen, J., Singh, T., et al., 2014. Pdx1 maintains beta cell identity and function by repressing an α cell program. Cell Metabolism 19(2):259—271.

[9] Ahlgren, U., Jonsson, J., Jonsson, L., 1998. b-Cell-specific inactivation of the mouse Ipf1/Pdx1 gene results in loss of the b-cell phenotype and maturity onset diabetes. Genes & Development 12(12):1763—1768.

[10] Hani, E.H., 1999. Defective mutations in the insulin promoter factor-1 (IPF-1) gene in late-onset type 2 diabetes mellitus. Journal of Clinical Investigation 104(9):R41—R48.

[11] Brissova, M., Shiota, M., Nicholson, W.E., Gannon, M., Knobel, S.M., Piston, D.W., et al., 2002. Reduction in pancreatic transcription factor PDX-1 impairs glucose-stimulated insulin secretion. Journal of Biological Chemistry 277(13):11225—11232.

[12] Johnson, J.D., Ahmed, N.T., Luciani, D.S., Han, Z., Tran, H., Fujita, J., et al., 2003. Increased islet apoptosis in Pdx1+/- mice. Journal of Clinical Investigation 111(8):1147—1160.

[13] Holland, A.M., Go, L.J., Naselli, G., MacDonald, R.J., Harrison, L.C., 2005. Conditional expression demonstrates the role of the homeodomain transcription factor Pdx1 in maintenance and regeneration of beta-cells in the adult pancreas. Diabetes 54:2586—2595.

[14] Fajans, S.S., Bell, G.I., Polonsky, K.S., 2001. Molecular mechanisms and clinical pathophysiology of maturity-onset diabetes of the young. The New England Journal of Medicine 345(13):971—980.

[15] Burtscher, I., Barkey, W., Lickert, H., 2013. Foxa2-venus fusion reporter mouse line allows live-cell analysis of endoderm-derived organ formation. Genesis 51(8):596—604.

[16] Willmann, S.J., Mueller, N.S., Engert, S., Sterr, M., Burtscher, I., Raducanu, A., et al., 2016. The global gene expression profile of the secondary transition during pancreatic development. Mechanisms of Development 139:51—64.

[17] Lantz, K.A., Vatamaniuk, M.Z., Brestelli, J.E., Friedman, J.R., Matschinsky, F.M., Kaestner, K.H., 2004. Foxa2 regulates multiple pathways of insulin secretion. Journal of Clinical Investigation 114(4):512—520.

[18] Gao, N., Le Lay, J., Qin, W., Doliba, N., Schug, J., Fox, A.J., et al., 2010. Foxa1 and Foxa2 maintain the metabolic and secretory features of the mature beta-cell. Molecular Endocrinology (Baltimore, Md) 24(8):1594—1604.

[19] Sund, N.J., Vatamaniuk, M.Z., Casey, M., Ang, S.W., Magnuson, M.A., Stoffers, D.A., et al., 2001. Tissue-specific deletion of Foxa2 in pancreatic β cells results in hyperinsulinemic hypoglycemia. Genes and Development 15(13):1706—1715.

[20] Gaulton, K.J., Ferreira, T., Lee, Y., Raimondo, A., Mägi, R., Reschen, M.E., et al., 2015. Genetic fine mapping and genomic annotation defines causal mechanisms at type 2 diabetes susceptibility loci. Nature Genetics 47(12):1415—1425.

[21] Gao, N., White, P., Doliba, N., Golson, M.L., Matschinsky, F.M., Kaestner, K.H., 2007. Foxa2 controls vesicle docking and insulin secretion in mature Beta cells. Cell Metabolism 6(4):267—279.

[22] Wang, H., Gauthier, B.R., Hagenfeldt-Johansson, K.A., Iezzi, M., Wollheim, C.B., 2002. Foxa2 (HNF3beta) controls multiple genes implicated in metabolism-secretion coupling of glucose-induced insulin release. Journal of Biological Chemistry 277(20):17564—17570.

[23] Wang, Z., York, N.W., Nichols, C.G., Remedi, M.S., 2014. Pancreatic β cell dedifferentiation in diabetes and redifferentiation following insulin therapy. Cell Metabolism 19(5):872—882.

[24] Russ, H.A., Sintov, E., Anker-Kitai, L., Friedman, O., Lenz, A., Toren, G., et al., 2011. Insulin-Producing cells generated from dedifferentiated human pancreatic beta cells expanded in vitro. PLoS One 6(9).

[25] Lee, C.S., Sund, N.J., Vatamaniuk, M.Z., Matschinsky, F.M., Stoffers, D.A., Kaestner, K.H., 2002. Foxa2 controls Pdx1 gene expression in pancreatic beta-cells in vivo. Diabetes 51(8):2546—2551.

[26] Copeland, N.G., Jenkins, N.A., Court, D.L., 2001. Recombineering: a powerful new tool for mouse functional genomics. Nature Reviews. Genetics 2(10):769—779.

[27] Liu, P., Jenkins, N.A., Copeland, N.G., 2003. A highly efficient recombineering-based method for generating conditional knockout mutations. Genome Research 13(3):476–484.

[28] Liao, W.P., Uetzmann, L., Burtscher, I., Lickert, H., 2009. Generation of a mouse line expressing Sox17-driven Cre recombinase with specific activity in arteries. Genesis 47(7):476–483.

[29] Uetzmann, L., Burtscher, I., Lickert, H., 2008. A mouse line expressing Foxa2-driven Cre recombinase in Node, notochord, floorplate, and endoderm. Genesis 46(10):515–522.

[30] Hitz, C., Wurst, W., Kühn, R., 2007. Conditional brain-specific knockdown of MAPK using Cre/loxP regulated RNA interference. Nucleic Acids Research 35(12):e90.

[31] Bader, E., Migliorini, A., Gegg, M., Moruzzi, N., Gerdes, J., Roscioni, S., et al., 2016. Identification of proliferative and mature β -cells in the islet of Langerhans. Nature 535(7612):430–434.

[32] Guo, Y., Mahony, S., Gifford, D.K., 2012. High resolution genome wide binding event finding and motif discovery reveals transcription factor spatial binding constraints. PLoS Computational Biology 8(8).

[33] Heinz, S., Benner, C., Spann, N., Bertolino, E., Lin, Y.C., Laslo, P., et al., 2010. Simple Combinations of lineage-determining transcription factors prime cis-regulatory elements required for macrophage and B cell identities. Molecular Cell 38(4):576–589.

[34] Potter, L.A., Choi, E., Hipkens, S.B., Wright, C.V.E., Magnuson, M.A., 2012. A recombinase-mediated cassette exchange-derived cyan fluorescent protein reporter allele for Pdx1. Genesis 50(4):384–392.

[35] Murtaugh, L.C., 2007. Pancreas and beta-cell development: from the actual to the possible. Development 134(3):427–438.

[36] Marshak, S., Benshushan, E., Shoshkes, M., Havin, L., Cerasi, E., Melloul, D., 2000. Functional conservation of regulatory elements in the pdx-1 gene: PDX-1 and hepatocyte nuclear factor 3beta transcription factors mediate beta-cell-specific expression. Molecular and Cellular Biology 20(20):7583–7590.

[37] Blum, B., Hrvatin, S., Schuetz, C., Bonal, C., Rezania, A., Melton, D.A., 2012. Functional beta-cell maturation is marked by an increased glucose threshold and by expression of urocortin 3. Nature Biotechnology 30(3):261–264.

[38] Nishimura, W., Kondo, T., Salameh, T., El Khattabi, I., Dodge, R., Bonner-Weir, S., et al., 2006. A switch from MafB to MafA expression accompanies differentiation to pancreatic beta-cells. Developmental Biology 293(2):526–539.

[39] Stolovich-Rain, M., Enk, J., Vikesa, J., Nielsen, F., Saada, A., Glaser, B., et al., 2015. Weaning triggers a maturation step of pancreatic β cells. Developmental Cell 32(5):535–545.

[40] Perelis, M., Marcheva, B., Ramsey, K.M., Schipma, M.J., Hutchison, A.L., Taguchi, A., et al., 2015. Pancreatic β cell enhancers regulate rhythmic transcription of genes controlling insulin secretion. Science 350(6261):4250.

[41] Jia, S., Ivanov, A., Blasevic, D., Müller, T., Purfürst, B., Sun, W., et al., 2015. Insm 1 cooperates with Neurod 1 and Foxa 2 to maintain mature pancreatic b -cell function 34(10):1417–1433.

[42] Hoffman, B.G., Robertson, G., Zavaglia, B., Beach, M., Cullum, R., Lee, S., et al., 2010. Locus co-occupancy, nucleosome positioning, and H3K4me1 regulate the functionality of FOXA2-, HNF4A-, and PDX1-bound loci in islets and liver. Genome Research 20(8):1037–1051.

[43] Rutter, G.A., Pullen, T.J., Hodson, D.J., Martinez-Sanchez, A., 2015. Pancreatic beta-cell identity, glucose sensing and the control of insulin secretion. The Biochemical Journal 466(2):203–218.

[44] Lee, C.S., Sund, N.J., Behr, R., Herrera, P.L., Kaestner, K.H., 2005. Foxa2 is required for the differentiation of pancreatic α-cells. Developmental Biology 278(2):484–495.

[45] Fujitani, Y., Fujitani, S., Boyer, D.F., Gannon, M., Kawaguchi, Y., Ray, M., et al., 2006. Targeted deletion of a cis-regulatory region reveals differential gene dosage requirements for Pdx1 in foregut organ differentiation and pancreas formation. Genes and Development 20(2):253–266.

[46] Gerrish, K., Gannon, M., Shih, D., Henderson, E., Stoffel, M., Wright, C.V.E., et al., 2000. Pancreatic β cell-specific transcription of the pdx-1 gene. The role of conserved upstream control regions and their hepatic nuclear factor 3β sites. Journal of Biological Chemistry 275(5):3485–3492.

[47] Gerrish, K., Cissell, M.A., Stein, R., 2001. The role of hepatic nuclear factor 1 alpha and PDX-1 in transcriptional regulation of the pdx-1 gene. The Journal of Biological Chemistry 276(51):47775–47784.

[48] Samaras, S.E., Cissell, M.A., Gerrish, K., Wright, C.V.E., Gannon, M., Stein, R., 2002. Conserved sequences in a tissue-specific regulatory region of the pdx-1 gene mediate transcription in Pancreatic beta cells: role for hepatocyte nuclear factor 3 beta and Pax6. Molecular and Cellular Biology 22(13):4702–4713.

[49] Hunter, C.S., Stein, R., 2013. Characterization of an apparently novel β-cell line-enriched 80-88 kDa transcriptional activator of the MafA and Pdxl genes. Journal of Biological Chemistry 288(6):3795–3803.

[50] Vanhoose, A.M., Samaras, S., Artner, I., Henderson, E., Hang, Y., Stein, R., 2008. MafA and MafB regulate Pdx1 transcription through the area II control region in pancreatic beta cells. Journal of Biological Chemistry 283(33): 22612–22619.

[51] Yang, Y.-P., Magnuson, M.A., Stein, R., Wright, C.V.E., 2016. The mammal-specific Pdx1 Area II enhancer has multiple essential functions in early endocrine-cell specification and postnatal β-cell maturation. Development 144:248–257.

[52] Sharma, S., Jhala, U.S., Johnson, T., Ferreri, K., Leonard, J., Montminy, M., 1997. Hormonal regulation of an islet-specific enhancer in the pancreatic homeobox gene STF-1. Molecular and Cellular Biology 17(5):2598–2604.

[53] Gerrish, K., Van Velkinburgh, J.C., Stein, R., 2004. Conserved transcriptional regulatory domains of the pdx-1 gene. Molecular Endocrinology 18(3):533–548.

[54] Vital, P., Larrieta, E., Hiriart, M., 2006. Sexual dimorphism in insulin sensitivity and susceptibility to develop diabetes in rats. Journal of Endocrinology 190(2): 425–432.

[55] Yuchi, Y., Cai, Y., Legein, B., De Groef, S., Leuckx, G., Coppens, V., et al., 2015. Estrogen receptor α regulates β-cell formation during pancreas development and following injury. Diabetes 64(9):3218–3228.

[56] Root-Bernstein, R., Podufaly, A., Dillon, P.F., 2014. Estradiol binds to insulin and insulin receptor decreasing insulin binding in vitro. Frontiers in Endocrinology 5:1–13.

[57] Alonso-Magdalena, P., Ropero, A.B., Carrera, M.P., Cederroth, C.R., Baquié, M., Gauthier, B.R., et al., 2008. Pancreatic insulin content regulation by the Estrogen receptor ERα. PLoS One 3(4).

[58] Li, Z., Tuteja, G., Schug, J., Kaestner, K.H., 2012. Foxa1 and Foxa2 are essential for sexual dimorphism in liver cancer. Cell 148(1–2):72–83.

[59] Gannon, M., Tweedie Ables, E., Crawford, L., Lowe, D., Offield, M.F., Magnuson, M.A., et al., 2008. Pdx-1 function is specifically required in embryonic beta cells to generate appropriate numbers of endocrine cell types and maintain glucose homeostasis. Developmental Biology 314(2):406–417.

[60] Yang, Y., Thorel, F., Boyer, D.F., Herrera, P.L., Wright, C.V.E., 2011. Context-specific α-to- β-cell reprogramming by forced Pdx1 expression service re programming by forced Pdx1 expression. Genes and Development 25:1680–1685.

[61] Weedon, M.N., Cebola, I., Patch, A., Flanagan, S.E., Franco, E. De., Caswell, R., et al., 2013. Recessive mutations in a distal PTF1A enhancer cause isolated pancreatic agenesis. Nature Genetic 46(1):61–64.

